(1) 7

Third Semiannual Technical Report

ARPA Order No.	1827
Program Code:	3F10
Name of Contractor:	University of Wisconsin-Milwaukee
Effective Date of Grant:	1 June 1973
Grant Expiration:	31 May 1975
Amount of Grant Dollars:	$94,472
Grant Number:	AFOSR 73-2543
Co-Principal Investigators:	Dr. Robert W. Taylor Dr. David E. Willis
Telephone:	Area Code 414, 963-4561
Program Manager:	Mr. William J. Best
Telephone:	Area Code 202, 964-5454
Short Title of Work:	Multiple Seismic Events
Report Number:	144-E123-10-T
Date:	15 March 1975

Sponsored by

Advanced Research Projects Agency

ARPA Order Number 1827

Approved for Public Release; Distribution Unlimited

SECURITY CLASSIFICATION OF THIS PAGE (When Data Entered)

REPORT DOCUMENTATION PAGE

READ INSTRUCTIONS BEFORE COMPLETING FORM

1. REPORT NUMBER (14) 144-E123-10-T
2. GOVT ACCESSION NO.
3. RECIPIENT'S CATALOG NUMBER

4. TITLE (and Subtitle) (6) Multiple Seismic Events.
5. TYPE OF REPORT & PERIOD COVERED: Scientific Interim
6. PERFORMING ORG. REPORT NUMBER

7. AUTHOR(s) (10) Robert W. Taylor, David E. Willis
8. CONTRACT OR GRANT NUMBER(s): AFOSR-73-C-2543

9. PERFORMING ORGANIZATION NAME AND ADDRESS
University of Wisconsin-Milwaukee
Department of Geological Sciences
Milwaukee, Wisconsin 53201
10. PROGRAM ELEMENT, PROJECT, TASK AREA & WORK UNIT NUMBERS
AO 1827-8
62701E

11. CONTROLLING OFFICE NAME AND ADDRESS
Air Force Office of Scientific Research
1400 Wilson Boulevard
Arlington, Virginia 22209
12. REPORT DATE: 15 March 1975
13. NUMBER OF PAGES

14. MONITORING AGENCY NAME & ADDRESS (if different from Controlling Office) (9) Semiannual Technical Rept. no. 3, 1 Jun - 31 Nov 74
15. SECURITY CLASS. (of this report): Unclassified
15a. DECLASSIFICATION/DOWNGRADING SCHEDULE

16. DISTRIBUTION STATEMENT (of this Report)
(12) 125 P.
Approved for public release; distribution unlimited
(15) AF-AFOSR-2543-73

17. DISTRIBUTION STATEMENT (of the abstract entered in Block 20, if different from Report)
ARPA Order-1827

18. SUPPLEMENTARY NOTES
Third Semiannual Technical Report

19. KEY WORDS (Continue on reverse side if necessary and identify by block number)
Earthquakes, multiple nuclear shots, detection, identification, magnitudes, unmanned observatories, Cepstrum analysis, radiation pattern

20. ABSTRACT (Continue on reverse side if necessary and identify by block number)
It is shown in this study that the relationships of the delay times of secondary arrivals to the distance and azimuth of the recording stations provide a potential method of differentiating the source characteristics of an event. Cepstrum analysis is the method used to detect the delay times of secondary arrivals and was applied in a first zone study to selected Nevada Test Site events and one natural earthquake.

NEXT Page

DD FORM 1 JAN 73 1473 EDITION OF 1 NOV 65 IS OBSOLETE

406422

Unclassified

SECURITY CLASSIFICATION OF THIS PAGE (When Data Entered)

20. Abstract (cont'd)

The theoretical basis of cepstrum analysis was extended to include three secondary arrivals, and a formula was established for recovering the scaling factor of secondary arrivals with respect to the initial P arrival from an event.

The results indicate that cepstrum analysis can be used to detect the delay time of secondary arrivals, but it is difficult to interpret the delay-distance and delay-azimuth relationships and thereby identify the secondary arrivals. The detection of multiple events appeared possible in some cases, but station coverage requirements are severe. Knowledge of pP within 500 km of a source has possibly been extended.

Technical Report Summary

This is the third semiannual report dealing with an investigation of multiple seismic events and first zone discriminants. Reported here are the results obtained from studying secondary arrivals from a series of underground nuclear shots at the Nevada Test Site and a natural earthquake in the same general source region utilizing Cepstrum analysis techniques.

Cepstrum analysis, when applied to real data at first zone distances, yields a number of peaks in the resulting cepstra. The signal to noise level appears rather low and the peaks cannot be readily differentiated on the basis of amplitude. Lacking any significant differences in amplitude, it is necessary to consider all of the resulting peaks. When the delays associated with all the peaks are considered as a function of station distance and azimuth, tentative identifications are possible. The scatter of the resulting data, however, is high and some subjective evaluation is required. In view of the subjective elements in the identification, it does not appear that the method can be converted to a simple machine procedure.

The identification of arrivals does appear possible when sufficient data are available and subjective evaluations are allowed. Selected arrivals exhibit the characteristics of single sources and multiples of horizontally separated events.

A delay arrival, occurring at approximately 0.70 sec at 200 km with moveout of about 0.08 sec per 100 km, occurred for five of the six nuclear events. This is tentatively identified as pP. Very little data is available on pP at these distance and depth ranges. Thus, if this identification is correct, the knowledge of pP is extended.

Due to the necessity of considering the measured delays as a function of distance and azimuth, station coverage requirements for the detection of multiple events are severe. The detection of P-P delays appears to require stations at 20° azimuth intervals. The detection of the pP arrival requires at least 8 stations located at 50-75 km intervals over a 500 km range.

The "a" scaling factor was not recovered for the nuclear events considered in this study. The failure to recover the value resulted from limitations in available computer time. In addition, the available station coverage of azimuth and distance was somewhat limited and far from the ideal given above. Despite these limitations, the detection of multiple events appeared possible in some cases.

On the basis of theoretical considerations and limited tests, values of the "a" factor can be recovered with some degree of accuracy. While recovery is possible, the resulting "a" is both theoretically and practically

ambiguous, and because of this may prove of little value in the identification of multiple events. However, despite the ambiguous nature of "a", this value would be useful in the identification of pP.

No obvious propagation path effects due to differences in geology are evident from the data. While the results from an actual earthquake appear different from the results obtained from nuclear events, insufficient data was available to establish a quantitative difference. It is interesting to note, however, that for the available data, the variance associated with the predominant peaks of the earthquake was 0.5 seconds, while the variance associated with the predominant peaks of nuclear events was approximately 0.1 seconds.

UWM THE UNIVERSITY OF WISCONSIN-MILWAUKEE / MILWAUKEE, WISCONSIN 53201

DEPARTMENT OF GEOLOGICAL SCIENCES
SABIN HALL
GREENE MUSEUM
TELEPHONE: (414) 963-4561

March 15, 1975

AFOSR Grant No. 73-2543
Investigation of Multiple Seismic
Events and First Zone Discriminants
ARPA Order No. 1827
Program Code 3F10
The University of Wisconsin-Milwaukee

Report No. 144-E123-10-T
Effective Date of Grant 1 June 1973
Grant Expiration 31 May 1975
$94,470
Project Scientists: R. W. Taylor
and D. E. Willis

Air Force Office of Scientific Research
ATTN: NPG
1400 Wilson Boulevard
Arlington, Virginia 22204

Subject: Third Semiannual Technical Report for Period Covering 1 June 1974 through 31 November 1974.

Dear Sir:

This report is a summary of research dealing with multiple seismic events and first zone discriminants. The research is divided into the following categories and will be discussed individually.

Introduction

The purpose of the research reported here is to evaluate one of the methods for the discrimination of multiple nuclear events from single nuclear and natural events at distances less than 1000 km. The basis for the method of discrimination investigated is the relationship of the delay of arrivals, following the initial P arrival, to azimuth and distance. These relationships should be characteristic of the event type. Cepstrum analysis is used to determine the delay of the secondary arrivals (Bogart, Healy, and Tukey, 1973). This method of analysis will be applied to records of selected events within the Nevada Test Site. This study will be a near source application of cepstrum analysis to events at distances ranging from 150 km to 415 km. Where possible, the relationships of any detected arrivals to distance and azimuth will be used to predict the nature of the event.

This report is based on the thesis prepared by Zimdars (1974) which was sponsored by this project. The results of our investigations into spectral and correlation analyses between the seismic signals from earthquakes and nuclear events will be presented in the next scheduled semiannual report.

Theoretical Considerations

Source Parameters and Multiple Arrivals

One method of determining the multiple nature of an event is to detect the multiple nature of the direct P arrivals which occur from the multiple sources. Associated with a multiple source, there is, thus, a P-P delay time, the time difference between the arrival of the direct P wave from one event and the arrival of the direct P from a second event. The major problems of this approach are caused by the existence of contaminating secondary arrivals. For natural earthquakes and single nuclear sources there exists a surface reflected P wave, pP, of similar shape but different polarity. In addition to pP for a single nuclear source, there is another possible secondary arrival caused by the slapdown of surface materials (King and others, 1974; Springer, 1974). Thus, each single nuclear explosive source may consist of three P phases, a direct P, pP, and a slapdown arrival P_s, and these have the associated delay time, pP-P and P_s-P. All of these arrivals will occur within the normal P wave coda.

A multiple source composed of two events consists of two sets of the three P phases and has the associated delay times, pP_1-P_1, $P_{s_1}-P_1$, P_2-P_1, pP_2-P_1, and $P_{s_2}-P_1$. The magnitude of the delay time and the order of the arrival of the phases at a particular station is dependent upon the location of the events and the shot times.

The possibility of the existence of a number of secondary arrivals makes it difficult to relate a secondary arrival from a single record to any source characteristics. The different secondary arrivals must be differentiated from each other. A possible method of differentiating the secondary arrivals exists in their differing delay to distance and delay to azimuth relationships. Thus, the use of the arrivals from a number of stations located at different distances and azimuths provide a possible relationship to the source characteristics.

In the following sections the relation of delay to azimuth and distance will be considered for each of the various potential secondary arrivals. In general, to keep the involved parameters reasonable, multiple events will be considered as vertically or horizontally separated and simultaneously detonated. The generalization to inclined separation or delayed firing will normally present little difficulty.

P-P

The delay distance curves for two events separated horizontally and two events separated vertically may be quantitatively determined using the simplified diagrams of Figures 1 and 2. Choosing a 1 km distance between events and a depth of burial of .5 km, the calculated distance delay curves for three velocities are shown in Figures 3

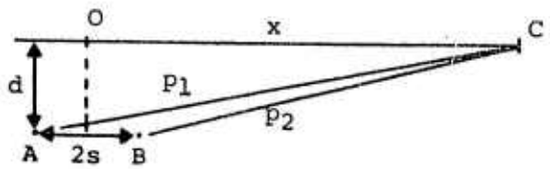

O - Midpoint of epicenter line

C - Station on surface of the earth

A, B - Explosion points

x - Distance to station

d - Depth of burial

2s - Distance between events

p_1, p_2 - Path of P wave of velocity, V

$$p_1 = (d^2 + (x + s)^2)^{1/2} \qquad p_2 = (d^2 + (x - s)^2)^{1/2}$$

$$\text{Delay time} = \frac{p_1 - p_2}{V}$$

$$= \frac{(d^2 + (x + s)^2)^{1/2} - (d^2 + (x - s)^2)^{1/2}}{V}$$

Figure 1. Schematic diagram of P wave paths for two horizontally separated events. Calculations are for the delay time of the direct P arrivals.

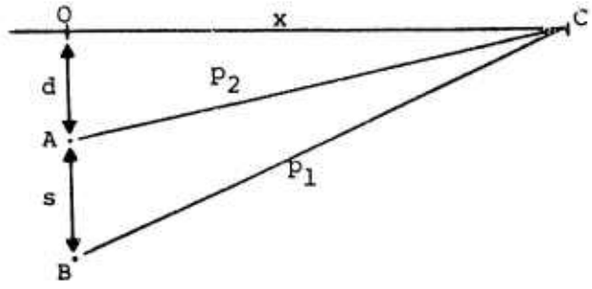

O - Epicenter

C - Station on surface of the earth

A, B - Explosion points

x - Distance to station

d - Depth of burial

s - Distance between events

p_1, p_2 - Path of P wave of velocity, V

$$p_1 = (x^2 + (d + s)^2)^{1/2} \qquad p_2 = (x^2 + d^2)^{1/2}$$

$$\text{Delay time} = \frac{p_1 - p_2}{V}$$

$$= \frac{(x^2 + (d + s)^2)^{1/2} - (x^2 + d^2)^{1/2}}{V}$$

Figure 2. Schematic diagram of P wave paths for two vertically separated events. Calculations are for the delay time of the direct P arrivals.

and 4. For two events separated horizontally the delay approaches constant values of .40, .25, and .17 seconds within 5 km of the source for velocities of 2.50, 4.00, and 6.00 km/sec, respectively. For two events vertically separated by 1 km, the delay approaches zero within 50 km of the source. The maximum delay in this case occurs at the epicenter of the events and for this model has values of .40, .25, and .17 seconds for velocities of 2.50, 4.00, and 6.00 km, respectively.

In order to generalize the delay distance plots, dimensionless plots were prepared. The abscissa of the plot is the ratio of the station distance to the distance between sources, and the ordinate is the percent of maximum delay. Dimensionless plots for horizontally and vertically separated multiple sources are given in Figure 5. It is evident that the delay approaches a constant value within 5 source separations of the epicenter for horizontally separated events. For vertically separated events the delay approaches a constant value within 50 source separations of the epicenter.

For two events vertically and horizontally separated by a similar amount the distance-delay plot has the form of the plot for horizontally separated events. Only the beginning section of the plot indicates that the events have a vertical separation. A plot for events having a

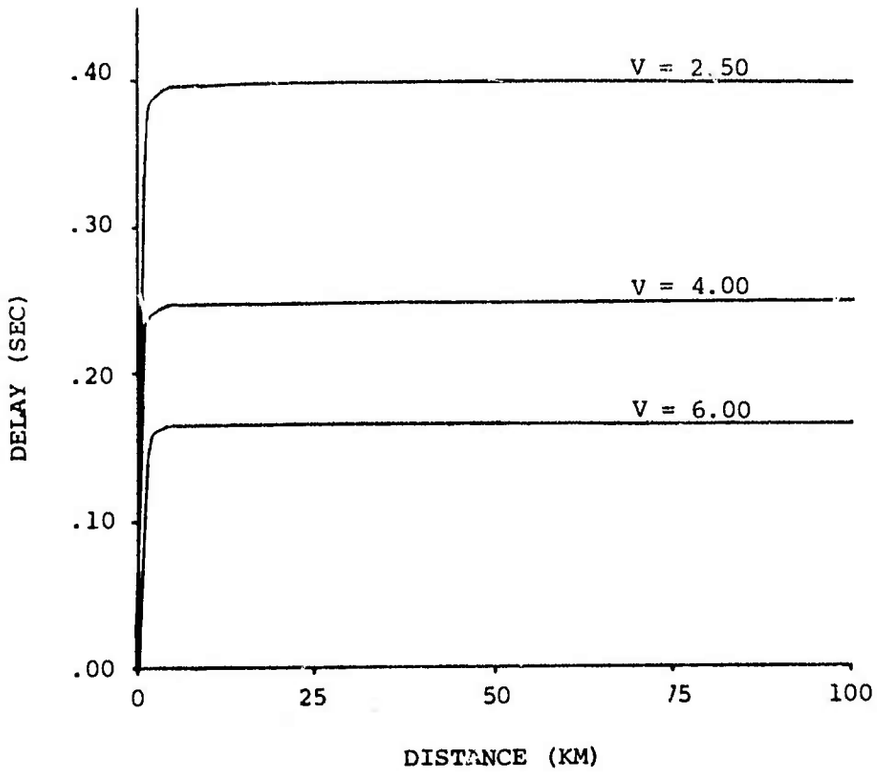

Figure 3. Three delay-distance plots for horizontally separated events. Distance between events is 1 km. Depth of burial is .5 km. Velocities (V) are 2.50, 4.00, and 6.00 km/sec.

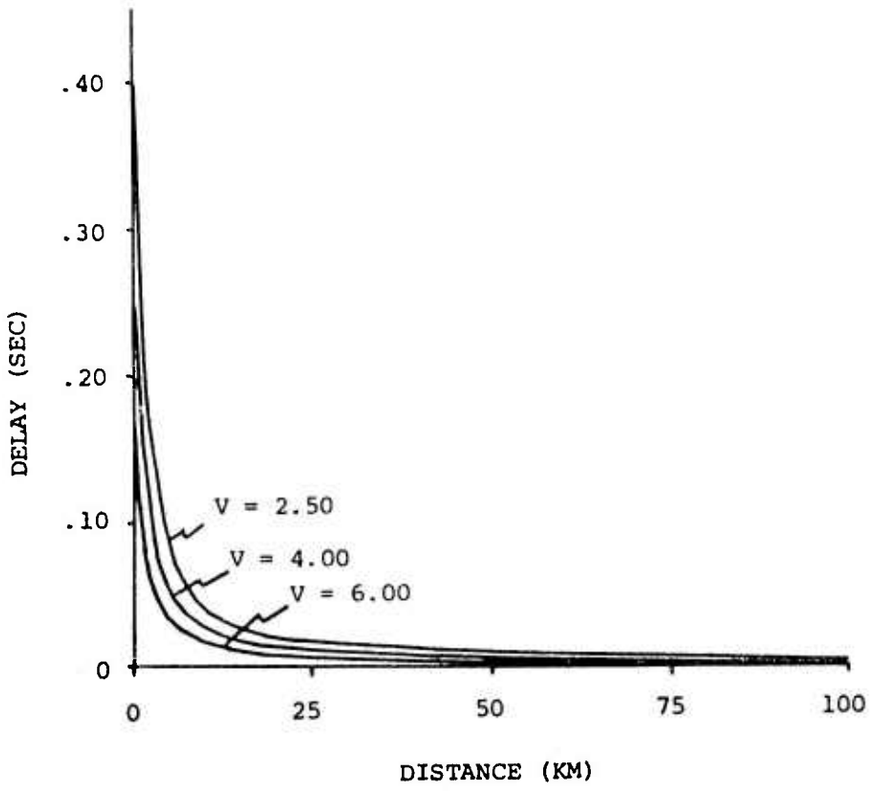

Figure 4. Three delay-distance plots for vertically separated events. Distance between events is 1 km. Depth of burial is .5 km. Velocities (V) are 2.50, 4.00, and 6.00 km/sec.

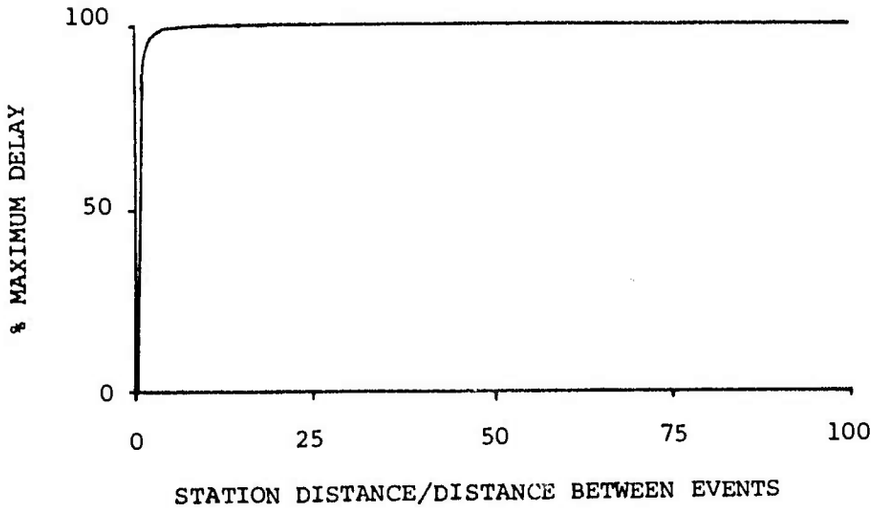

a

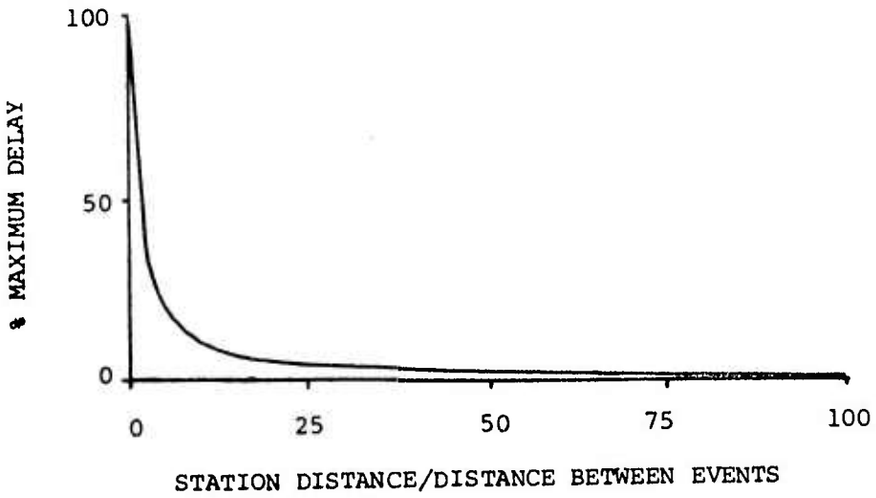

b

Figure 5. a) Dimensionless plot for two events separated horizontally.
b) Dimensionless plot for two events separated vertically.

horizontal separation of 1.0 km and a vertical separation of 1.0 km is shown in Figure 6.

Azimuth-delay plots for a horizontal separation of events were determined for distances between events of 1, 5, and 10 km and a velocity of 2.50 km/sec. The diagram and plots are shown in Figures 7 and 8. The delay times calculated are dependent upon the azimuth of the recording station, the depth of burial, and the distance between events and virtually independent of the distance to the recording station. For the calculated model, the trend of the line connecting the epicenter of the events is east-west. The origin of the plot is the midpoint of the line connecting the epicenters. The maximum delay occurs at azimuths of 90° and 270°. The P-P delay at stations which are located on a line perpendicular to the midpoint of the epicenter line is zero. Both direct P phases from the multiple source will arrive at approximately the same time. The P-P delay will be much less than the maximum delay in a 10 degree wedge on both sides of the line perpendicular to the midpoint of the epicenter line.

The delay-azimuth relation for events separated vertically is shown in Figure 9 for completeness only. It is evident from the figure that the delay time is dependent upon the distance between sources and not upon the azimuth. The expected delay azimuth plot for any

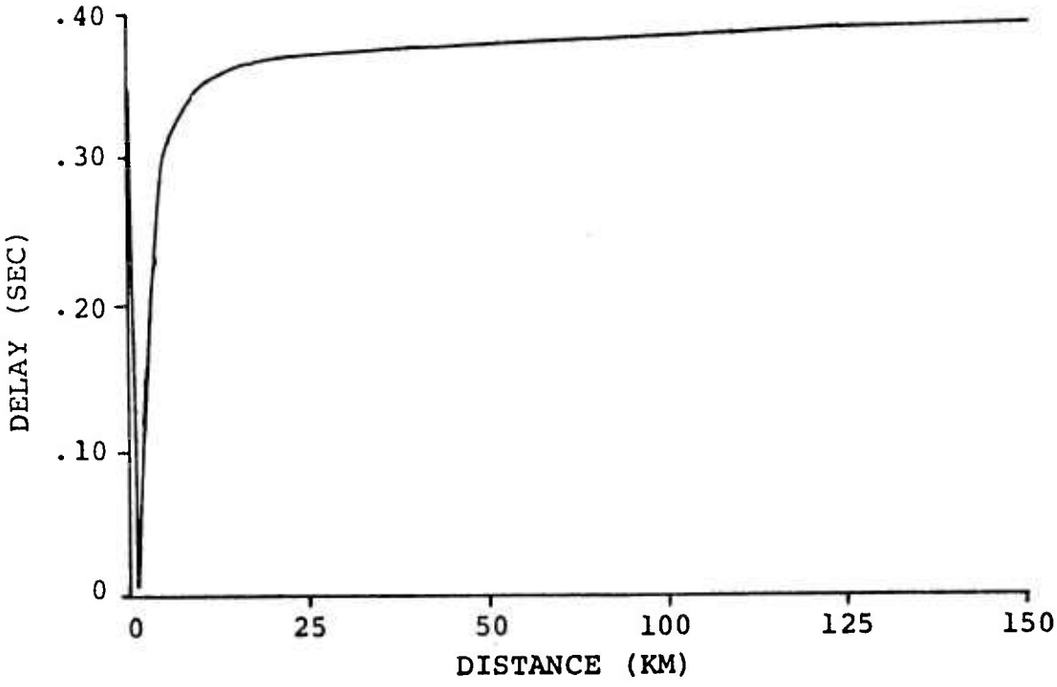

Figure 6. Delay-distance plot for an event separated vertically and horizontally. Vertical separation is 1 km and horizontal separation is 1 km. Velocity is 2.50 km/sec.

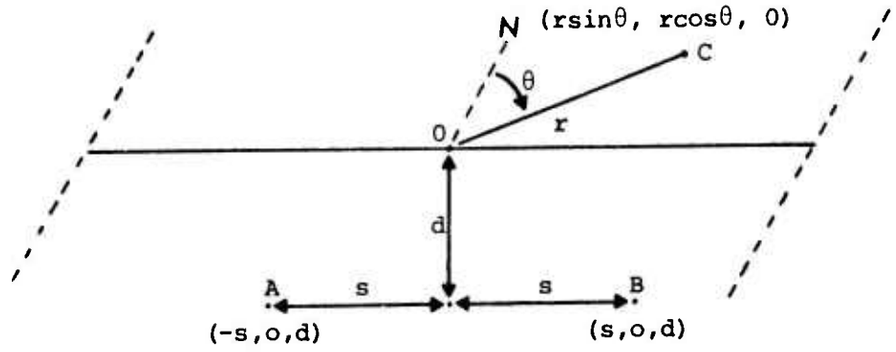

0 - Midpoint of epicenter line

A, B - Explosion points

C - Station on surface of earth

r - Distance to station

d - Depth of burial

2s - Distance between events

θ - Azimuth

V - velocity

$$\overline{AC} = ((r\sin\theta + s)^2 + r^2\cos^2\theta + d^2)^{1/2}$$

$$\overline{BC} = ((r\sin\theta - s)^2 + r^2\cos^2\theta + d^2)^{1/2}$$

$$\text{Delay time} = \frac{|\overline{AC} - \overline{BC}|}{V}$$

$$= \frac{|(r^2 + s^2 + d^2 + 2rs\sin\theta)^{1/2} - (r^2 + s^2 + d^2 - 2rs\sin\theta)^{1/2}|}{V}$$

Figure 7. Diagram of distance, depth, and azimuth relationships for two horizontally separated events. Calculations are for the delay time of the direct P arrivals.

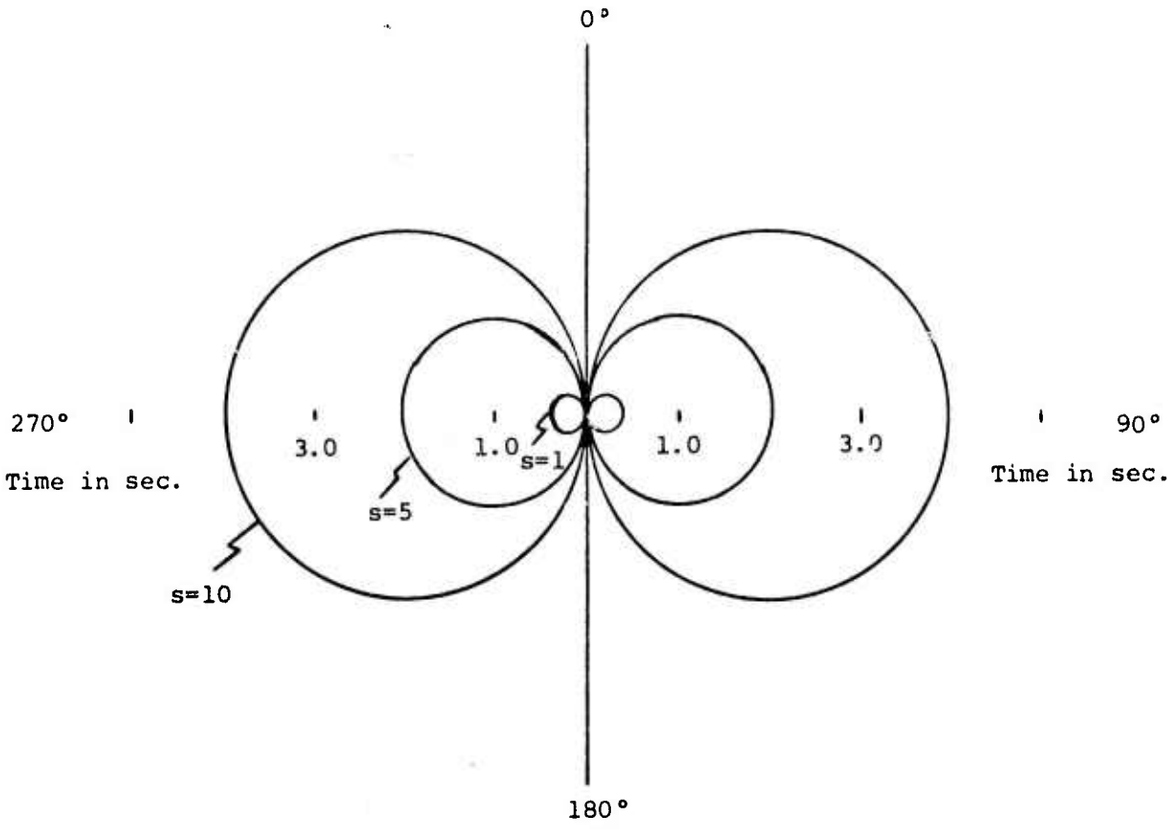

Figure 8. Three delay-azimuth plots for horizontally separated events. Depth of burial is .5 km. Velocity is 2.50 km/sec. Distances between events (s) are 1, 5, and 10 km.

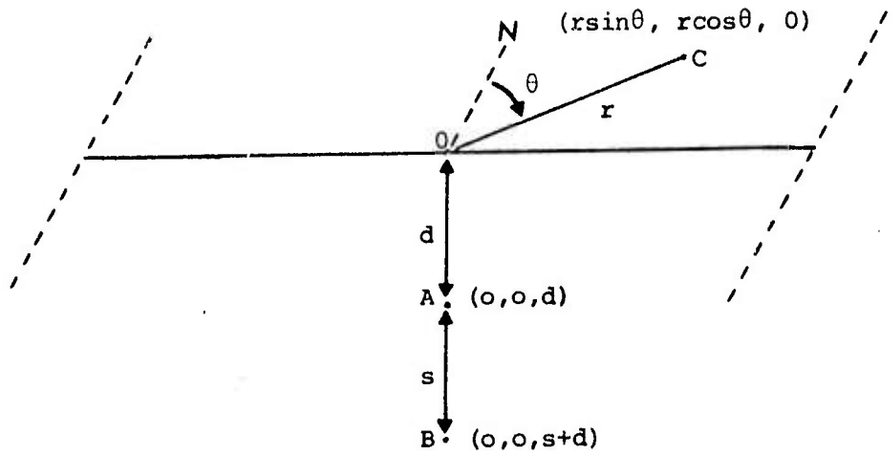

0 - Epicenter

A, B - Explosion points

C - Station on surface of earth

r - Distance to station

d - Depth of burial

s - Distance between events

θ - Azimuth

V - velocity

$$\overline{AC} = (r^2\sin^2\theta + r^2\cos^2\theta + d^2)^{1/2}$$

$$\overline{BC} = (r^2\sin^2\theta + r^2\cos^2\theta + (s + d)^2)^{1/2}$$

$$\text{Delay time} = \frac{|\overline{AC} - \overline{BC}|}{V} = \frac{|(r^2 + d^2)^{1/2} - (r^2 + (s + d)^2)^{1/2}|}{V}$$

Figure 9. Diagram of distance, depth, and azimuth relationships for two vertically separated events. Calculations are for the delay time of the direct P arrivals.

reasonable vertical separation of sources is a point at the origin.

pP-P

The pP phase of a shallow event is difficult or impossible to identify on a seismogram. The 1968 Seismological Tables for P phases lists a pP-P interval of 3.4 seconds for an event at distances of 2° to 13° and a depth of 15 kilometers. An increasing pP-P interval with increasing epicentral distance is indicated by the table listings. The station distances in this study range from 1° to 4° and the shot depths from .15 to .56 kilometer. The pP-P delay times for thirty-seven U.S. underground tests have been estimated by Springer (1974) from surface-zero accelerograms and range from .17 to 1.00 seconds. Table 1 is a listing of Springer's estimates. The three lowest estimates of .17, .21, and .24 seconds were for shots detonated in granite. The shot mediums in this study are alluvium and tuff, and the lowest estimates by Springer for shots in alluvium and tuff are .34 and .33 seconds, respectively.

Based upon the above information, the pP-P delay times for the shots in this study are expected to be within the .20 to 1.5 second range. The pP-P delay may be constant over the 1° to 4° epicentral distance range or an increasing pP-P delay with increasing distance is

possible. When the pP-P delay is constant over the epicentral distance range, the expected delay-distance plot for pP-P is a horizontal line, and the delay-azimuth plot is a circle with center at the origin. For the case of pP-P increasing with distance from the station, the delay-distance plot is a curve showing the increasing delay with distance, and the delay-azimuth plot is a circle with center at the origin for those stations of similar epicentral distance.

P_S-P

Surface material above an underground nuclear explosion is thrown upward by spallation, which is the parting of near-surface layers originally in contact (Eisler and Chilton, 1964). The parting is described by Springer (1974) as occurring when

> interference between the reflected tension wave and the incident compressive stress wave may produce a net tensile stress equal to the sum of lithostatic pressure (overburden) and tensile strength of the rock. Separation of the rock layers above this point occurs because some of the stress wave energy is imparted to the separated layers in the form of kinetic energy. That is, a layer of the earth separates and continues ballistically upward. The material eventually falls under the force of gravity and lands with a considerable shock.

The forcible landing of the spalled layers causes the slapdown phase. The occurrence of spallation depends upon the yield of the explosion and the depth of burial. Spallation would not occur for a very low yield explosion

or for an explosion buried at great depth. Also, no spallation would occur if an explosion was not contained.

The slapdown phase follows the P phase by the same interval at all stations. The P_S-P delay distance plot is a horizontal line, and the delay azimuth plot is a circle with center at the origin.

P_S-P delays of .87, 1.35, and 1.85 seconds were determined for the LONGSHOT, MILROW, and CANNIKIN nuclear explosions by King and others (1974) using a spectral ratio method. Springer (1974) estimated P_S-P delays from surface-zero accelerograms for twenty-seven U.S. underground explosions. His slapdown estimates range from .75 to 3.07 seconds and are listed in Table 1.

The differentiation of the secondary arrivals by their delay to distance and delay to azimuth relationships provide a possible method of determining the source characteristics of an event. The delay to distance and azimuth relationships for P, pP, and P_S are summarized in Figure 10. It is evident from the figure that when taken together the relationship of delay to distance and azimuth define the source type involved. Thus, it may be possible to use plots of this nature to differentiate the various source types if the interference of the P-coda is significantly low.

TABLE 1

Estimated Delay Times Determined from Surface-Zero Accelerograms (Modified from Springer, 1974, Table 1, p. 586; Springer and Kinnaman, 1971, Table 1, p. 1074)

Shot Name	Date	Depth of Burial (km)	pP-P (sec)	P_s-P (sec)
RAINIER	9/19/57	.25	0.33	0.75
GNOME	12/10/61	.36	0.36	1.32
HARD HAT	2/15/62	.29	0.17	-*
SHOAL	10/26/63	.37	0.21	0.90
SALMON	10/22/64	.83	0.58	-*
HANDCAR	11/05/64	.40	0.37	0.92
LONG SHOT	10/29/65	.70	0.45	1.76
DURYEA	4/14/66	.54	0.59	1.39
PILE DRIVER	6/02/66	.46	0.24	1.32
VULCAN	6/25/66	.32	0.41	-*
HALFBEAK	6/30/66	.82	0.72	2.93
NEW POINT	12/13/66	.24	0.35	-*
GREELEY	12/20/66	1.22	0.97	-*
AGILE	2/23/67	.73	0.83	-*
COMMODORE	5/20/67	.75	0.84	-*
SCOTCH	5/23/67	.98	0.91	1.73
LANPHER	10/18/67	.71	0.86	-*
GASBUGGY	12/10/67	1.29	0.87	1.17
HUPMOBILE	1/18/68	.25	0.34	0.99
FAULTLESS	1/19/68	.98	0.80	2.17
KNOX	2/21/68	.65	0.67	2.47
BOXCAR	4/26/68	1.16	0.96	3.07
NOGGIN	9/06/68	.58	0.75	2.92
				or 3.72
HUTCH	7/16/69	.55	0.59	1.92
JORUM	9/16/69	1.16	0.98	2.78
MILROW	10/02/69	1.22	0.74	2.49
CALABASH	10/29/69	.63	0.70	-*
HANDLEY	3/26/70	1.21	0.95	2.84
CARPETBAG	12/17/70	.66	0.67	2.31
HARBELL	6/24/71	.52	0.63	1.03
CATHAY	10/08/71	.38	0.54	1.02
CANNIKIN	11/06/71	1.79	1.00	-*
CHAENACTIS	12/14/71	.33	0.41	0.80
MONERO	5/19/72	.54	0.69	1.08
				or 1.25
DIAMOND SKULLS	7/20/72	.42	0.47	1.59
OSCURO	9/21/72	.56	0.69	2.12
DELPHINIUM	9/26/72	.30	0.40	0.90

* Data unavailable or nonexistent.

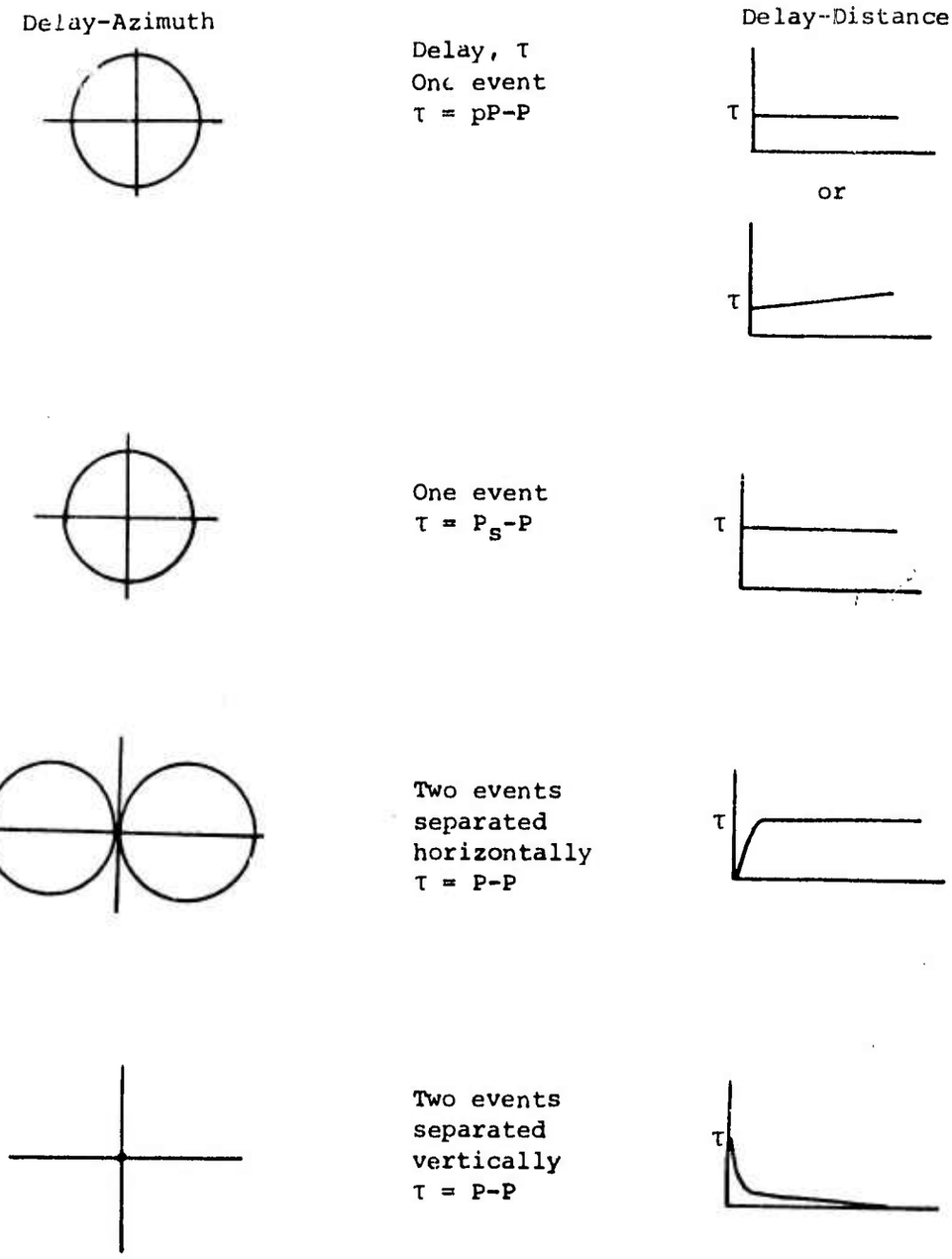

Figure 10. Summary of delay-distance and delay-azimuth relationships for P, pP, and P_S.

Method for the Detection of Multiple Arrivals

Cepstrum analysis was introduced by Bogert, Healy, and Tukey (1963) as a method for detecting the existence and timing of echoes. The authors defined the cepstrum as the spectrum of the spectrum of a time series. The method involves the application of two Fourier transforms to the data set.

The authors demonstrated the potential of applying time series techniques of spectral analysis to a series in the frequency domain. Using an artificial time series with an echo, the echo was detected by obtaining the Fourier amplitude spectrum of the series, determining the logarithm of the spectrum, and obtaining the Fourier amplitude spectrum of the logarithm of the spectrum. The logarithm of the spectrum is a frequency series and the Fourier transform of the frequency series yields a series in the time domain. This is essentially the spectrum of a spectrum and was termed the cepstrum. A peak in the cepstrum indicates the existence of an echo at the corresponding time in the original series.

For purposes of completeness and understanding, the original work of Bogert, Healy, and Tukey (1963) is outlined here. Consider a time series, $f(t)$, with echo to consist of $s(t)$ and $s(t)$ multiplied by a constant value a and delayed by time τ. The series with echo is given by

$$f(t) = s(t) + as(t - \tau). \tag{1}$$

The Fourier transform, F, of $f(t)$ is

$$F(\omega) = S(\omega)(1 + ae^{j\omega\tau}) \tag{2}$$

with the amplitude spectrum being

$$|F(\omega)| = |S(\omega)|(1 + 2a\cos\omega\tau + a^2)^{1/2}. \tag{3}$$

Taking the logarithm of the spectrum converts the multiplicative effect of the echo into an additive effect and yields

$$\log|F(\omega)| = \log|S(\omega)| + 1/2 \log(1 + 2a\cos\omega\tau + a^2). \tag{4}$$

Applying the log expansion,

$$\log(1 + X) = X - \frac{X^2}{2} + \frac{X^3}{3} \ldots \text{ where } -1<X\leq 1 \tag{5}$$

and assuming $a<1$ the expression may be reduced to

$$\log|F(\omega)| = \log|S(\omega)| + a\cos\omega\tau. \tag{6}$$

The log spectrum is a frequency series. The Fourier transform of the log spectrum, which converts the frequency series into the time domain, is given by

$$C(t) = F\log|S(\omega)| + a\delta(t - \tau). \tag{7}$$

The amplitude spectrum of C(t),

$$|C(t)| = |\mathcal{F}\log|S(\omega)|| + a|\delta(t - \tau)| \qquad (8)$$

is the cepstrum. The Fourier transform of the function $\cos\omega\tau$ is the delta function, $\delta(t - \tau)$, which has an amplitude of zero at all t except $t = \tau$, where its amplitude tends to infinity. Thus, a peak occurs in the cepstrum at time $t = \tau$, as a result of the echo in the original series which was delayed by time τ.

The condition requiring a to be less than 1 was satisfied when applying cepstrum analysis to the detection of echoes, since the amplitude of an echo is normally less than the amplitude of the first arrival. The $a<1$ condition is also valid for the detection of reflected phases from an earthquake or single nuclear event for the same reason. An a value greater than 1 is possible when applying cepstrum analysis to the detection of a multiple nuclear event. The second direct P arrival from a multiple event may have an amplitude on the order of, or greater than, the amplitude of the first direct P.

A logarithm expansion which allows a to be greater than 1 is

$$\log X = \log b + \frac{(x - b)}{b} - \frac{(x - b)^2}{2b^2} + \frac{(x - b)^3}{3b^3} \ldots. \qquad (9)$$

where $0<X\leq 2b$.

Letting $x = 1 + 2a\cos\omega\tau + a^2$ and $b = 1 + a^2$ and applying this expansion when taking the logarithm of the spectra

and disregarding second order terms, the expression for the log spectrum becomes

$$\log|F(\omega)| = \log|S(\omega)| + 1/2 \log(1 + a^2) + \frac{a}{1 + a^2} \cos\omega\tau \quad (10)$$

The Fourier transform of the log spectrum is

$$C(t) = F(\log|S(\omega)| + 1/2 \log(1 + a^2)) + \frac{a}{1 + a^2} \delta(t - \tau) \quad (11)$$

and the amplitude spectrum, which is the cepstrum is

$$|C(t)| = |F(\log|S(\omega)| + 1/2 \log(1 + a^2))| + \frac{a}{1 + a^2}|\delta(t - \tau)|. \quad (12)$$

Except for constant terms and scaling factors this is equivalent to the original expression and would produce an amplitude peak at time τ. Cepstrum analysis can therefore be expected to detect a secondary arrival stronger than the first arrival.

While cepstrum analysis has received some application in the simple detection of secondary arrivals, it does not appear that anyone has attempted the recovery of the a scaling factor (Flinn and others, 1973; Cohen, 1970). Knowledge of a would be useful in differentiating the secondary arrivals. King and others (1974) estimated the

amplitude of the pP and P_S phases of the LONGSHOT, MILROW, and CANNIKIN explosions to be .3-.5 times the corresponding direct P amplitudes. If the a factor could be recovered for the secondary arrivals, any values of $a \geq 1$ would clearly suggest the arrival of a second direct P from a multiple source.

From the expression for the cepstrum, equation (12), the value of the peak in the cepstrum at time $t = \tau$ is

$$P = |C(t)| - |F(\log|S(\omega)| + 1/2 \log(1 + a^2))| = \frac{a}{1 + a^2}|\delta(t - \tau)|. \tag{13}$$

In digital applications the amplitude of $\delta(t - \tau)$ has a finite value which may be denoted $|\delta(t - \tau)|c$. Letting

$$Q = \frac{P}{|\delta(t - \tau)|c} = \frac{a}{1 + a^2} \tag{14}$$

then

$$Qa^2 - a + Q = 0, \tag{15}$$

and solving for a yields

$$a = \frac{1 \pm \sqrt{1 - 4Q^2}}{2Q}. \tag{16}$$

Designating the roots of the equation as a_1 and a_2, it can be shown that $a_1 = \frac{1}{a_2}$. The reciprocal property of the roots limits the usefulness of the recovered a values.

A value of a in the range $.8<a<1.25$ may aid in differentiation of a second direct P from other secondary arrivals. Values of a outside of this range will be useful only if other information about the secondary arrivals is available.

The theoretical basis for cepstrum analysis and the recovery of a discussed above involve only a single secondary arrival. To extend the theoretical base to include three secondary arrivals consider a signal

$$f(t) = s(t) + a_1 s(t - \tau_1) + a_2 s(t - \tau_2) + a_3 s(t - \tau_3) \quad (17)$$

where $\tau_1<\tau_2<\tau_3$.

The Fourier transform is

$$F(\omega) = S(\omega)(1 + a_1 e^{j\omega\tau_1} + a_2 e^{j\omega\tau_2} + a_3 e^{j\omega\tau_3}) \quad (18)$$

and the amplitude spectrum is

$$|F(\omega)| = |S(\omega)|(1 + a_1^2 + a_2^2 + a_3^2 + 2a_1\cos\omega\tau_1 + 2a_2\cos\omega\tau_2 + 2a_3\cos\omega\tau_3 + 2a_1a_2\cos\omega(\tau_1 - \tau_2) + 2a_1a_3\cos\omega(\tau_1 - \tau_3) + 2a_2a_3\cos\omega(\tau_2 - \tau_3))^{1/2}. \quad (19)$$

The expression for the log spectrum is

$$\log|F(\omega)| = \log|S(\omega)| + 1/2\ \log(1 + a_1^2 + a_2^2 + a_3^2 + 2a_1\cos\omega\tau_1 + 2a_2\cos\omega\tau_2 + 2a_3\cos\omega\tau_3 + 2a_1a_2\cos\omega(\tau_1 - \tau_2) + 2a_1a_3\cos\omega(\tau_1 - \tau_3) + 2a_2a_3\cos\omega(\tau_2 - \tau_3)). \quad (20)$$

Applying the log expansion,

$$\log|F(\omega)| = \log|S(\omega)| + 1/2 \log(1 + a_1^2 + a_2^2 + a_3^2)$$
$$+ \frac{1}{1 + a_1^2 + a_2^2 + a_3^2}(a_1\cos\omega\tau_1 + a_2\cos\omega\tau_2 + a_3\cos\omega\tau_3$$
$$+ a_1a_2\cos\omega(\tau_1 - \tau_2) + a_1a_3\cos\omega(\tau_1 - \tau_3) \qquad (21)$$
$$+ a_2a_3\cos\omega(\tau_2 - \tau_2)),$$

yielding as the cepstrum

$$|C(t)| = |F(\log|S(\omega)| + 1/2 \log(1 + a_1^2 + a_2^2 + a_3^2)|$$
$$+ \frac{1}{1 + a_1^2 + a_2^2 + a_3^2}(a_1|\delta(t - \tau_1)| + a_2|\delta(t - \tau_2)|$$
$$+ a_3|\delta(t - \tau_3)| + a_1a_2|\delta(t - (\tau_1 - \tau_2))| \qquad (22)$$
$$+ a_1a_3|\delta(t - (\tau_1 - \tau_3))| + a_2a_3|\delta(t - (\tau_2 - \tau_3))|.$$

It is evident that the cepstrum will become more complex with the addition of more secondary arrivals. The peaks occurring at $\tau_2 - \tau_1$, $\tau_3 - \tau_1$, and $\tau_3 - \tau_2$ may make interpretation of the cepstrum more difficult. This will be true especially in the case of a multiple event where one of the factors a_1, a_2, or a_3 could have a value greater than 1. It is also evident that with the addition of a number of secondary arrivals it is not possible to determine the actual value of a for a particular secondary arrival from a single record.

Data Sources

Seismograms of selected Nevada Test Site events were obtained from Lawrence Livermore Laboratories and Sandia Laboratories. Seismograms of the Massachusetts Mountain earthquake, which occurred within the Nevada Test Site, were obtained from Lawrence Livermore Laboratories (Rohrer and Springer, 1972; Fisher and others, 1972). Records of other earthquakes occurring within or near the Nevada Test Site and thus having propagation paths similar to the nuclear events, were requested but were not available.

The location of the Nevada Test Site, the Lawrence Livermore stations, and the Sandia stations are shown in Figure 11. ELK, KNB, LAC, and MNV are Lawrence Livermore stations, and BMN, DAC, ELY, LEE, NEL, and TPH are Sandia stations. Table 2 is a listing of the stations and their locations. The station coverage with respect to Nevada Test Site is illustrated in Figure 12.

The nuclear explosion records obtained for analysis include a multiple event, BLENTON/THISTLE, a single event, DIDO QUEEN, and five events A through E of unknown nature. Information relating to BLENTON/THISTLE and DIDO QUEEN is given in Table 3. Table 4 is a listing of the depth of burial and shot medium for the events of unknown nature. Typical records of the events analyzed are displayed in Appendix A.

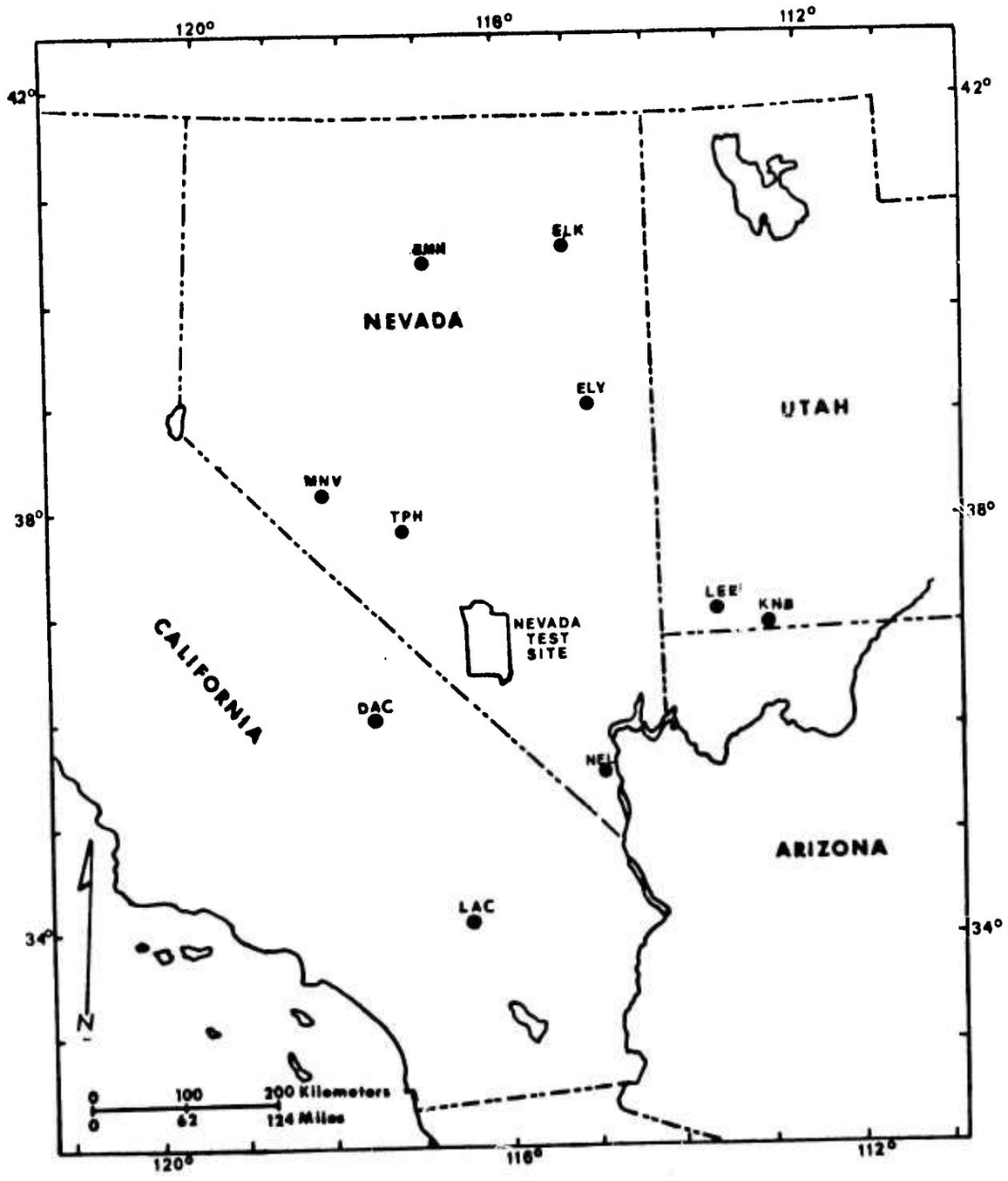

Figure 11. Location of Nevada Test Site and Lawrence Livermore (ELK, KNB, MNV, and LAC) and Sandia (BMN, DAC, ELY, LEE, NEL, and TPH) stations.

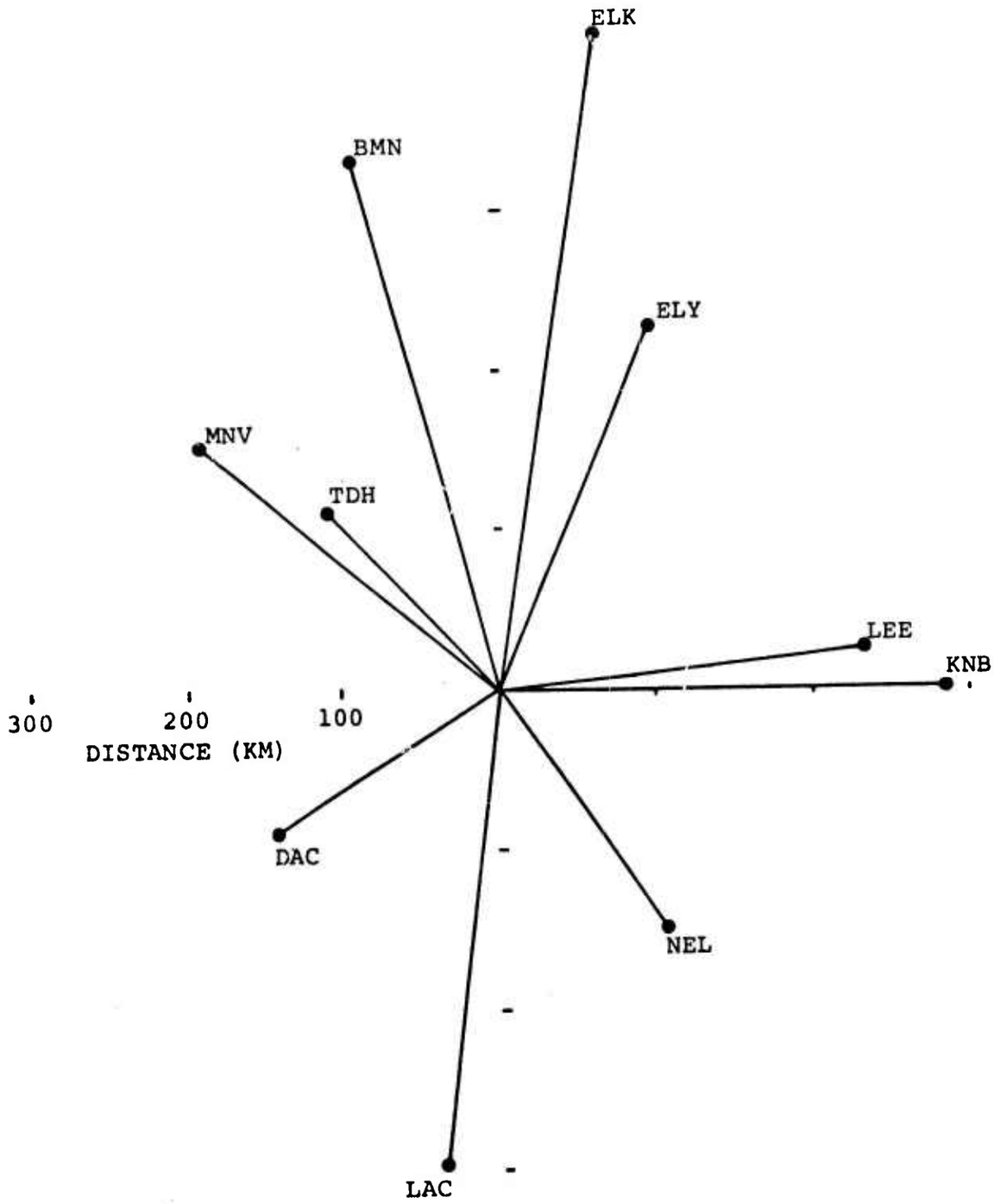

Figure 12. Station coverage of Nevada Test Site. Distance and azimuth stations with respect to the Nevada Test Site.

TABLE 2

Seismic Stations

Code	Station	Latitude	Longitude
BMN	Battle Mountain, Nev.	40°25'53.3"N	117°13'18.4"W
DAC	Darwin, California	36°16'37.2"N	117°35'37.2"W
ELK	Elko, Nevada	40°44'41.4"N	115°14'19.6"W
ELY	Ely, Nevada	39°07'52.8"N	114°53'31.2"W
KNB	Kanab, Utah	37°00'59.8"N	112°49'20.7"W
LAC	Landers, California	34°23'23.2"N	116°24'41.4"W
LEE	Leeds, Utah	37°14'34.8"N	113°22'36.0"W
MNV	Mina, Nevada	38°25'56.0"N	118°09'15.8"W
NEL	Nelson, Nevada	35°42'44.0"N	114°50'37.0"W
TPH	Tonopah, Nevada	38°04'29.0"N	117°13'21.0"W

TABLE 3

BLENTON/THISTLE and DIDO QUEEN Data

	BLENTON	THISTLE	DIDO QUEEN
Date	4/30/69	4/30/69	6/5/73
Shot Time	1700:00.04	1700:00.04	1700:00.00
Location	37°04'53.4"N 116°00'50.2"W	37°05'25.0"N 116°00'20.3"W	37°11'06.1"N 116°12'54.1"W
Depth of Burial	.56 km	.56 km	.39 km
Shot Medium	Tuff	Tuff	Tuff

TABLE 4

Depth and Shot Medium for Events A-E

Event	Depth	Shot Medium
A	.24 km	Alluvium
B	.56 km	Tuff
C	.31 km	Tuff
D	.44 km	Tuff
E	.39 km	Alluvium

Geologic Setting

Nevada, southeastern California, and western Utah lie within the Basin and Range province described by Thornbury (1965). This province is characterized by north-south trending mountain ranges and intermontane basins formed as a result of block faulting. The Basin and Range province is bounded on the west by the Sierra Nevada and on the east by the Colorado Plateau. The physiographic provinces of the Nevada, California, and Utah area are outlined in Figure 13.

The Nevada Test Site is located in a structurally complex, highly faulted segment of the Basin and Range province. The geologic and physiographic features of the Nevada Test Site and surrounding area are shown in Figure 14. The test site is approximately fifty miles east of the Cordilleran eugeosyncline eastern boundary and about one hundred miles west of the miogeosyncline eastern boundary. The area is also north and east of the Las Vegas Valley-Walker Lane shear zone.

The events analyzed in this study were detonated in the Yucca Flats area of the Nevada Test Site, and the epicenter of the Massachusetts Mountain earthquake was located in the southern part of this area. A generalized geologic map of the Yucca Flats area with the location of the earthquake epicenter and the area in which the nuclear events were detonated are given in Figure 15. Upper

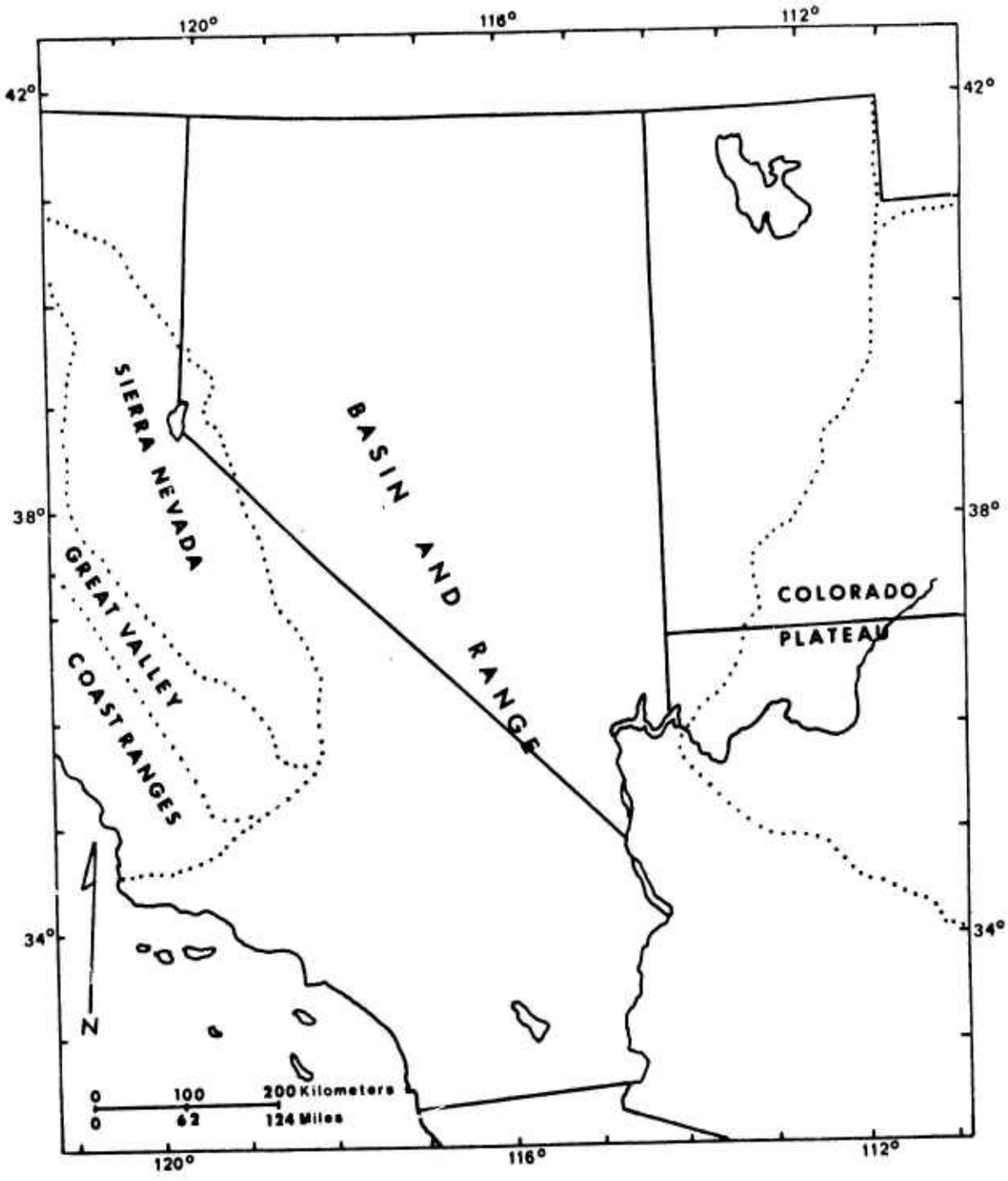

Figure 13. Physiographic provinces of the Nevada, California, and Utah area (modified from Lobeck, 1957).

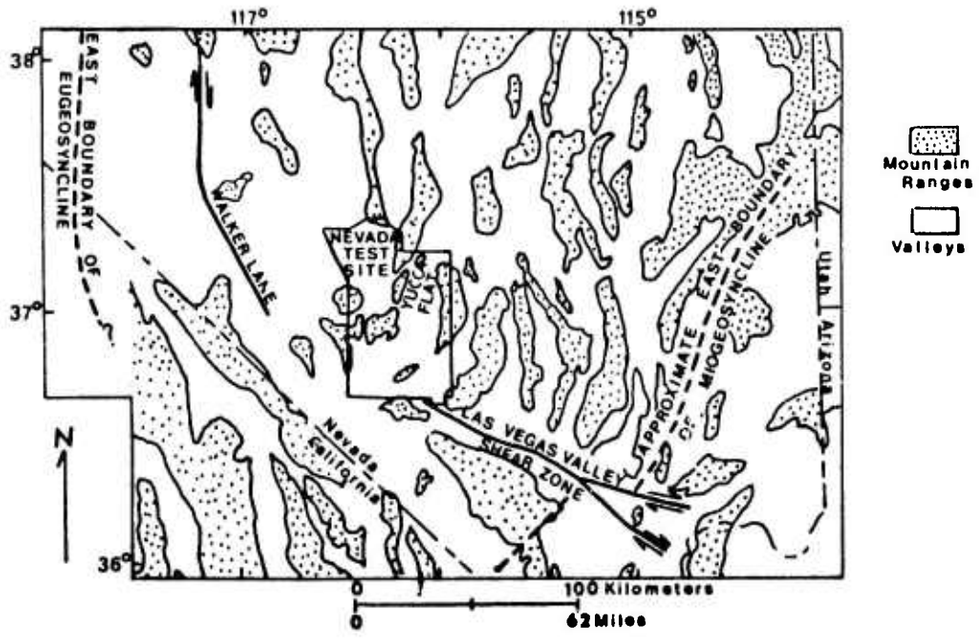

Figure 14. Index map of the geologic and physiographic features of the Nevada Test Site and surrounding area (modified from Ekren, 1968, p. 12).

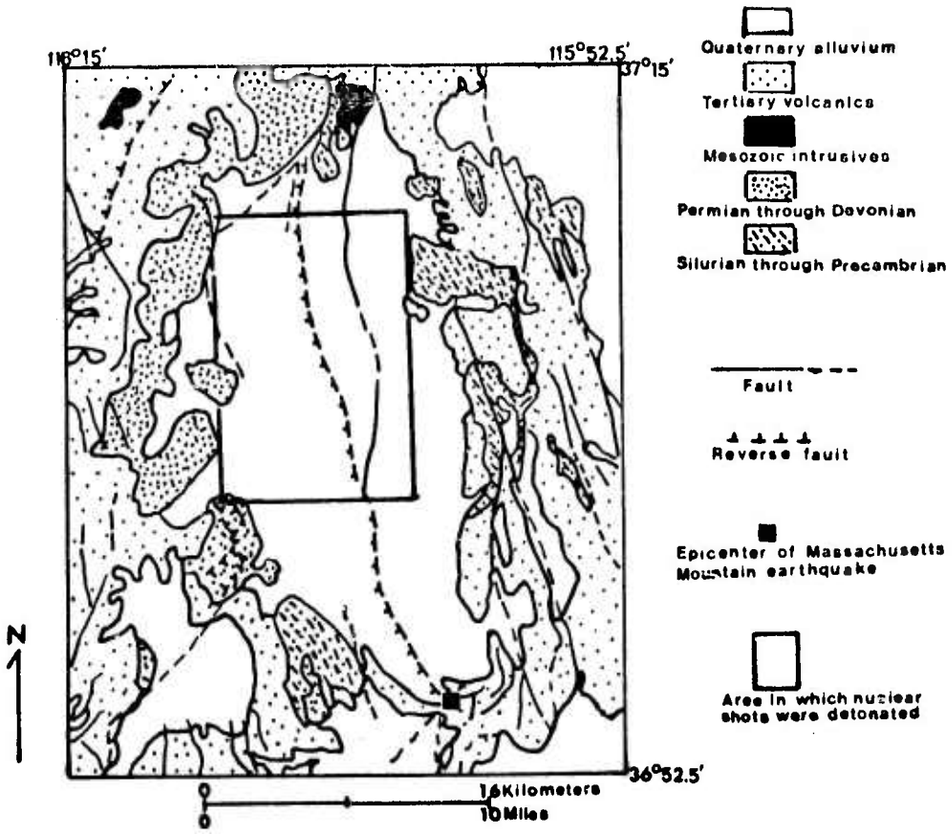

Figure 15. Generalized geologic map of Yucca Flats area with epicenter of Massachusetts Mt. earthquake and area in which nuclear events were detonated (modified from Hinrichs, 1968, p. 242).

Precambrian and Paleozoic sedimentary rocks, Mesozoic intrusives, Tertiary volcanics, and Quaternary alluvium are exposed in the area. Quartzite is the major lithology of the Upper Precambrian and lower part of the Cambrian. The remaining portion of the Paleozoic is composed of carbonates, conglomerates, quartzites, and shales. Granitic intrusives are the only Mesozoic rocks in the area. Tertiary rocks consist mainly of rhyolitic tuffs. The total thickness of the Yucca Flats stratigraphic section is 44,500 feet and is divided as follows: Precambrian and Paleozoic rocks 38,800 feet; Tertiary rocks 3,700 feet; and Quaternary sediments 2,000 feet (Hinrichs, 1968).

DIGITAL ANALYSIS

The seismograms were prepared for computer processing by digitizing the records using a Computer Equipment Corporation Digitizer. A FORTRAN program written by Taylor (1974) was used to obtain the cepstra and a listing is provided in Appendix B. The program digitally performs the following operations on the input data:

1. Interpolation of data at equal increments.
2. Normalized autocorrelation.
3. Calculation of Fourier transform.
4. Calculation of amplitude spectra.
5. Determination of log spectra.
6. Normalized autocorrelation.
7. Calculation of Fourier transform.
8. Calculation of amplitude spectra, which is the cepstrum.

An example of the results of the different operations performed to obtain a cepstrum is shown in Figures 16 through 19. The normalized autocorrelation, the amplitude spectrum, the log spectrum, the normalized autocorrelation of the log spectrum, and the cepstrum are given for the BLENTON/THISTLE event recorded at the KNB station.

The input data were interpolated at an increment of .05 second. This increment, or Δt, was adequate to satisfy the Sampling Theorem

$$\Delta t < \frac{1}{2f_n} \qquad \text{(Huang, 1966)} \qquad (23)$$

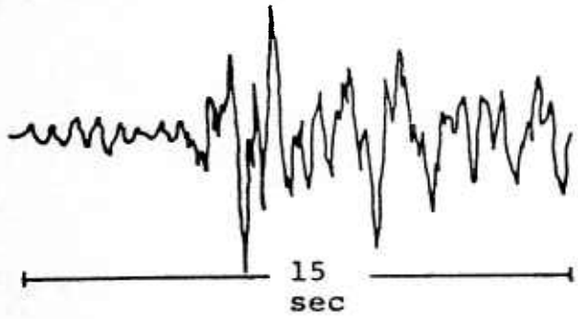

a)

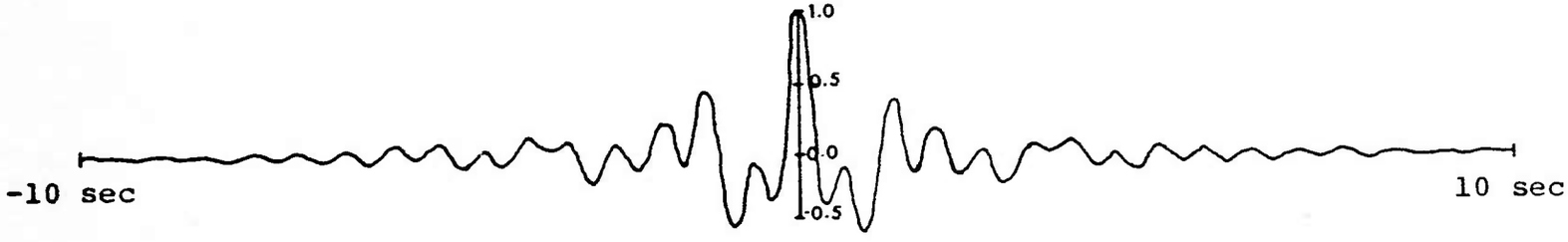

b)

Figure 16. a) Seismogram of BLENTON/THISTLE event recorded at KNB station.
b) Normalized autocorrelation of 10 seconds of the BLENTON/THISTLE signal recorded at KNB. Correlation coefficients on the vertical scale.

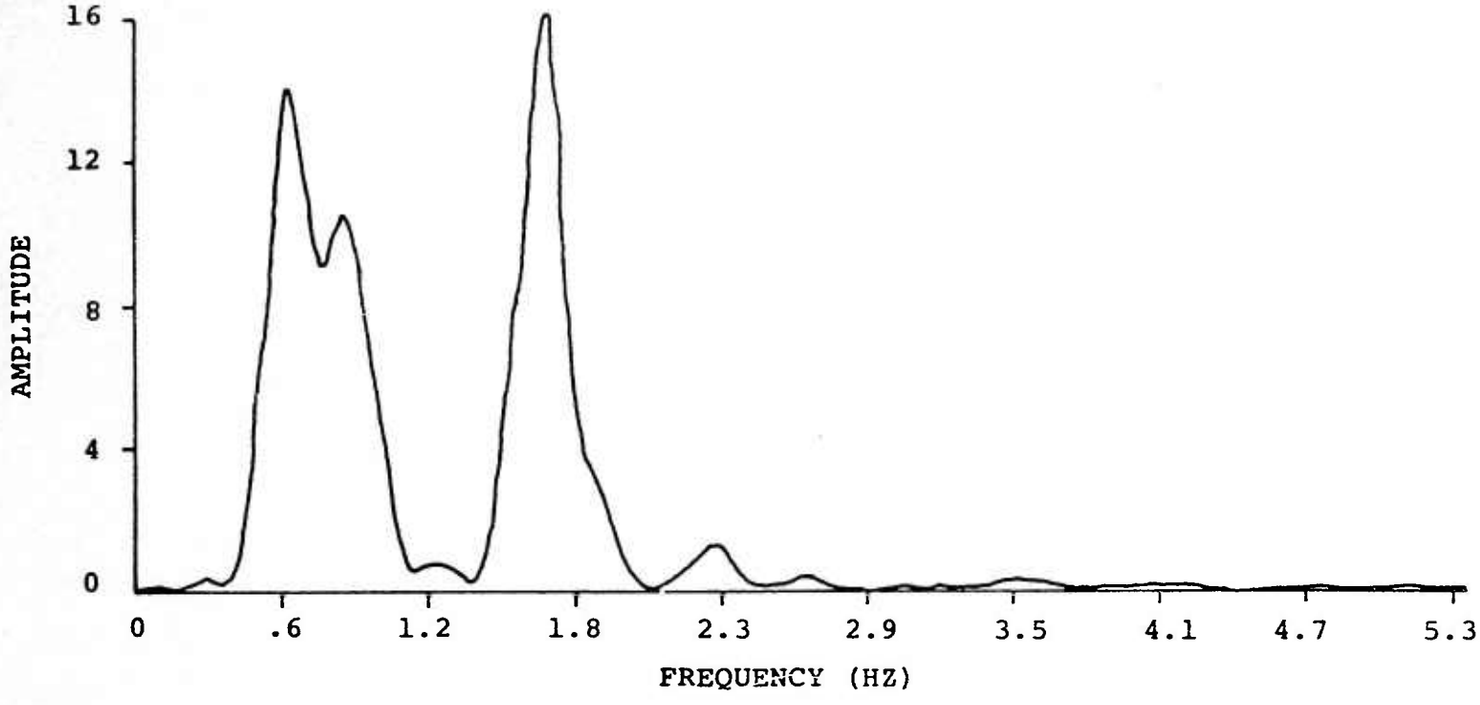

Figure 17. Amplitude spectrum of BLENTON/THISTLE event - KNB station.

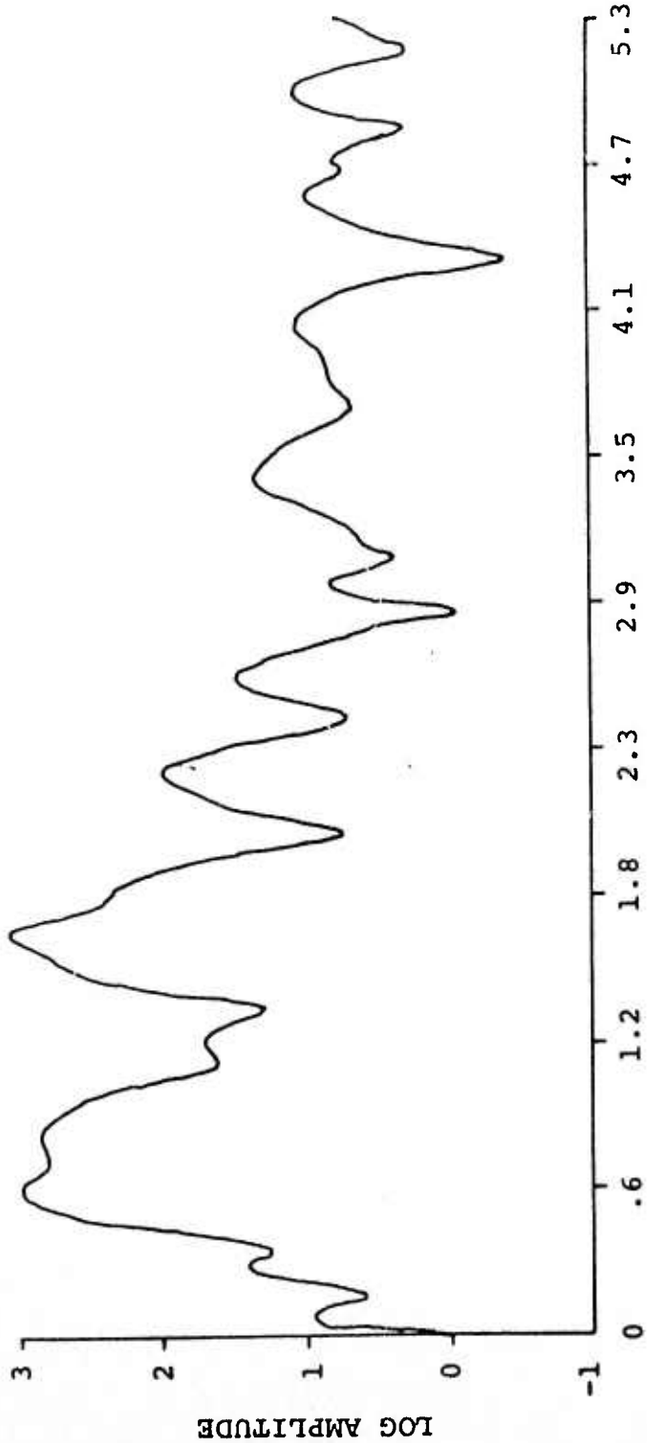

Figure 18. Log spectrum of BLENTON/THISTLE event - KNB station.

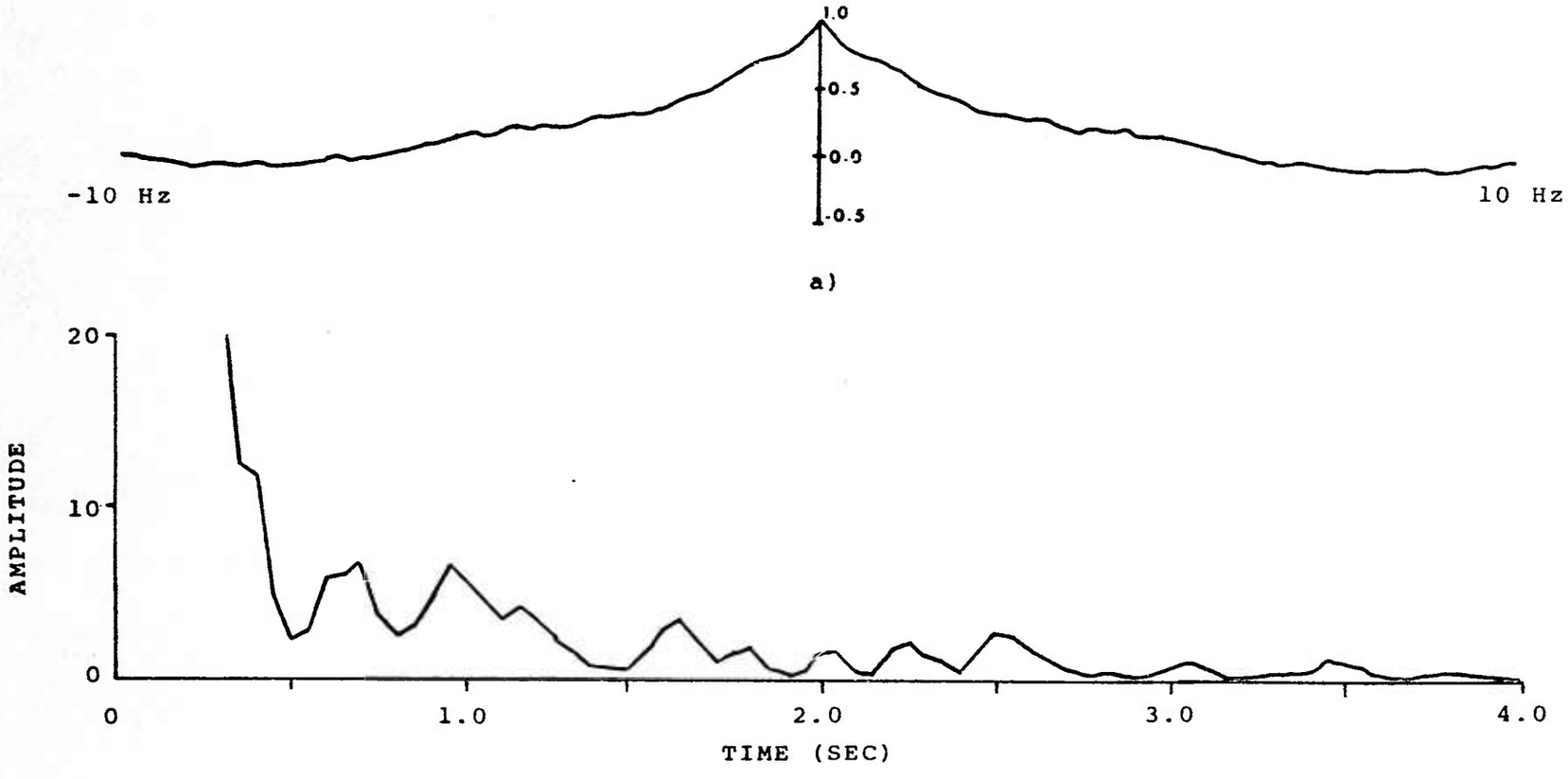

Figure 19. a) Normalized autocorrelation of log spectra of BLENTON/THISTLE recorded at KNB. Correlation coefficient on the vertical scale.
b) Cepstrum of BLENTON/THISTLE recorded at KNB.

where f_n is the maximum frequency present in the signal. The Nyquist or folding frequency is then

$$f_N = \frac{1}{2\Delta t} = 10 \text{ Hz} \tag{24}$$

or

$$\omega_N = 2\pi f_N = 62.8 \text{ radians/sec.} \tag{25}$$

The values of a Fourier transform computed digitally differ from the true transform values by a factor of Δt. With the application of two transforms to the data, the computer cepstrum values differ from the true cepstrum values by a factor of $\Delta\omega$, the frequency increment. The values of the Fourier transform and the transform of the transform were digitally computed using 2048 points. The value of the frequency increment is

$$\Delta\omega = \frac{2\pi}{2048\Delta t} = .0614 \text{ radians/sec.} \tag{26}$$

Denoting the true cepstrum value as C and the computer value as Cc,

$$C = \Delta\omega Cc. \tag{27}$$

The normalized autocorrelation which was performed on the data introduces a normalization factor into the computation for the true cepstrum value, and it is also necessary to take the square root of the computer value because of the property that the Fourier transform of an autocorrelation

equals the square of the amplitude. A final factor to be accounted for is that in the determination of the log spectra, the logarithm to the base 10 was used, but the logarithm expansion of equation (9) holds for the logarithm to the base e. Thus, the computer values must be multiplied by a factor of 2.3. The expression for the true cepstrum values then becomes

$$C = 2.3\Delta\omega\sqrt{NF}\ \sqrt{Cc} \tag{28}$$

where NF is the normalized factor.

The value of a peak in the cepstrum is the difference between two of the true cepstrum values. Equation (14) then becomes

$$Q = \frac{P}{|\delta(t-\tau)|c} = \frac{2.3\Delta\omega\sqrt{NF}(\sqrt{Cc_2} - \sqrt{Cc_1})}{|\delta(t-\tau)|c} = \frac{a}{1+a^2} \tag{29}$$

The amplitude of the delta function is 31.4 and can be obtained by evaluating the integral

$$\int_0^{62.8} (\cos\omega\tau)e^{j\omega t}d\omega \simeq \int_0^{62.8} \cos\omega\tau\cos\omega t d\omega. \tag{30}$$

The imaginary part of the above integral is insignificant in comparison to the real part. The equation for Q then becomes

$$Q = .0045\sqrt{NF}(\sqrt{Cc_2} - \sqrt{Cc_1}) = \frac{a}{1+a^2}, \tag{31}$$

The factors necessary in the calculations for the a scaling factor were not completely understood until the majority of the data had been processed. It was not possible to reprocess data to obtain the normalization factors. The a factors were only computed for the artificial double events created using the DIDO QUEEN records.

Results and Discussion

It has been observationally established that significant energy will follow the arrival of any P wave, and this following energy has been termed the P wave coda. Secondary arrivals will appear within the coda and suffer from the coda's contaminating influence. In addition, the digital spectra of the initial P arrival will exhibit effects due to contamination of the coda. Therefore, in the absence of any well defined secondary arrivals, variations in the cepstra are to be expected. The ambiguity in interpretation resulting from these peaks will depend upon the degree to which the secondary arrival peaks exceed the extraneous peaks. Greenfield (1969) measured coda power levels on the order of 0.1-1.0 of the primary P levels. The figure provided by Greenfield actually indicates power level ratios on the order of 0.01-0.1, but it appears that an error exists in the labeling of the figure. Ratios on the order of 0.1-1.0 would be exactly the same order as that expected for actual secondary arrivals. Thus, the identification of peaks relating to secondary arrivals may be difficult, and may prove to be somewhat subjective.

In addition to the problem of extraneous peaks it is necessary to consider the problem of what time domain window length to select for the processing of the data. A window length too short would eliminate desired second

arrivals, and a window length too long would pass additional contaminating energy with no increase in desired signal. It does not appear that any theoretical basis for selection of an optimum window length exists. Lacking a theoretical basis, the effects of window length are investigated in the following section.

Effects of Time Domain Window Length

The combination event BLENTON/THISTLE provides an ideal example for the study of window length effects. As previously noted, the event is known to be a simple horizontal dipole and the records of the event should contain a second arrival from the more distant event. Analysis of this event will also provide an indication of the magnitude associated with cepstral peaks.

Cepstra were generated for 8, 10, 15, and 20 second windows for the recordings at DAC and KNB. The results are shown in Figures 20 and 21. The peaks of the DAC cepstra are consistent for the different window lengths. The peaks of the KNB cepstra are consistent in the beginning two seconds, with some of the peaks in the 15 and 20 second windows becoming less pronounced. It also appears that as the window length of the KNB cepstra is increased more peaks occur beyond 2 seconds.

On the basis of these results a window length of 10 sec was selected as the optimum window. A careful study

Figure 20. Effect of window length on cepstra of BLENTON/THISTLE event. Window lengths of 8, 10, and 15 seconds for signal recorded at KNB and DAC.

Figure 20.

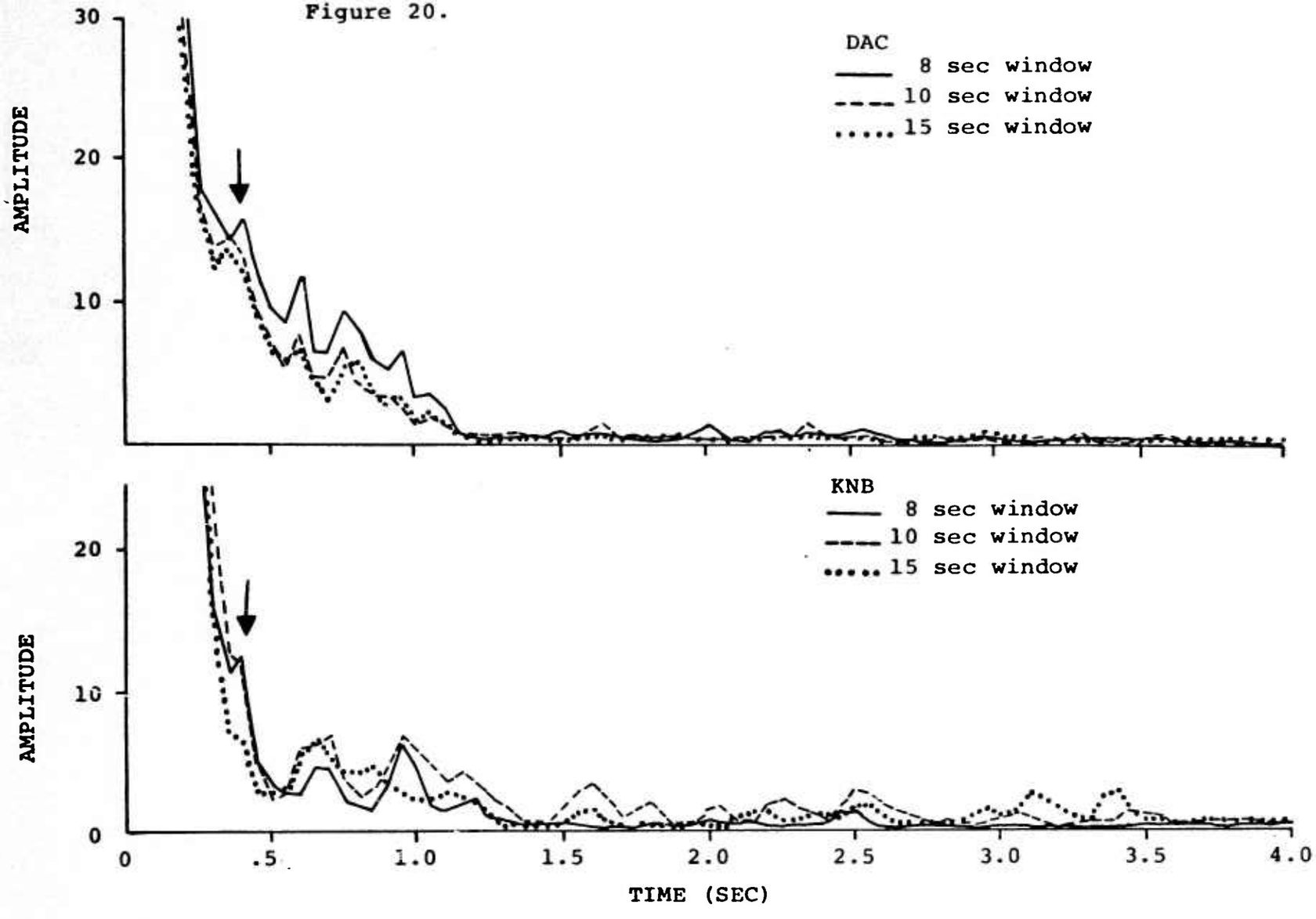
DAC
8 sec window
10 sec window
15 sec window
AMPLITUDE
30
20
10
KNB
8 sec window
10 sec window
15 sec window
AMPLITUDE
20
10
0
0
.5
1.0
1.5
2.0
2.5
3.0
3.5
4.0
TIME (SEC)

Figure 21. Effect of window length on cepstra of BLENTON/THISTLE event. Window lengths of 15 and 20 seconds for signal recorded at KNB and DAC.

Figure 21.

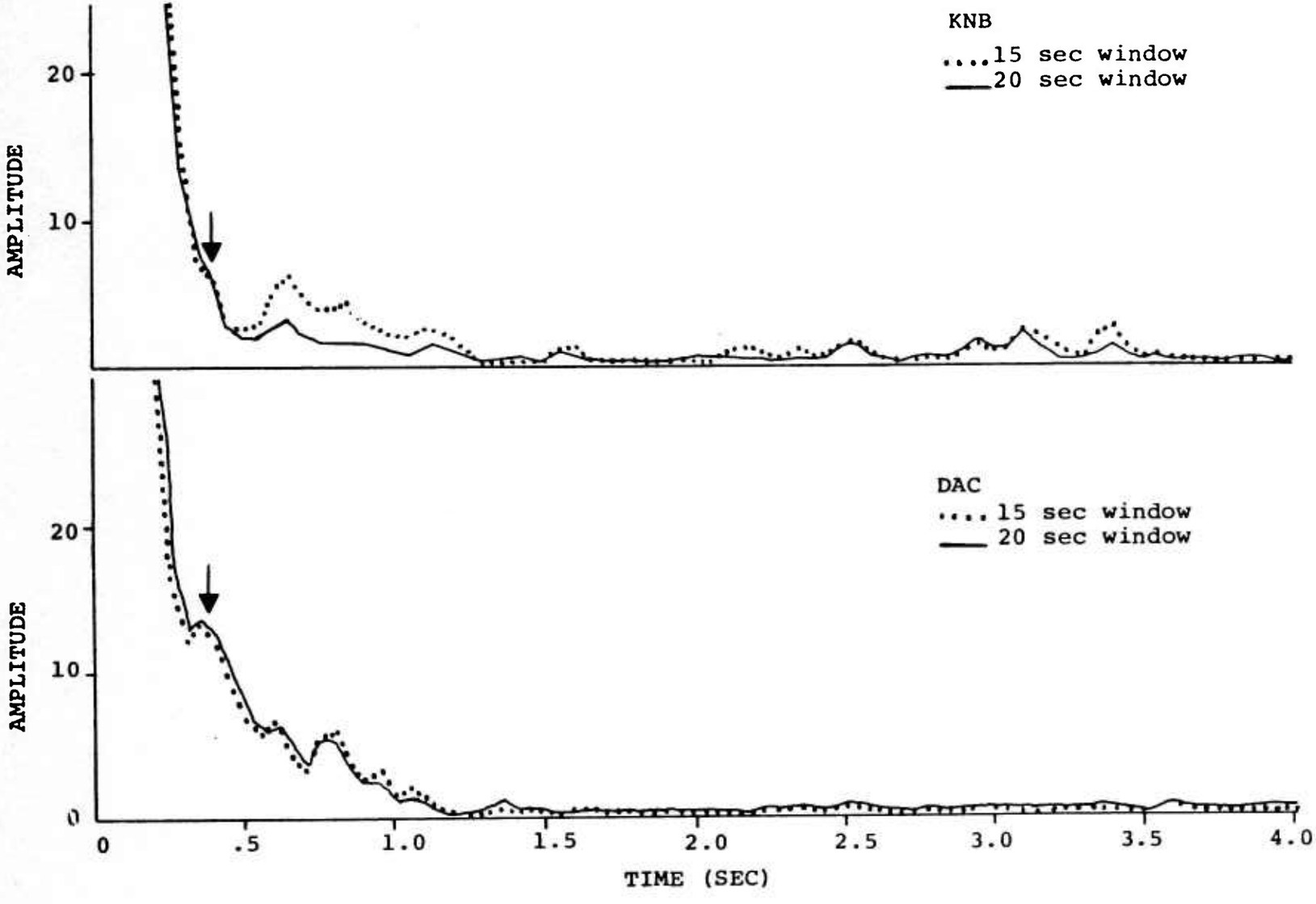
KNB
....15 sec window
____20 sec window
AMPLITUDE
20
10
DAC
.... 15 sec window
____ 20 sec window
AMPLITUDE
20
10
0
0
.5
1.0
1.5
2.0
2.5
3.0
3.5
4.0
TIME (SEC)

of Figure 20 would suggest that an 8 second window is more nearly optimum. It is not expected that such minor changes in window length can greatly affect the final results. The data in this study was, therefore, processed using a window length of 10 seconds. The information contained in the first 10 seconds of a signal was considered sufficient since the secondary arrivals of interest are expected to occur in the first 3 seconds of the record.

In addition to the effects of window length, Figures 20 and 21 indicate the problems that were previously anticipated in the identification of cepstral peaks. While the relative yields of the two events is not known, the expected arrival time of the second can be calculated and is indicated by the vertical arrows. It is evident that in all cases a peak does exist but in no case is it a pronounced peak.

Results from a Single Event (DIDO QUEEN) and an Artificially Created Double Event

Cepstrum analysis was applied to two records of the single event DIDO QUEEN. There were not enough records of processing quality available to analyze delay-distance and delay-azimuth relationships. The cepstra of DIDO QUEEN calculated from recordings at DAC and LEE are shown in Figure 22. Peaks occur in the DAC cepstrum at .70,

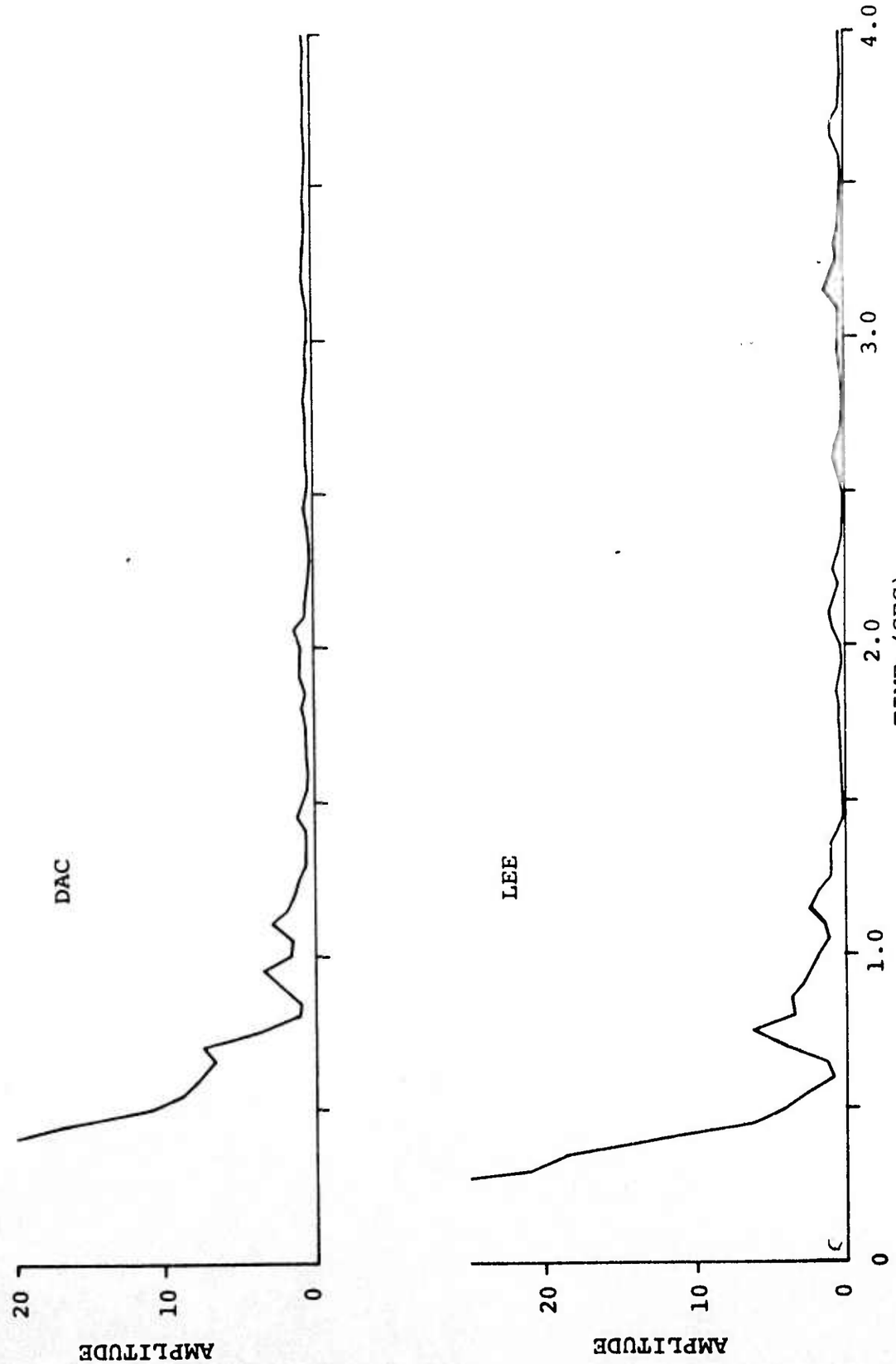

Figure 22. DIDO QUEEN cepstra for DAC and LEE.

.95, and 1.10 seconds and in the LEE cepstrum at .75 and 1.15 seconds. The peaks occurring at .70 and .75 seconds could be associated with the arrival of pP, but more records are needed to make a firm determination.

The DIDO QUEEN records were used to artificially create the record of a double event. An a value and a delay time value were chosen, the digitized signal was multiplied by a, delayed by the time value, and then added to the original digitized input to artificially create the signal for a double event. Cepstra of the artificially created double event were determined for various a and delay values. The LEE cepstra are shown in Figure 23 and the DAC cepstra in Figure 24. The peaks for the artificially created second direct P occur at the chosen delay time or .05 seconds later.

The a values for the artificial second direct P were computed using equation (31) and compared with the a value used in creating the artificial signal. Table 5 is a listing of the actual a values and the computed a values.

It is evident from Table 5 that the formula developed for the calculation of a is valid, although the percent error varies from 37% high to 32% low. A major contribution to the error percentage probably results from the various data smoothing operations included in the cepstral program. It does not appear that the effects of these

Figure 23. Cepstra for artificially created double event using DIDO QUEEN record at DAC.

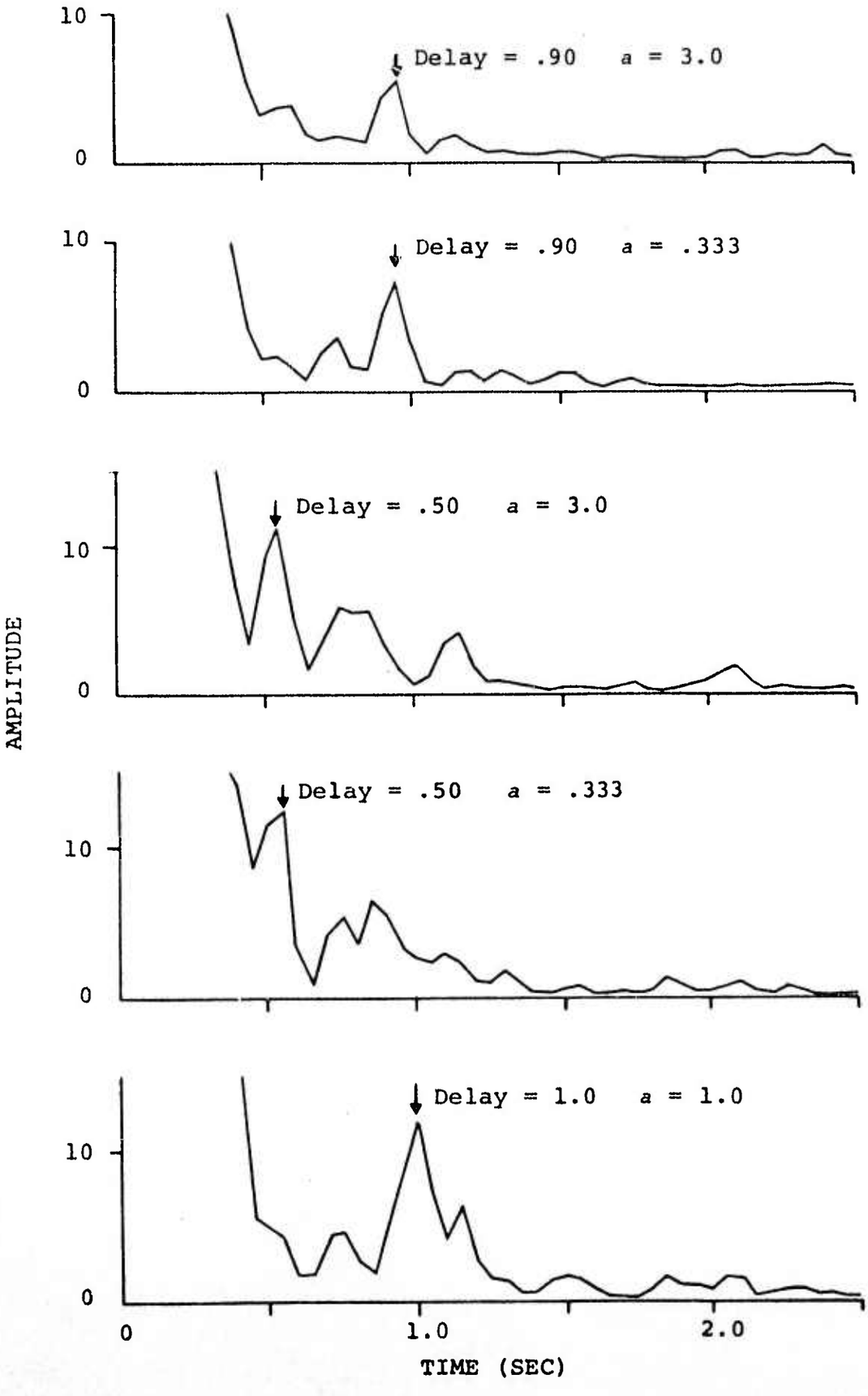
10
0
Delay = .90 a = 3.0
10
0
Delay = .90 a = .333
10
0
Delay = .50 a = 3.0
10
0
Delay = .50 a = .333
10
0
Delay = 1.0 a = 1.0
10
0
0
1.0
2.0
TIME (SEC)
AMPLITUDE

Figure 24. Cepstra for artificially created double event using DIDO QUEEN record at DAC.

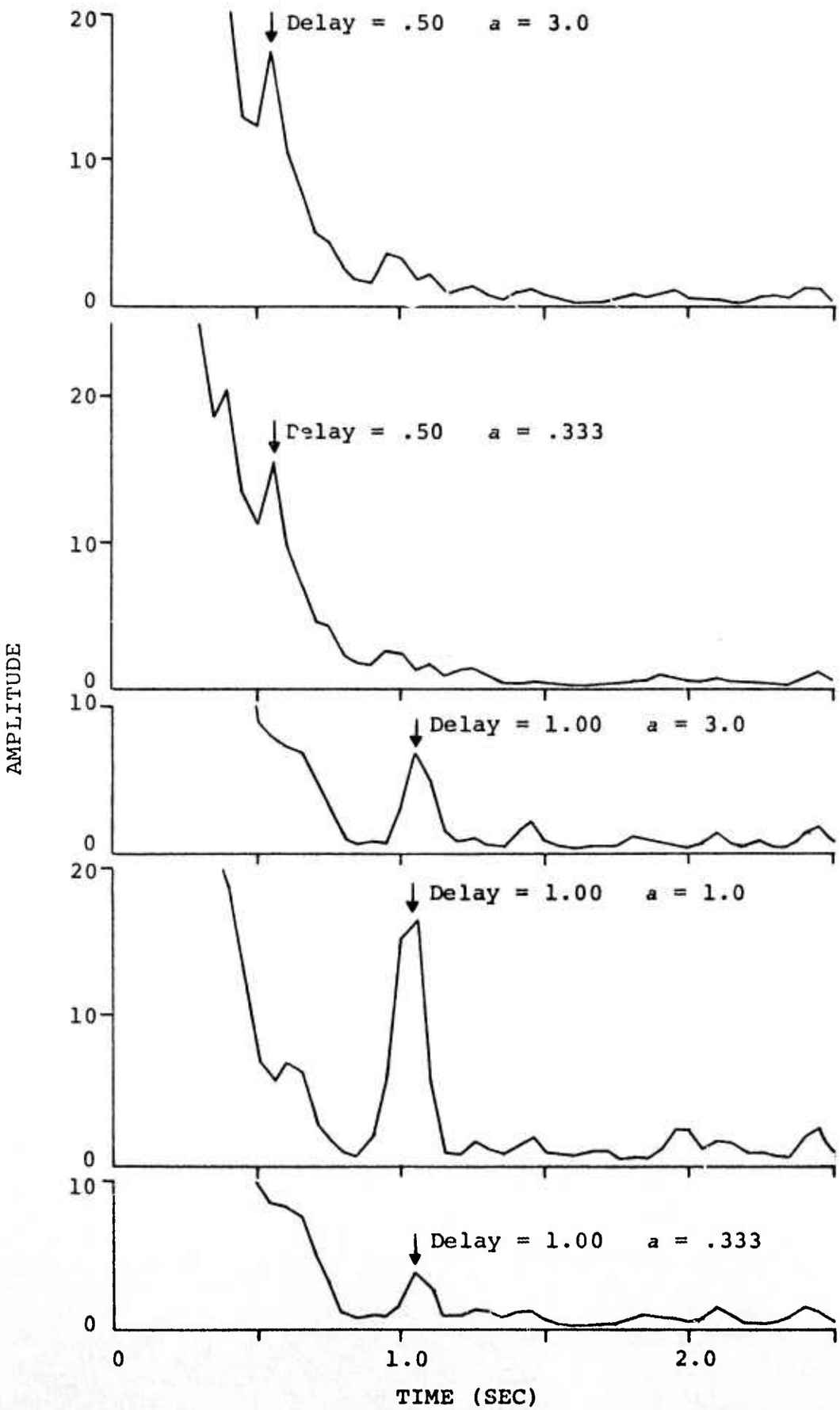
Delay = .50 a = 3.0
Delay = .50 a = .333
Delay = 1.00 a = 3.0
Delay = 1.00 a = 1.0
Delay = 1.00 a = .333
20
10
0
AMPLITUDE
0
1.0
2.0
TIME (SEC)

TABLE 5

Comparison of Actual a Values and Computed a Values for Artificially Created Double Events

Station	Delay Time (sec)	Actual a	Computed a	Reciprocal Root	% Error
DAC	.50	3.00	3.61	.277	20
DAC	.50	.333	.263	3.80	21
DAC	1.00	3.00	2.87	.349	4
DAC	1.00	1.00	1.22	.817	22
DAC	1.00	.333	.226	4.42	32
LEE	.50	3.00	4.12	.242	22
LEE	.50	.333	.296	3.38	9
LEE	.90	3.00	3.66	.273	37
LEE	.90	.333	.363	2.75	11
LEE	1.00	1.00	.701	1.42	30

operations may be accounted for on the basis of any reasonable theoretical treatment. To eliminate the smoothing operations results in an increased noise level more detrimental to calculations of *a* than the effects of smoothing. The average *a* calculated on the basis of several stations should yield a reasonable estimate of *a*. The *a* value obtained on the basis of a single station can be considered only an estimate of order. As previously noted, it is also evident from Table 5 that without additional information as to the nature of a secondary arrival it cannot be determined which root is the actual value of *a*. The recovered *a* values may therefore be of limited value.

The peaks occurring in the cepstra of the artificially created series are an indication of the sensitivity of a cepstral peak to an *a* value. The peaks having *a* values as low as 0.333 were clearly visible on the cepstra. Thus, it appears that secondary arrivals having *a* values of at least .333 have the potential of being detected by the cepstrum method.

Results from a Known Double Event (BLENTON/THISTLE)

The BLENTON/THISTLE event, which was previously used in a limited manner to study the effects of window length, provides an excellent starting point for any attempted

analysis of multiple arrivals. The explosions consisted of two shots which were detonated simultaneously and separated by 1.22 km. The trend of the line connecting the epicenters was N37°E. Additional known information concerning the shots is listed in Table 3. On the basis of the known information it would be expected that at least three significant secondary arrivals would exist with delays of P_2-P_1, pP_2-P_1, and pP_1-P_1, and there is the potential for other later arrivals resulting from slapdown effects. The P_2-P_1 delay should exhibit the previously discussed azimuthal and distance dependences. The pP_2-P_1 and pP_1-P_1 delays should individually exhibit no azimuth dependence, but may yield sectors of ambiguous identification because of the 1.22 km offset.

Cepstrum analysis was applied to nine BLENTON/THISTLE records. The cepstra are shown in Figures 25, 26, and 27. The delay of the peak of greatest amplitude of each cepstra and the delay of other peaks of lower amplitude were plotted versus the distance to the recording station. When two or more peaks have the same amplitude and are the peaks of greatest amplitude occurring on the cepstrum, these peaks are all plotted as peaks of greatest amplitude. The delay-distance plot for BLENTON/THISTLE is shown in Figure 28. There are peaks occurring in the .40-.50 sec range on the cepstra of six stations, and five of these peaks are the peaks of greatest amplitude for that cepstrum.

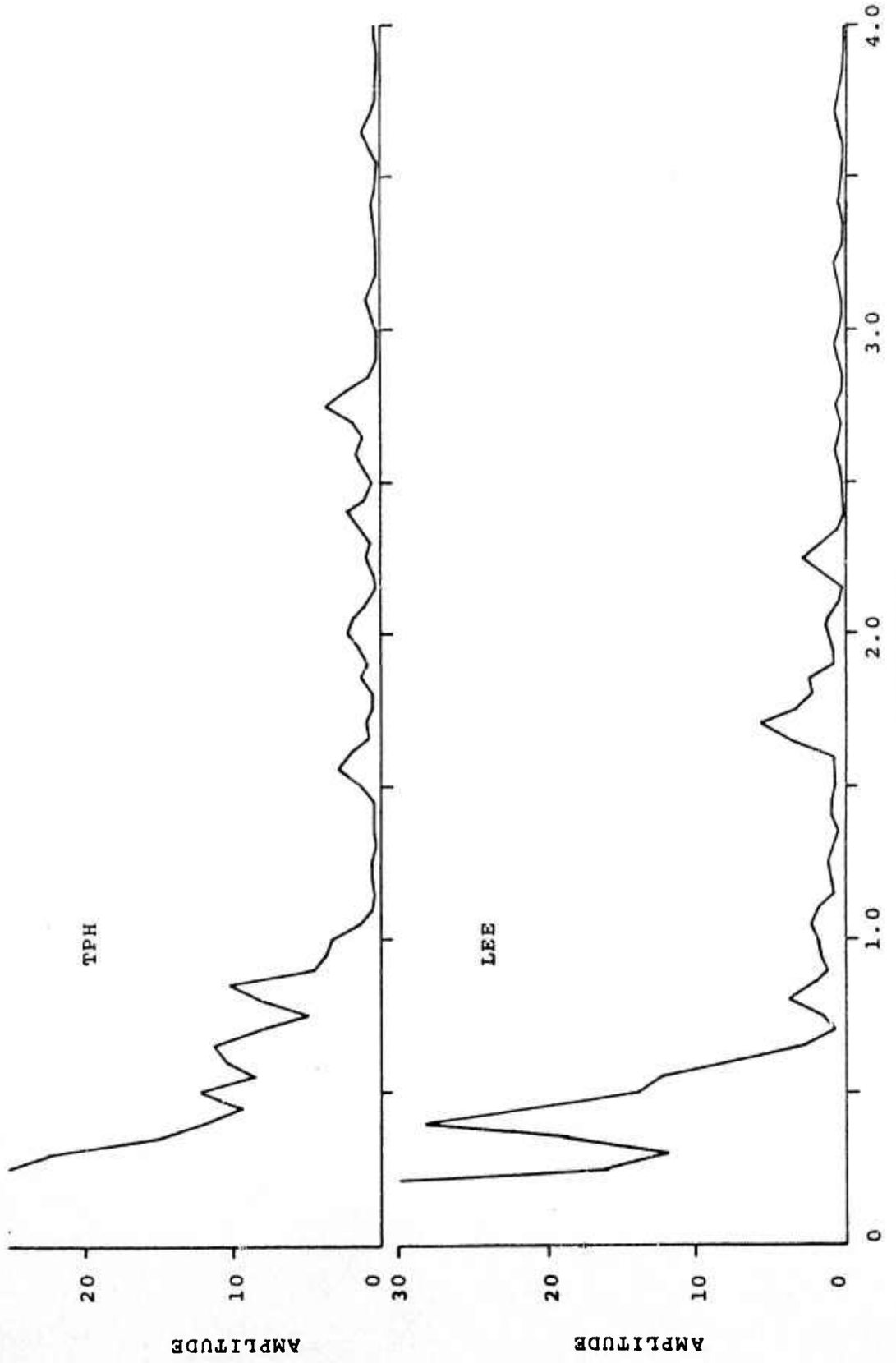

Figure 25. BLENTON/THISTLE cepstra for TPH and LEE.

Figure 26. BLENTON/THISTLE cpestra for MNV, NEL, ELY, and LAC.

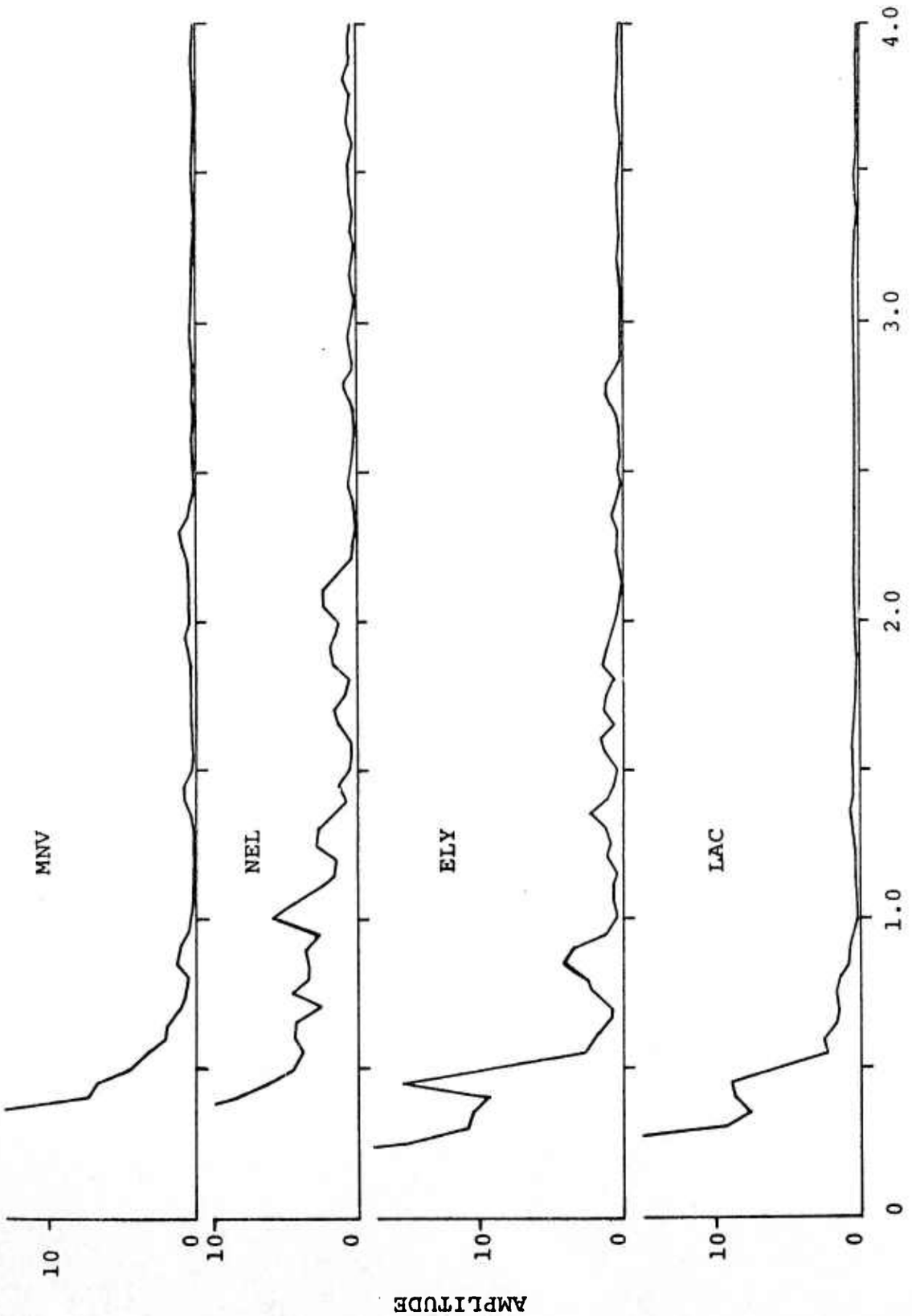
MNV
NEL
ELY
LAC
10
0
10
0
10
0
10
0
AMPLITUDE
0
1.0
2.0
3.0
4.0
TIME (SEC)

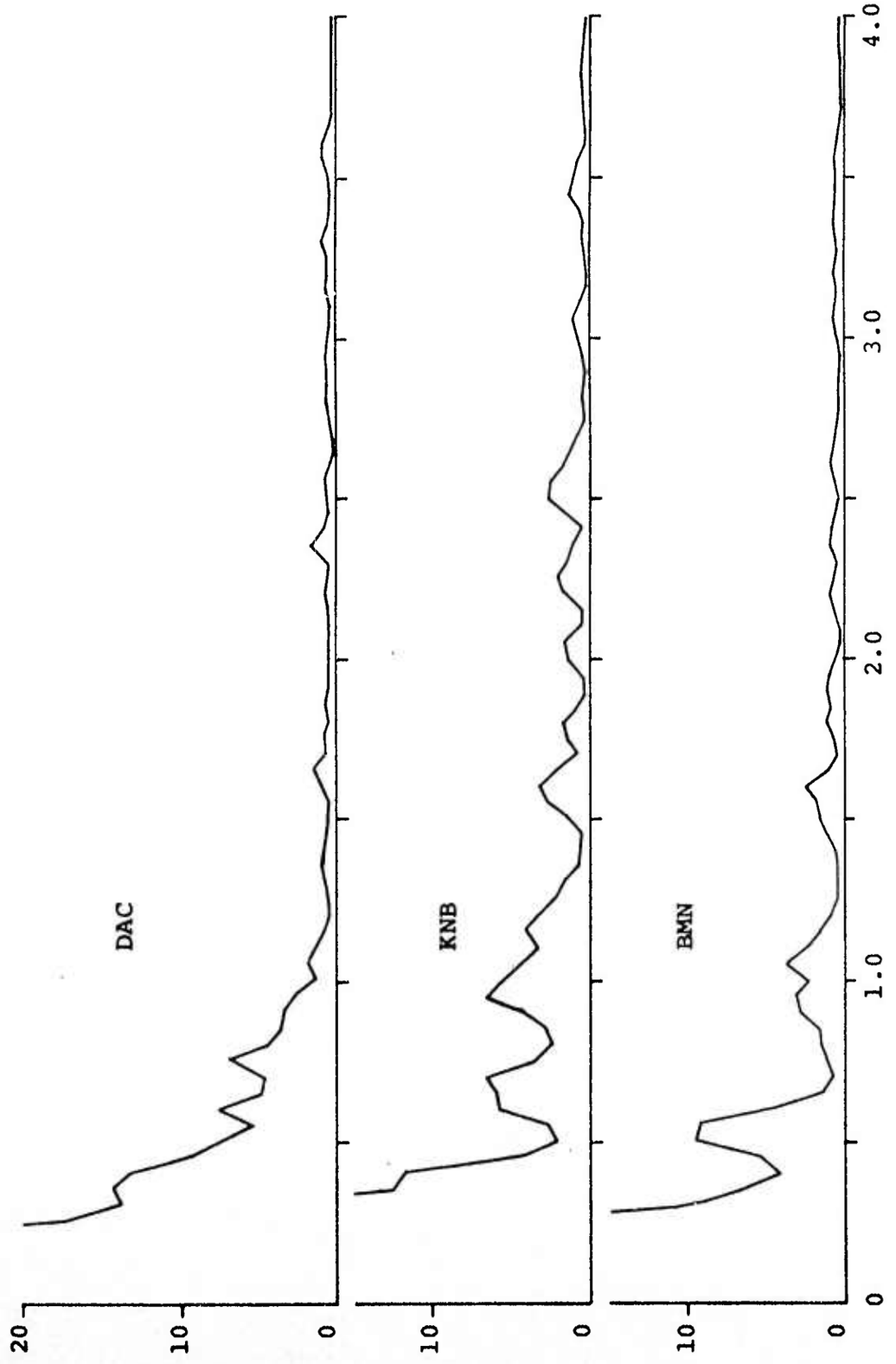

Figure 27. BLENTON/THISTLE cepstra for DAC, KNB, and BMN.

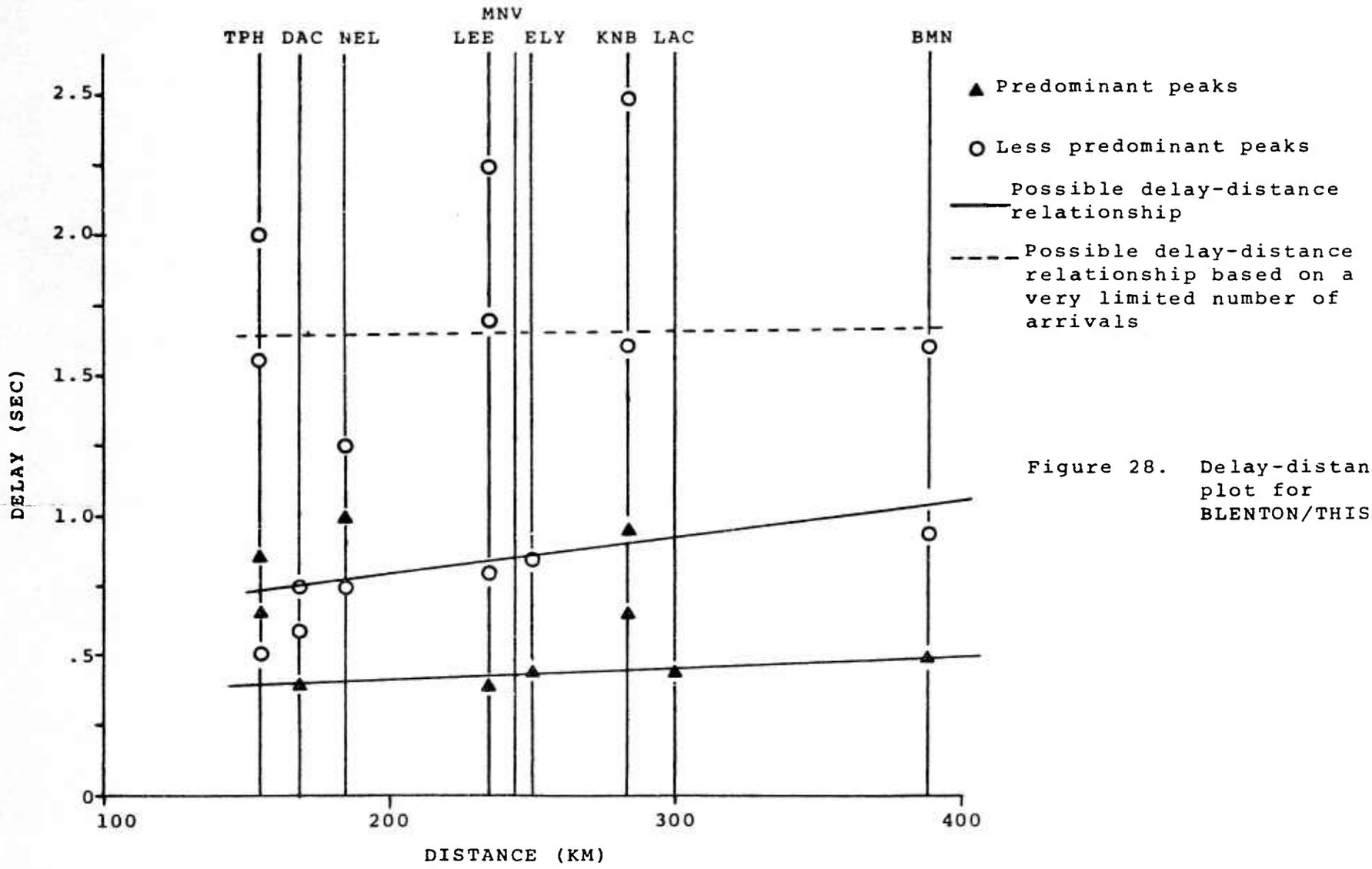

Figure 28. Delay-distance plot for BLENTON/THISTLE

Also, six stations have cepstral peaks in .75-1.05 sec range, and 4 stations have a later arrival in the 1.55-1.70 sec range. No peaks are visible on the MNV cepstrum. and the first peaks on the NEL and KNB cepstra do not occur until .75 and .65 seconds, respectively.

Figure 29 is the delay-azimuth plot of the BLENTON/THISTLE secondary arrivals. The trend of the line connecting the midpoint of the epicenters and the theoretical curve of P_2-P_1 for a source separation of 1.22 km is also shown on the plot. MNV lies on an azimuth perpendicular to the trend of the line connecting the midpoint of the epicenters, TPH and NEL lie within 15° of the perpendicular. The absence of arrivals at MNV and at NEL within .75 sec is consistent with the expected delay-azimuth relationship for two horizontally separated events. Using the .40-.50 sec arrivals and considering the absence of arrivals at MNV and NEL, the delay-azimuth relationship for two horizontally separated events is visible on the plot. The delay-azimuth relationships, together with the delay-distance relationship, indicate that the arrival at .40-.50 sec is the second direct P arrival from the multiple source.

From an analysis of the arrivals in the .75-1.05 sec range, an increasing delay with distance relationship is indicated. This arrival then may be the pP phase from one of the events. The later arrival at 1.55-1.70 sec could possible be a P_s phase, but a firm determination

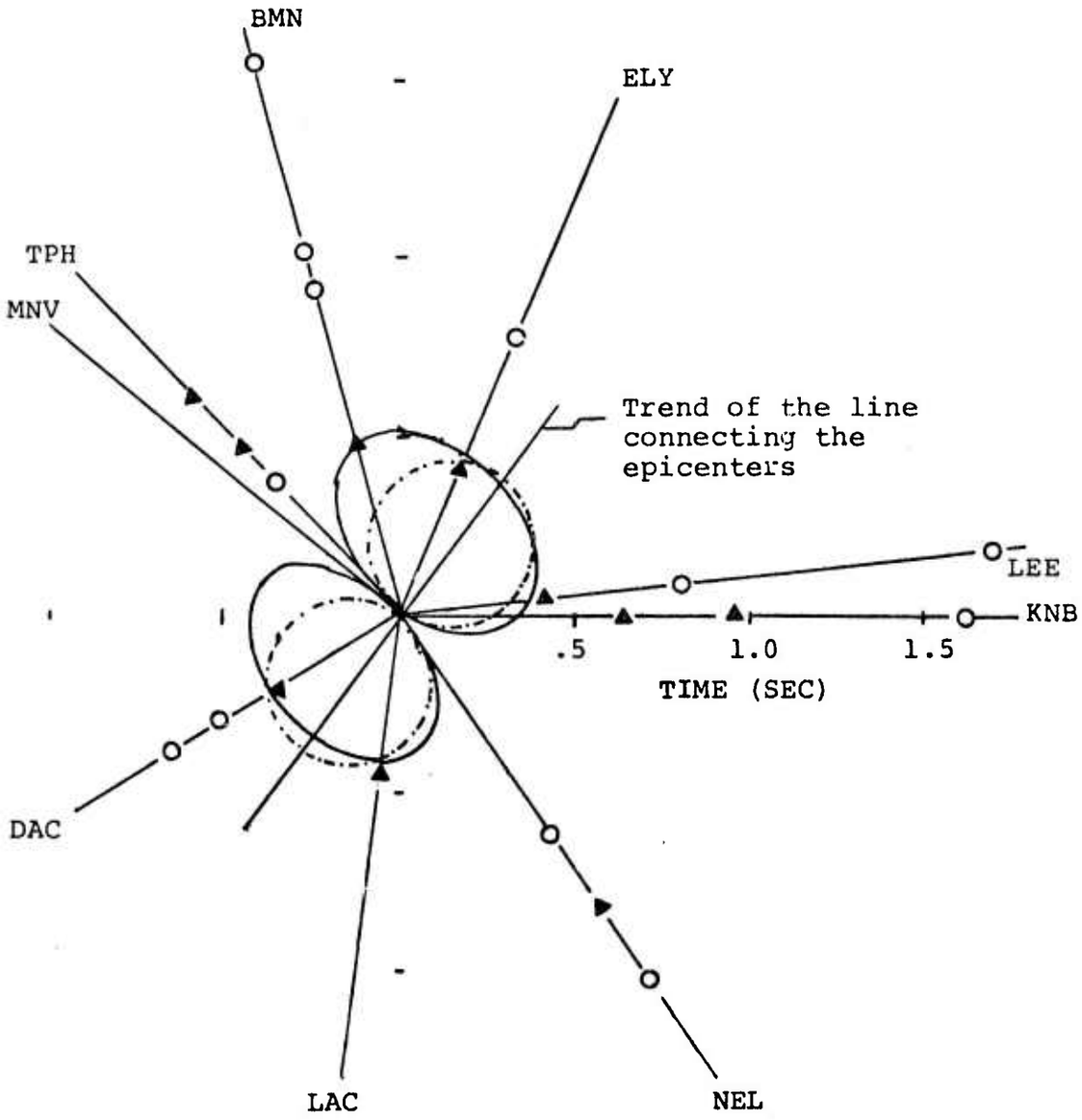

▲ Predominant peaks

O Less predominant peaks

—— Possible delay-azimuth relationship

-·-·- Theoretically computed relationship

Figure 29. Delay-azimuth plot for BLENTON/THISTLE.

could be accounted for by either of these fault systems. Four records of the Massachusetts Mountain earthquake were available for analysis. The cepstra are shown in Figure 30. The KNB and LAC cepstra show peaks with amplitudes of 3 or less, while the MNV and ELK cepstra have peaks with amplitudes ranging up to 8. The delay-distance plot in Figure 31 and the delay-azimuth plot in Figure 32 have a scatter of points, and it is not possible to distinguish a pattern for a secondary arrival on the basis of only four stations.

Despite the limited data available, it may be noted that the cepstra peaks appear primarily in a 0.5 sec to 1.0 sec window. If the published depth estimate of 4.6 km is accepted pP should appear beyond the 1 sec window. It thus appears reasonable to assume that the cepstral peaks are not the result of pP but rather result from multiple generation on the fault plane or differential path effects during propagation.

Results from EVENT A

Cepstrum analysis was applied to seven EVENT A records. The cepstra are shown in Figures 33 and 34. The delay-distance plot is given in Figure 35. The peaks of greatest amplitude occur over a range of .35-.90 seconds, with 5 stations having peaks of greatest amplitude in a .70-.90 sec range. There is no later arrival consistently

cannot be made on the basis of only four cepstra exhibiting peaks in this range.

The results from BLENTON/THISTLE indicate that cepstrum analysis is a potential method of detecting the secondary arrivals for an unknown event, and that it was possible to use the delay-distance and delay-azimuth relationships to identify secondary arrivals. However, the delay-distance and delay-azimuth plots may prove very difficult to interpret.

Results from the Massachusetts Mountain Earthquake

The Massachusetts Mountain earthquake occurred on August 5, 1971. The epicenter was located at latitude 36°54.94'N and longitude 115°59.42'W, and is shown on the Yucca Flats map of Figure 15. The focal depth of the earthquake was 4.6 km, and the magnitude of the event was 3.5. The epicenter was south of the Yucca Flats area of the Nevada Test Site; thus the earthquake had a great circle propagation path nearly identical to that of the nuclear shots detonated in that region. Fischer and others (1972) determined the nodal fault plane solution to be a plane striking N22°W and having a vertical dip or a plane striking N68°E and having a 86° dip to the northwest. The main earthquake occurred in an area having both northwest-trending right-lateral faults and northeast-trending left-lateral faults, and the focal plane solution

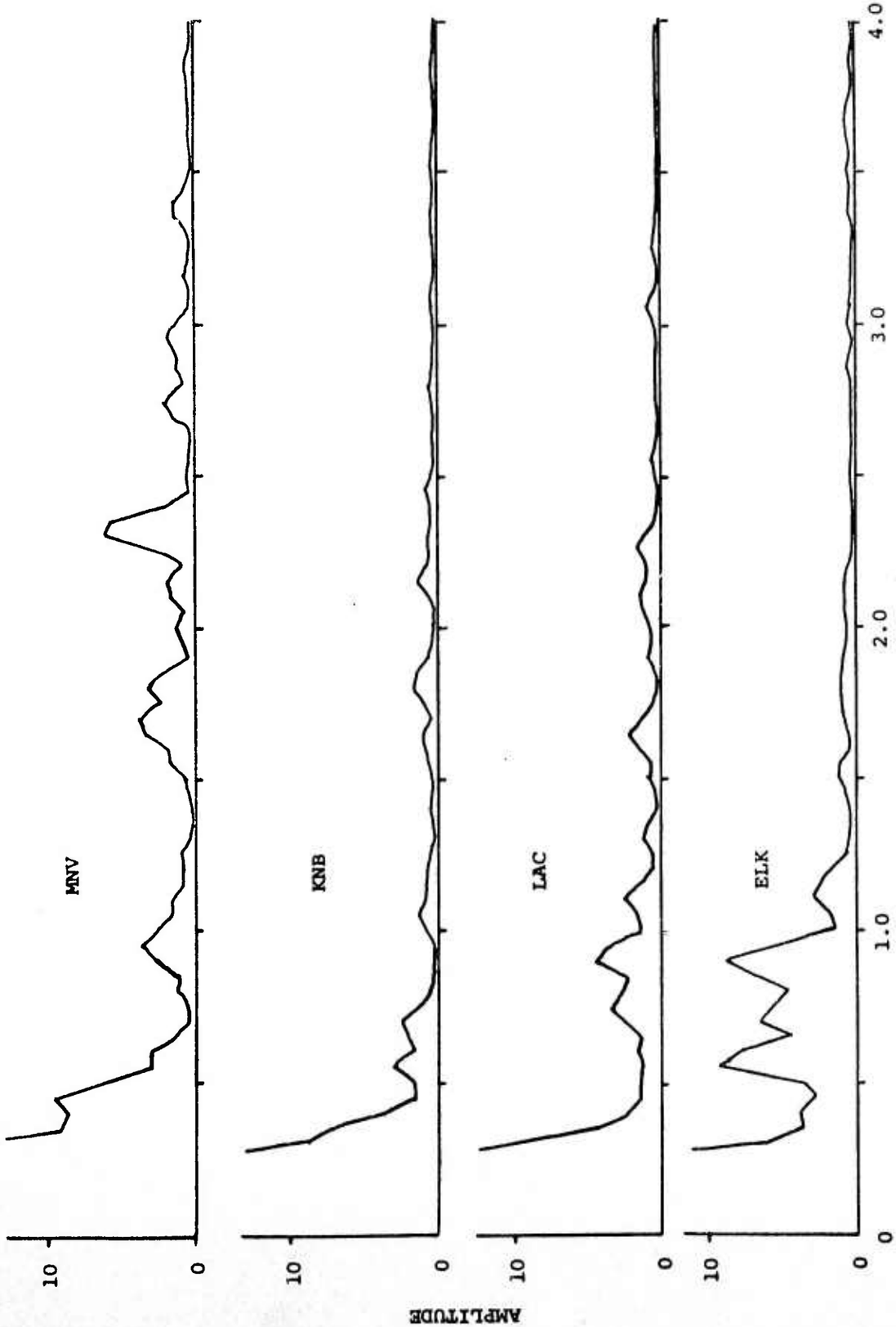

Figure 30. Massachusetts Mountain cepstra for MNV, KNB, LAC, and ELK.

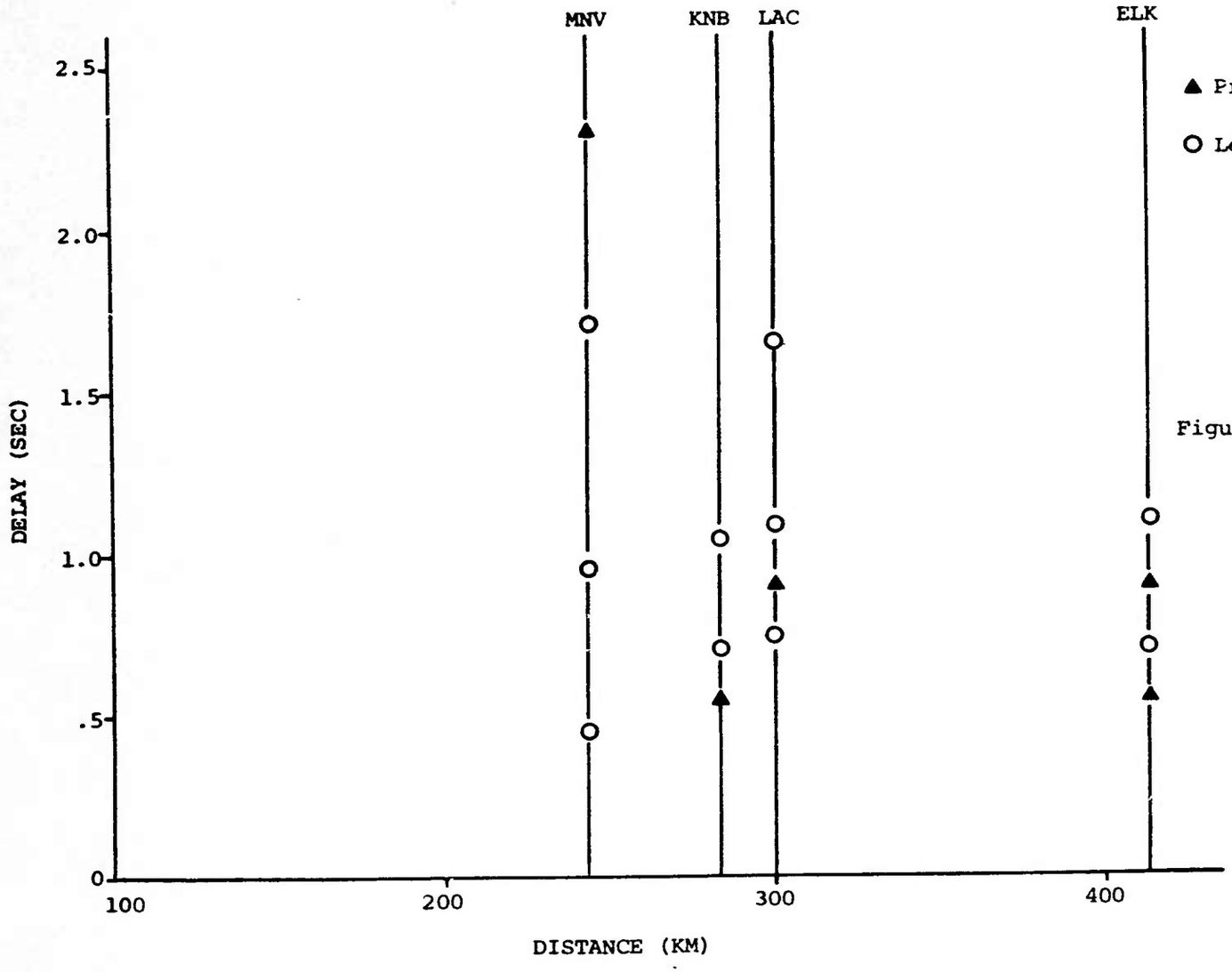

Figure 31. Delay-distance plot for Massachusetts Mountain Earthquake.

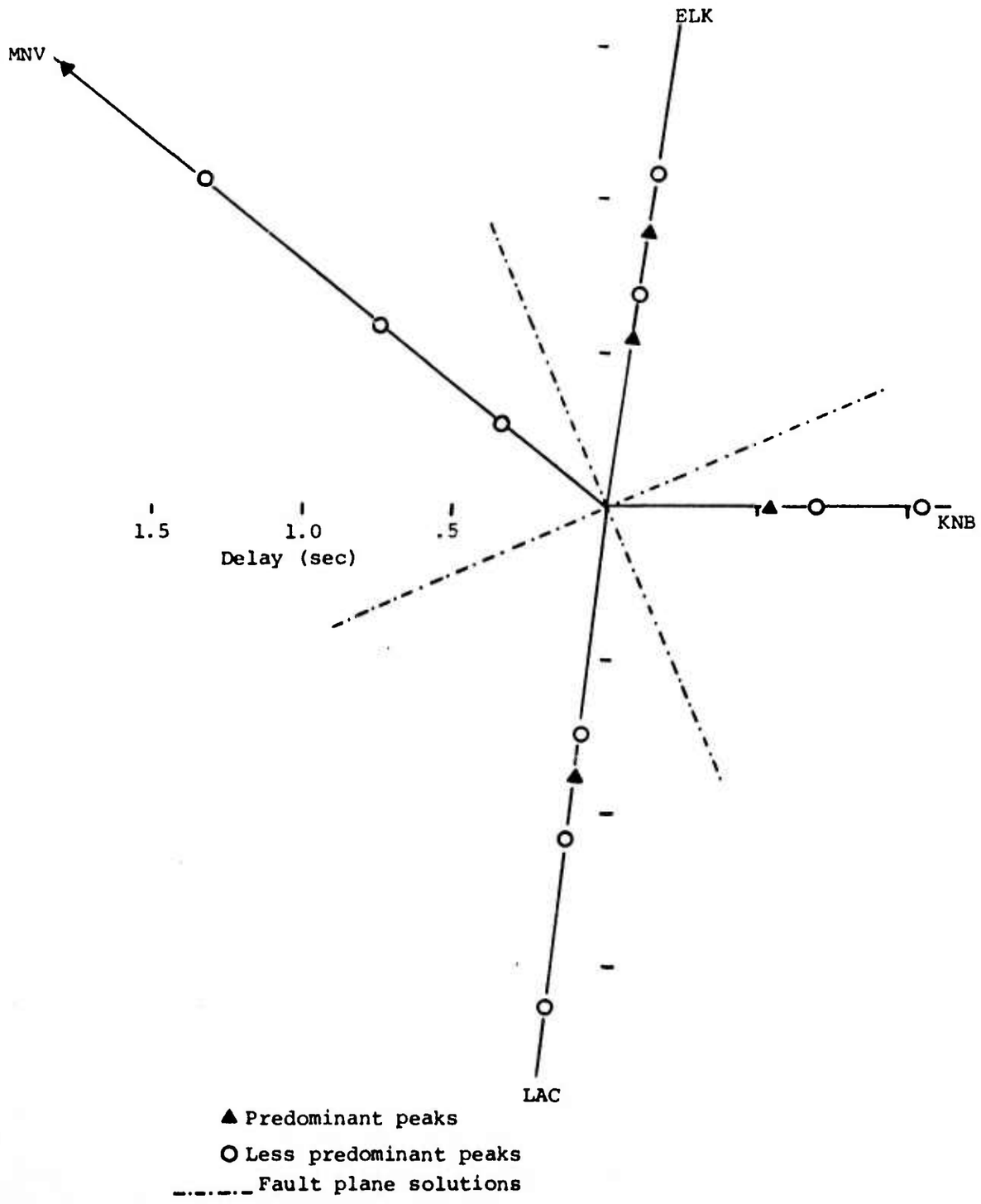

Figure 32. Delay-azimuth plot for Massachusetts Mountain earthquake.

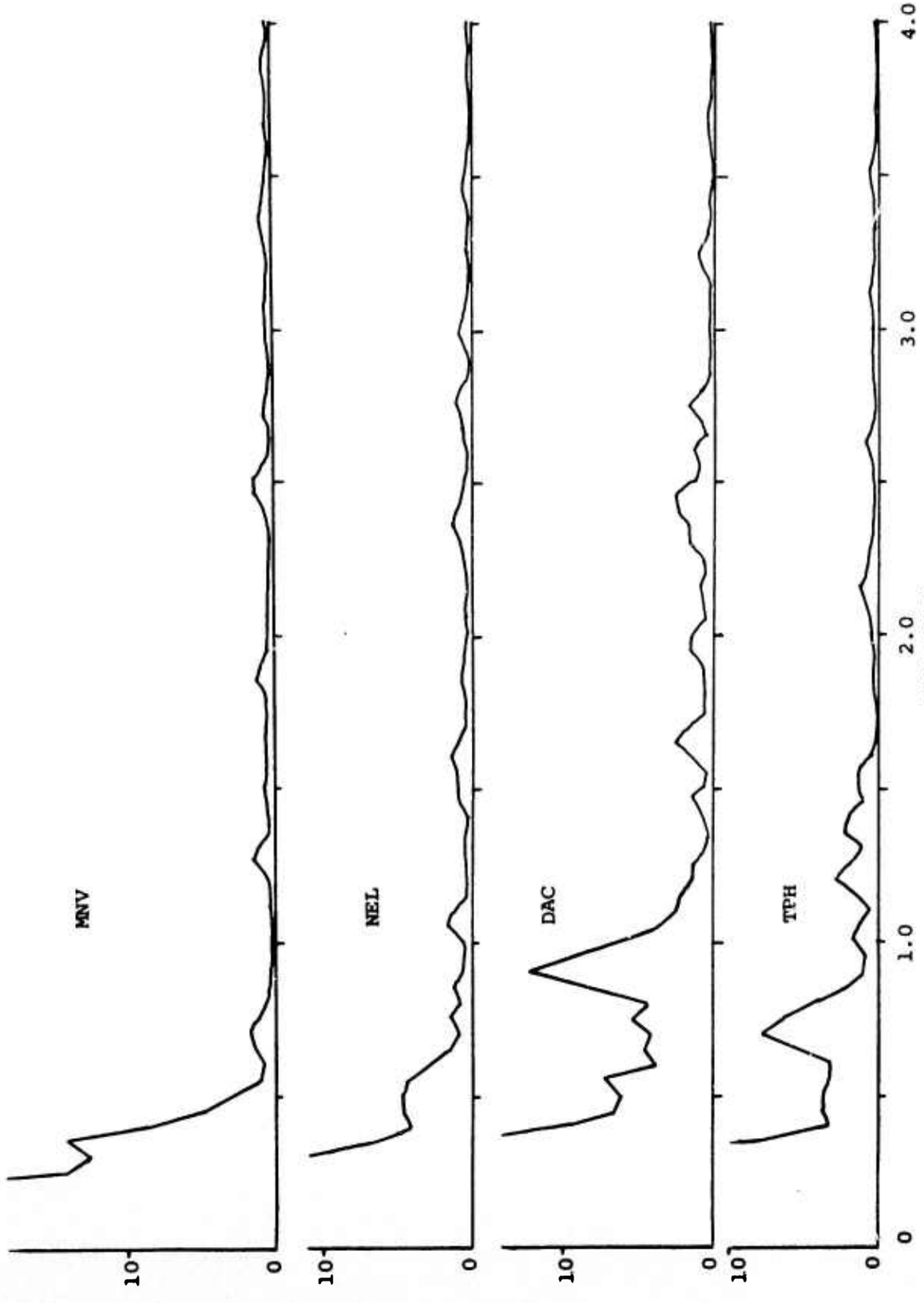

Figure 33. EVENT A cepstra for MNV, NEL, DAC, and TPH.

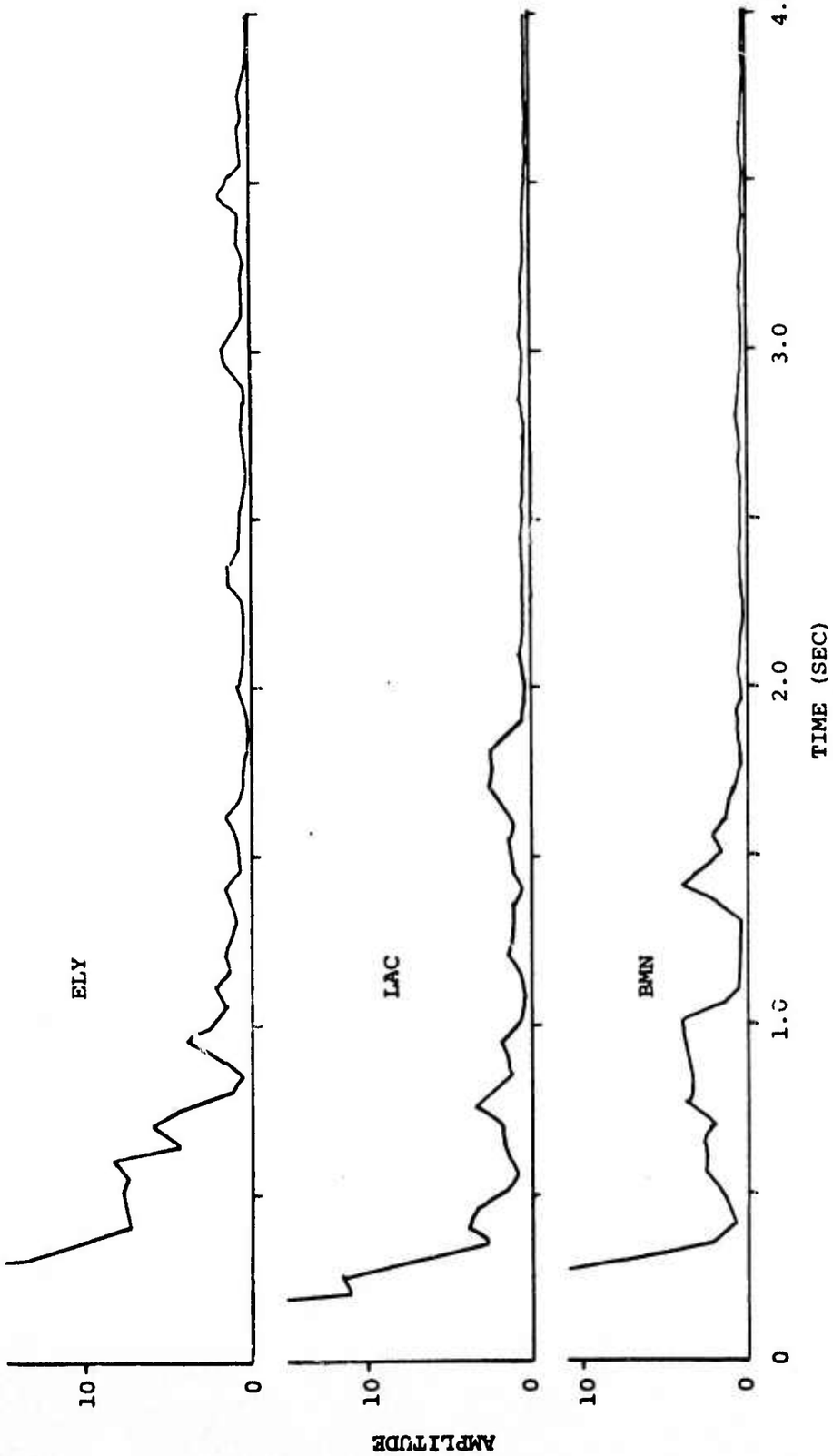

Figure 34. EVENT A cepstra for ELY, LAC, BMN.

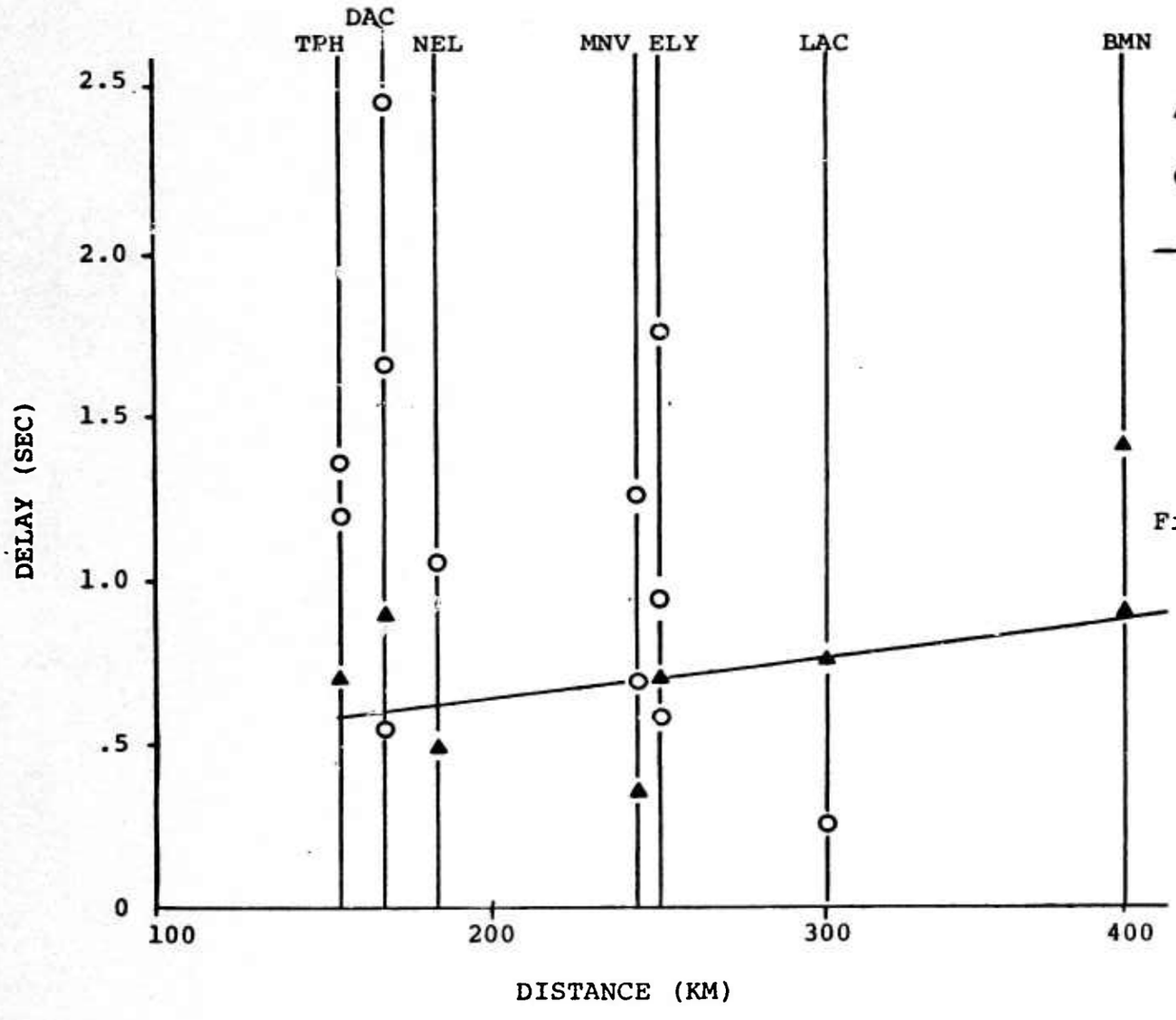

Figure 35. Delay-distance plot for EVENT A.

occurring which would indicate a slapdown arrival, nor is there an absence of arrivals at any station which would indicate a multiple event. A suggestion of a consistent secondary arrival does exist, and is indicated by the line drawn through five of the delay points in Figure 35. The slope of this line yields a moveout of 0.15 sec per 100 km and may result from pP.

The delay-azimuth plot shown in Figure 36 does not aid in distinguishing a relationship for a secondary arrival because of the lack of station coverage in the 90° and 270° azimuth area. The relationship for a single event or for horizontally separated events could be drawn on the delay-azimuth plot for the data available. It is not possible then to predict the nature of EVENT A.

Results from EVENT B

Ten EVENT B records were available for analysis. The cepstra are shown in Figures 37, 38, and 39, and the delay-distance plot in Figure 40. Eight of the cepstra have peaks occurring in the .40-.55 second range, and a second concentration of peaks occurs on eight of the cepstra in the .70-.90 second range. The TPH and NEL cepstra have no peaks occurring until .80 and.75 sec, respectively, and considering this absence of arrivals and the 171° difference in their azimuth with respect to the Nevada Test Site, TPH and NEL may possibly be located on azimuths

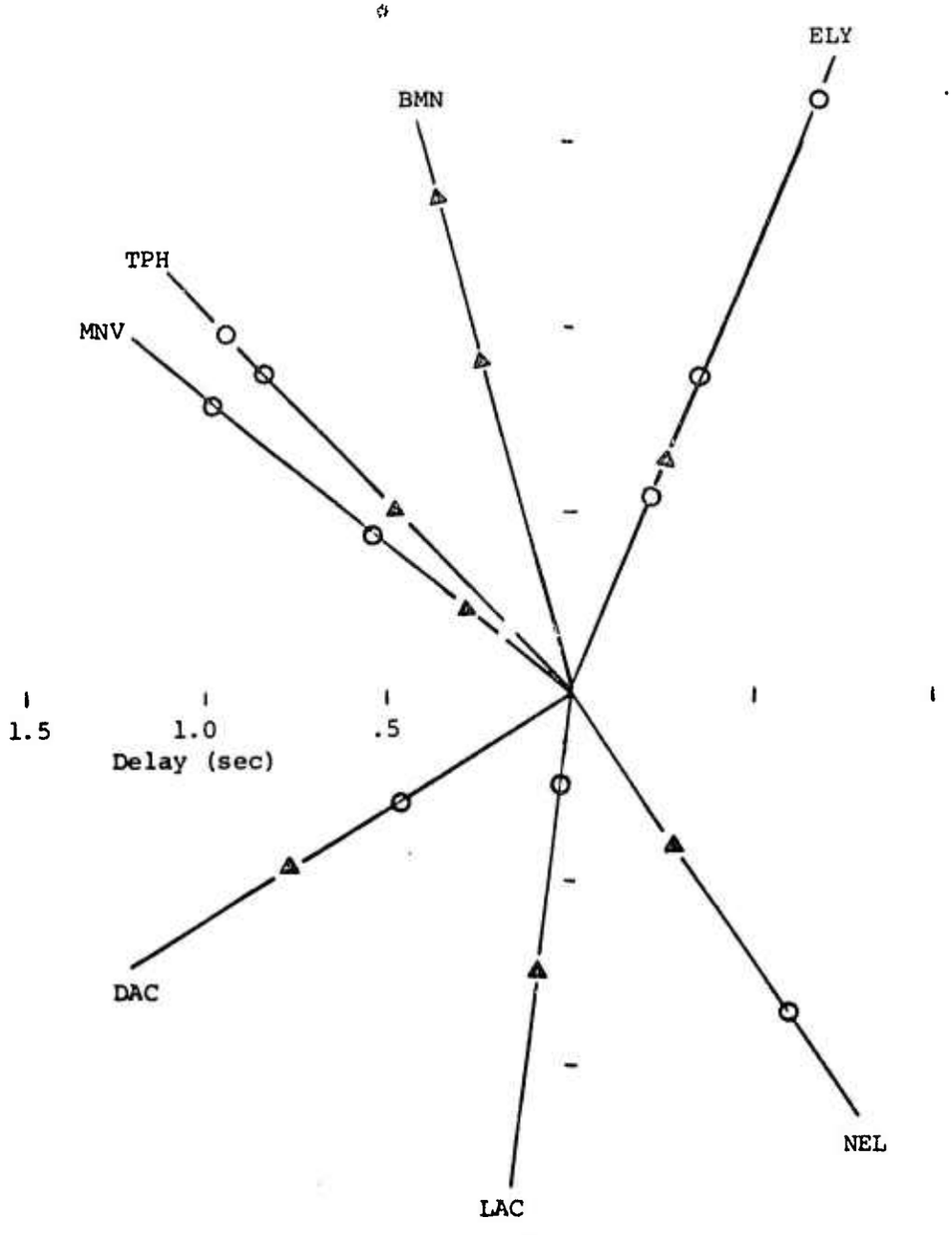

Figure 36. Delay-azimuth plot for EVENT A.

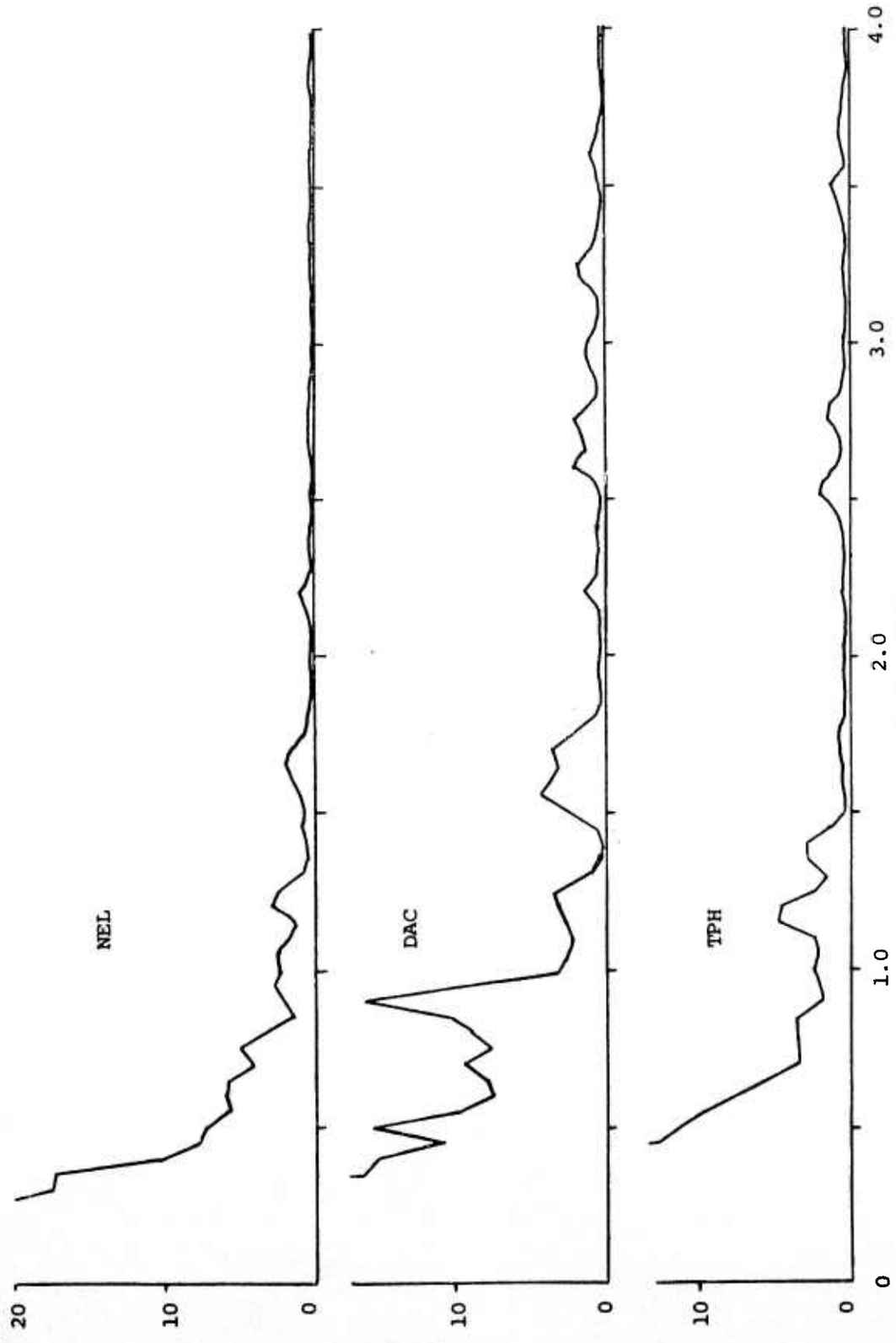

Figure 37. EVENT B cepstra for NEL, DAC, and TPH.

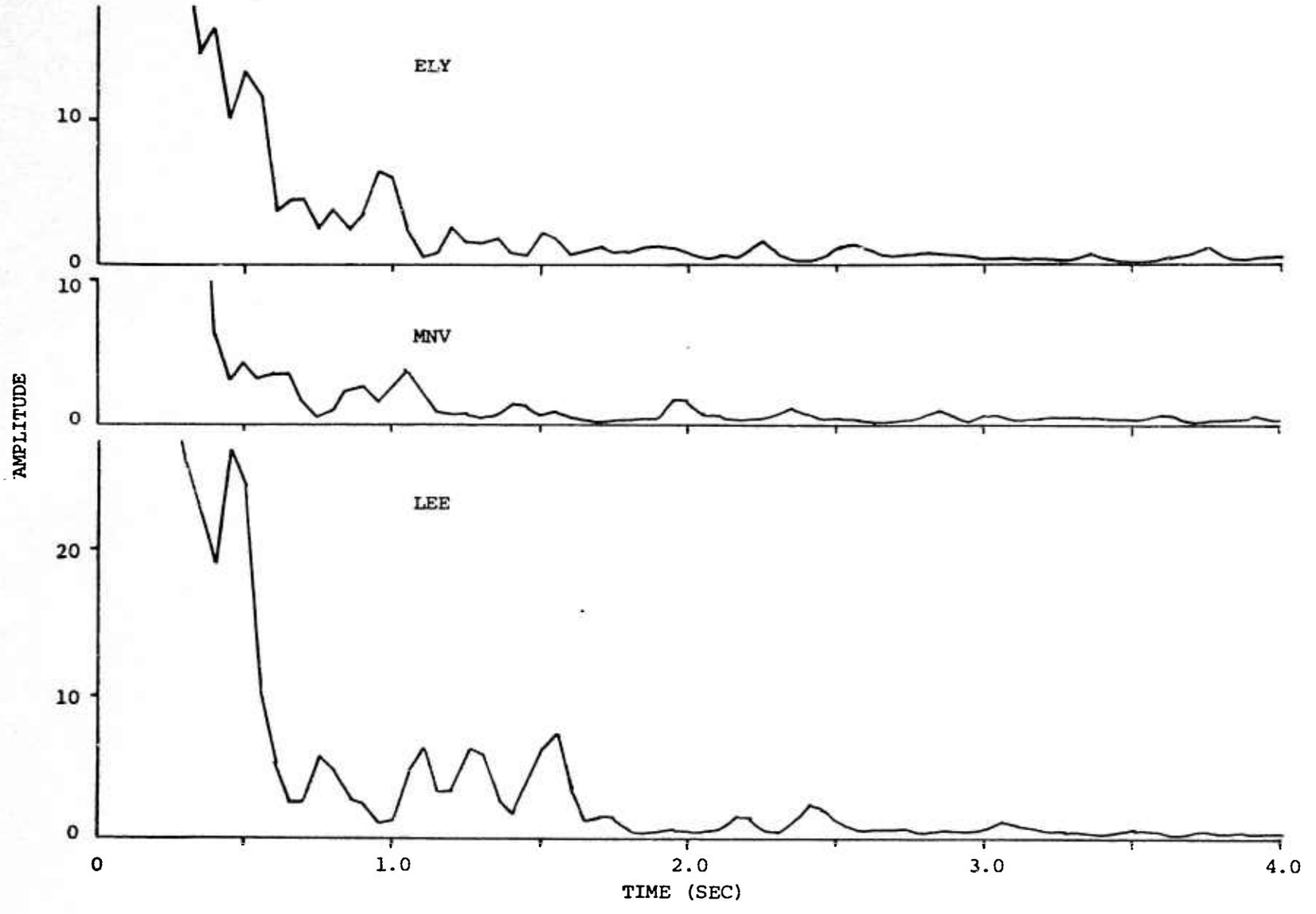

Figure 38. EVENT B cepstra for ELY, MNV, and LEE.

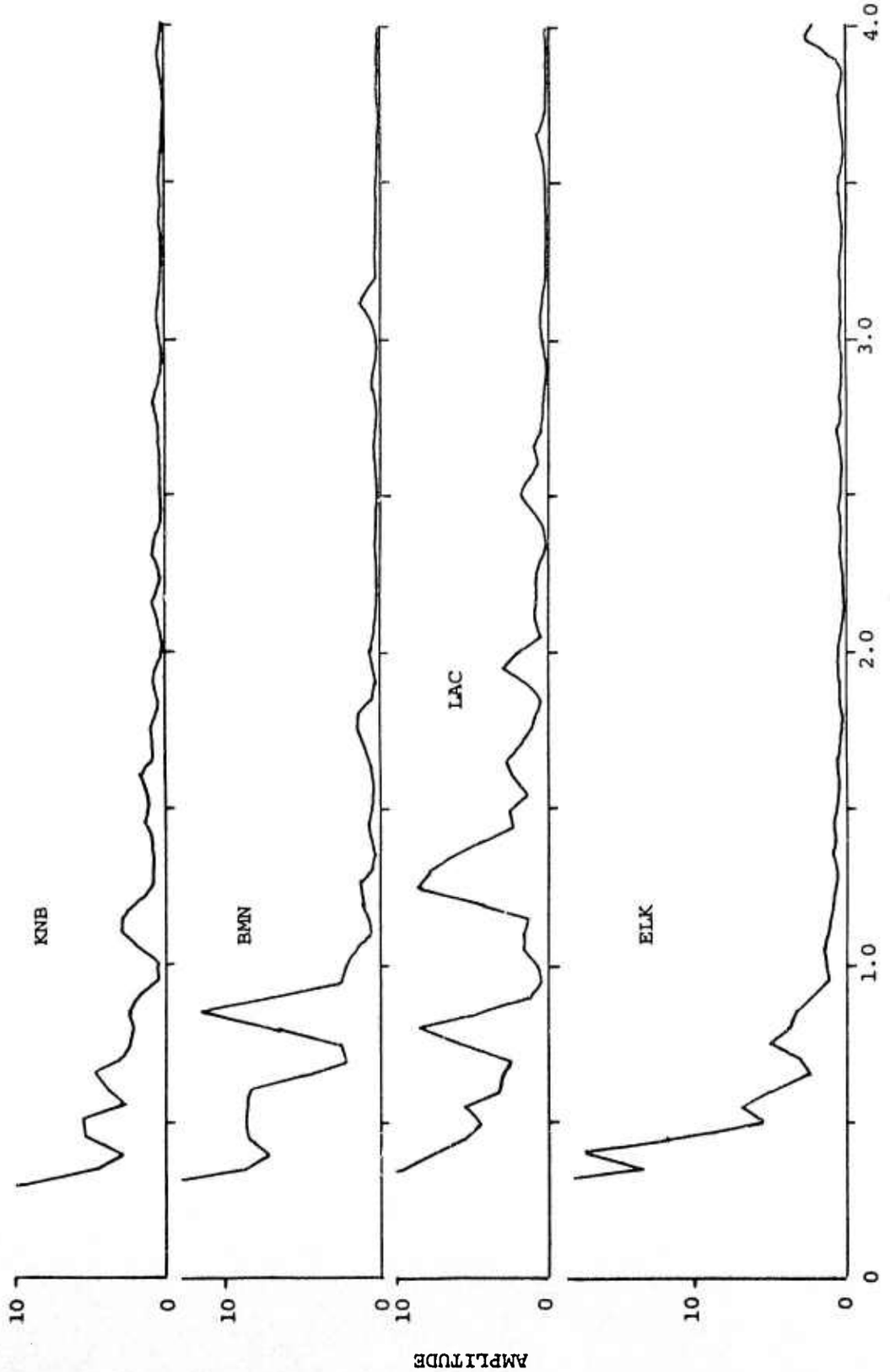

Figure 39. EVENT B cepstra for KNB, BMN, LAC, and ELK.

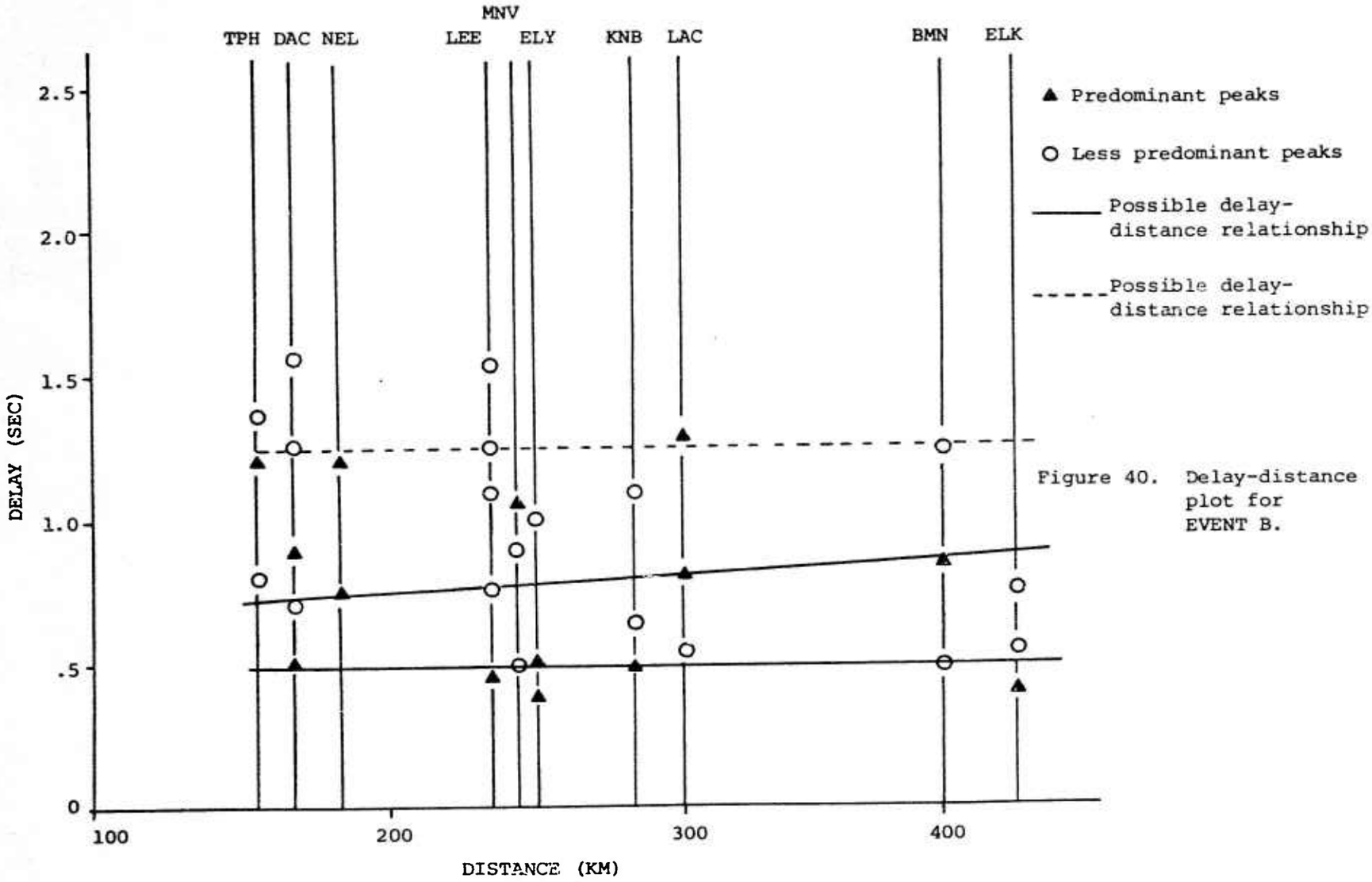

Figure 40. Delay-distance plot for EVENT B.

perpendicular to the trend of a line connecting the epicenter of a double event. Considering the peaks in the .40-.55 sec range of the delay-azimuth plot of Figure 41, the pattern for two events separated horizontally can be drawn on the plot. The concentration of peaks in the .70-.90 sec range may be associated with a pP arrival. A line possibly related to pP is shown on Figure 40. If this line is correct, it indicates a pP movement of 0.05 sec per 100 km. There is also a suggestion, indicated by the dashed line in Figure 40, of an event arriving with relatively constant delay. This could be a slapdown signal.

On the basis of the delay-distance and delay-azimuth relationships it appears that EVENT B is a horizontally separated dipole. The separation appears to be approximately 1 km and trends in a N60°E direction. A slapdown signal was possibly generated 1.23 seconds following detonation.

Results from EVENT C

Cepstrum analysis was applied to nine EVENT B records. The cepstra are shown in Figures 42 and 43 and Figure 44 is the delay-distance plot for EVENT B. Seven of the cepstra have their first peaks occurring in the .55-.70 sec range. A line through these points may be related to pP and is shown on Figure 44. If correct,

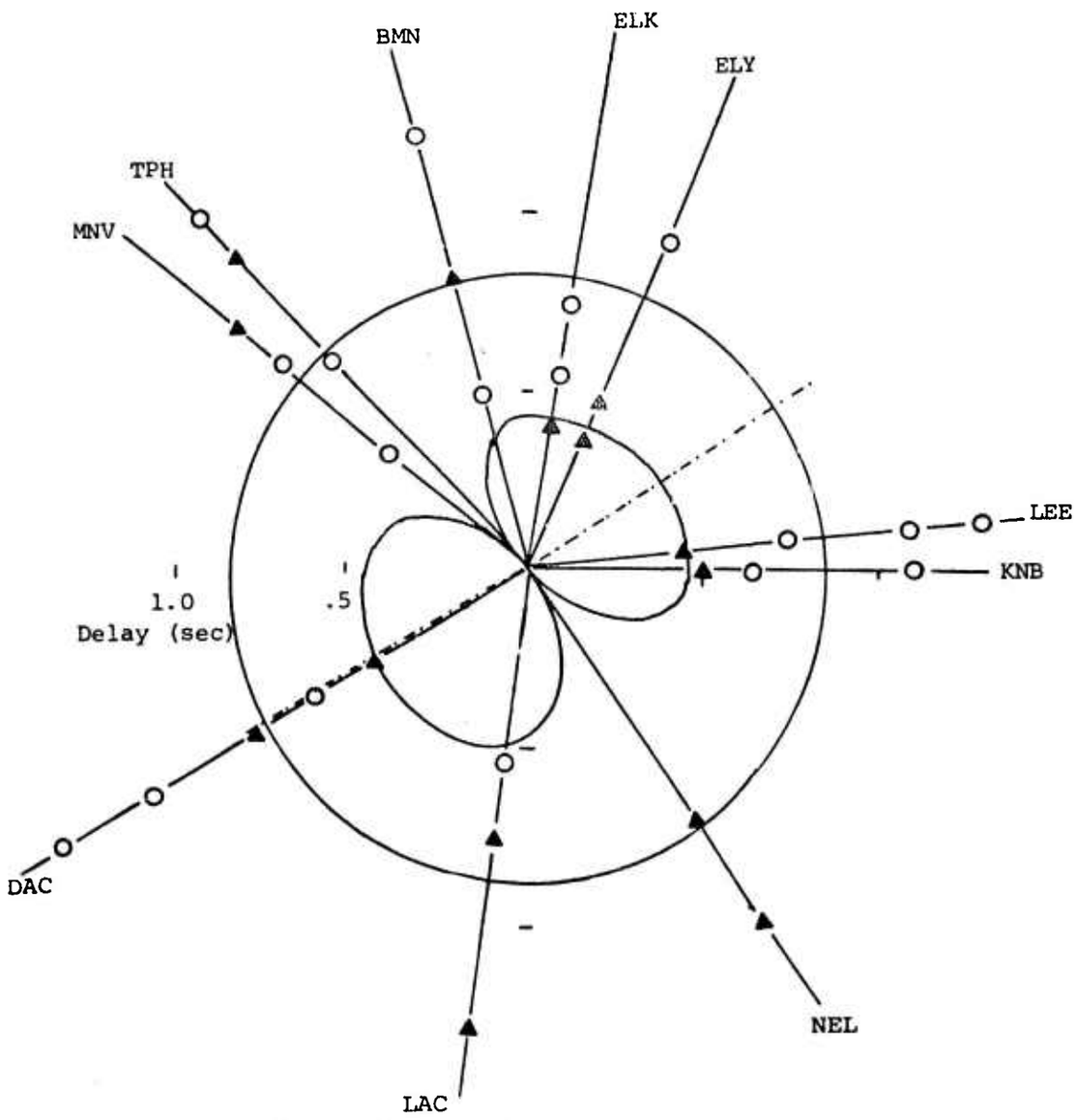

Figure 41. Delay-azimuth plot for EVENT B.

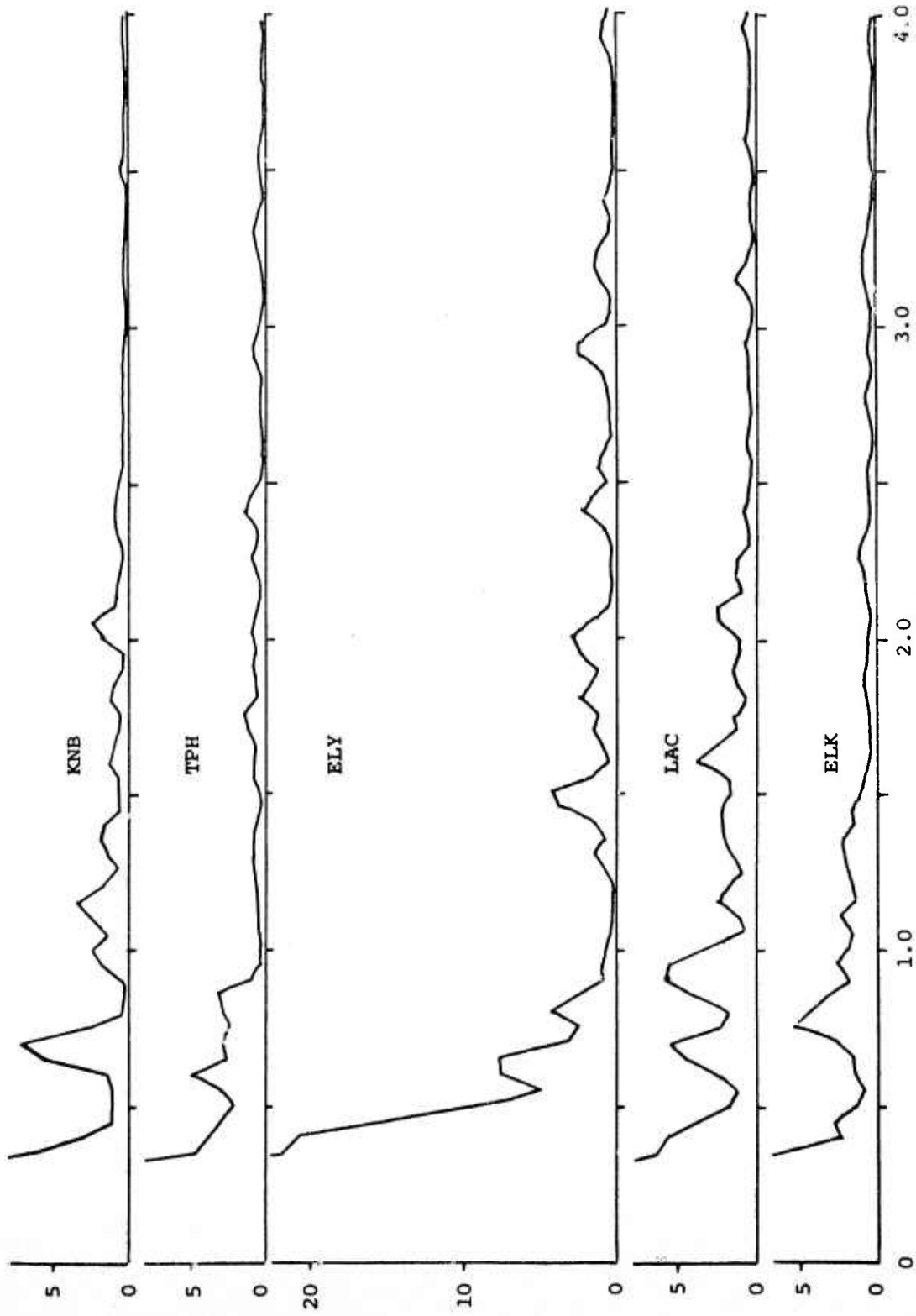

Figure 42. EVENT C cepstra for KNB, TPH, ELY, and LAC.

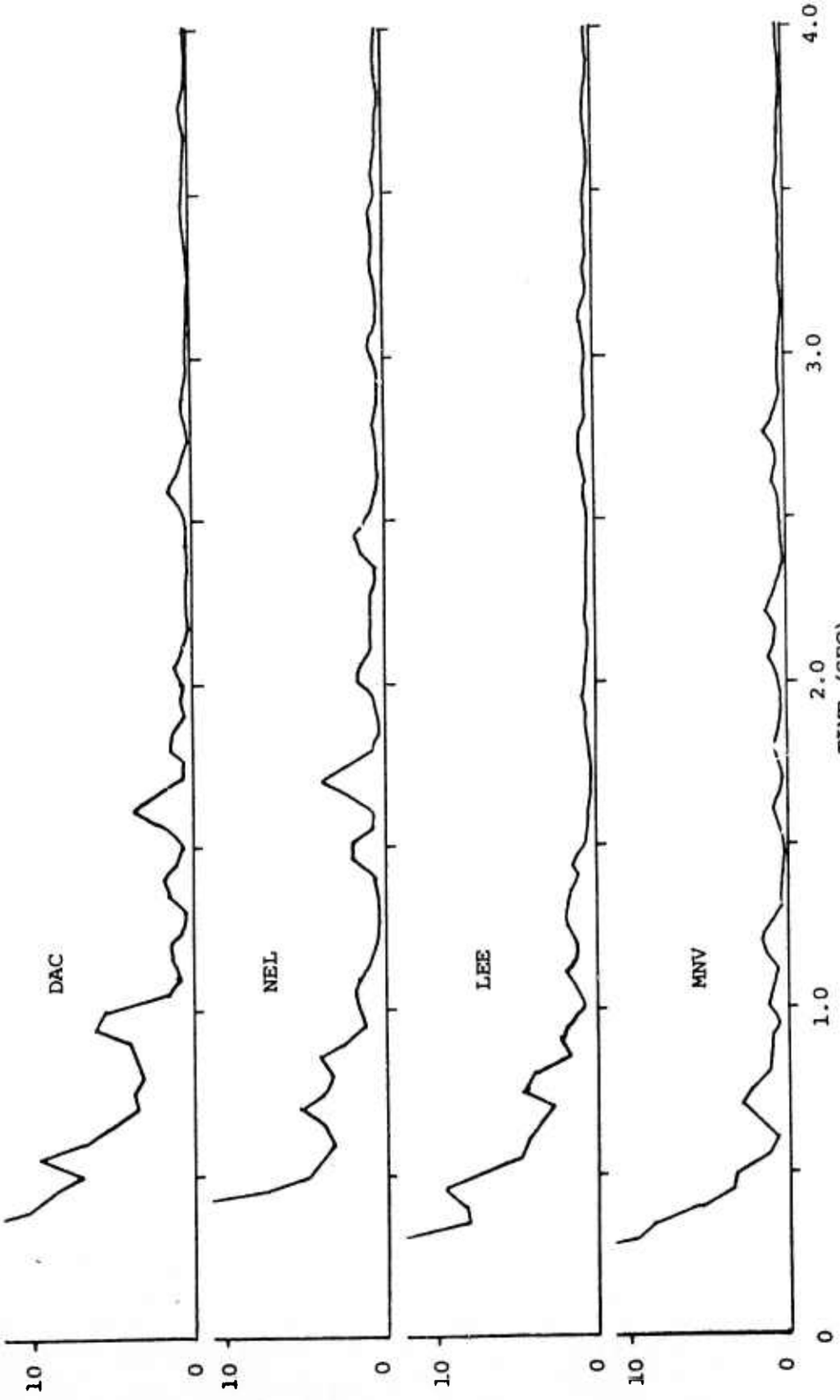

Figure 43. EVENT C cepstra for DAC, NEL, LEE, and MNV.

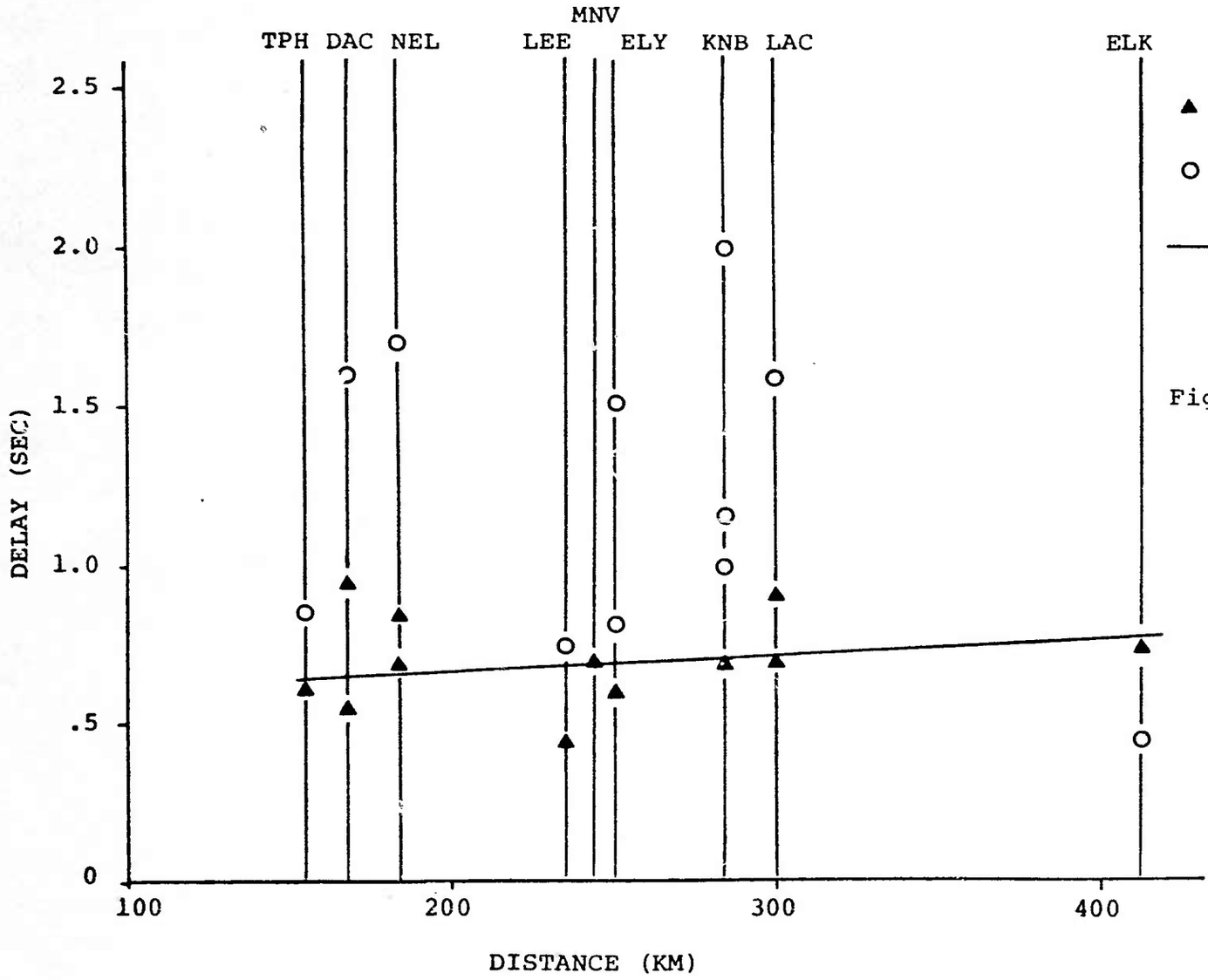

Figure 44. Delay-distance plot for EVENT C.

this line indicates a pP moveout of 0.07 sec per 100 km. The two other cepstra, LEE and ELK, have first peaks occurring at .45 sec. None of the stations exhibit an absence of peaks which would indicate a multiple event. The delay-azimuth plot is given in Figure 45. It appears that EVENT C is a single event with a pP arrival in the .55 to .70 sec range. DAC, NEL, ELY, and LAC have an arrival in the 1.5-1.7 range which could possible be a slapdown arrival.

Results from EVENT D

Cepstrum analysis was applied to nine EVENT D records. The cepstra are shown in Figures 46, 47, and 48, and the delay-distance plot is given in Figure 49. Six of the cepstra have first peaks occurring in the .45-.60 second range. A line of very small slope can be drawn on the delay-distance plot through these points, and this suggests a multiple event. LAC has a first peak at .30 sec, and ELK and LEE have no peaks until .75 and .85 seconds, respectively. From the delay-azimuth plot in Figure 50 it is evident that it is possible for LEE to lie on an azimuth perpendicular to the trend of a line connecting the epicenters of a double event, and the pattern for two events separated horizontally could be drawn through the data point. The theoretical curve for horizontally separated events having a P-P delay of .50

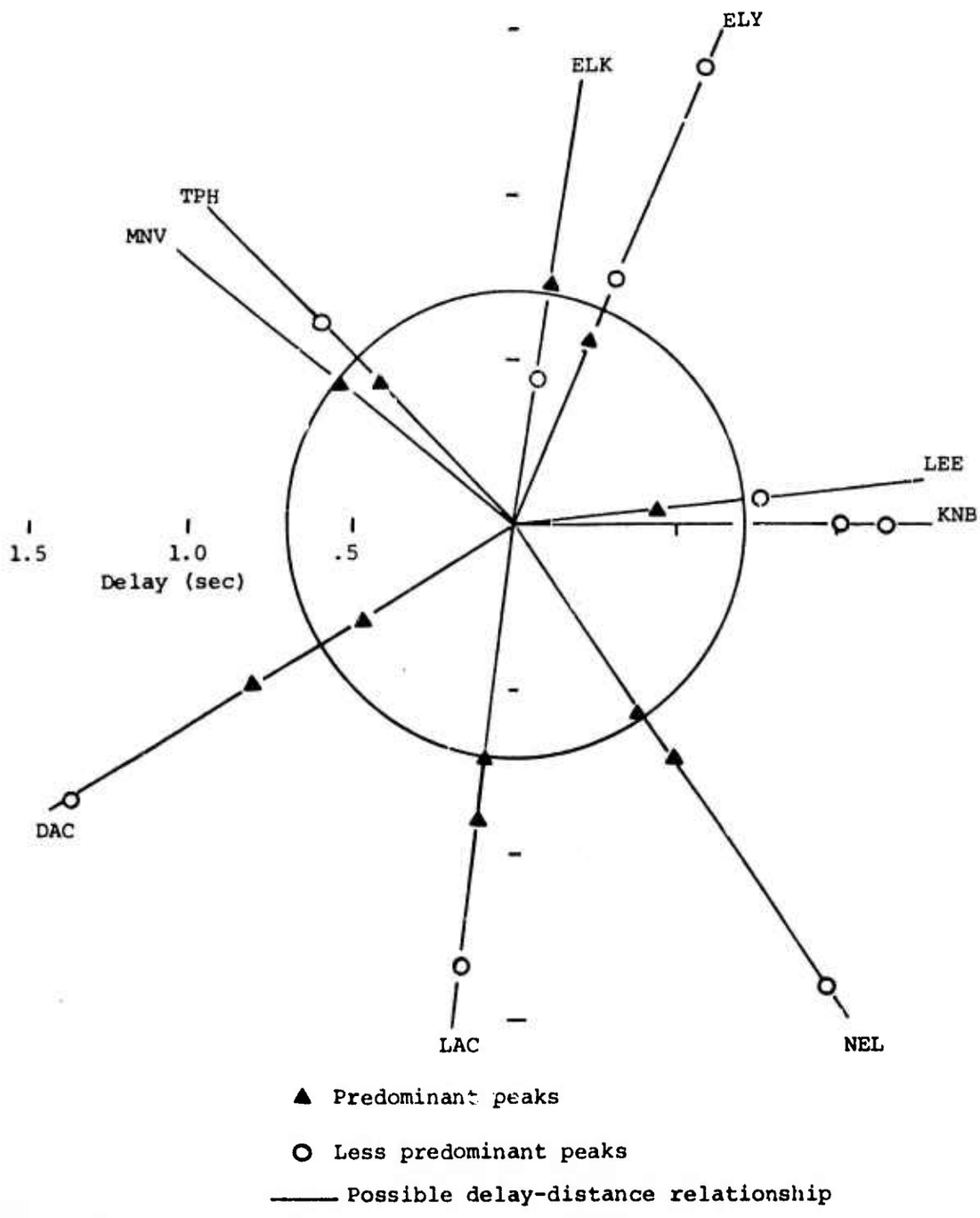

Figure 45. Delay-azimuth plot for EVENT C.

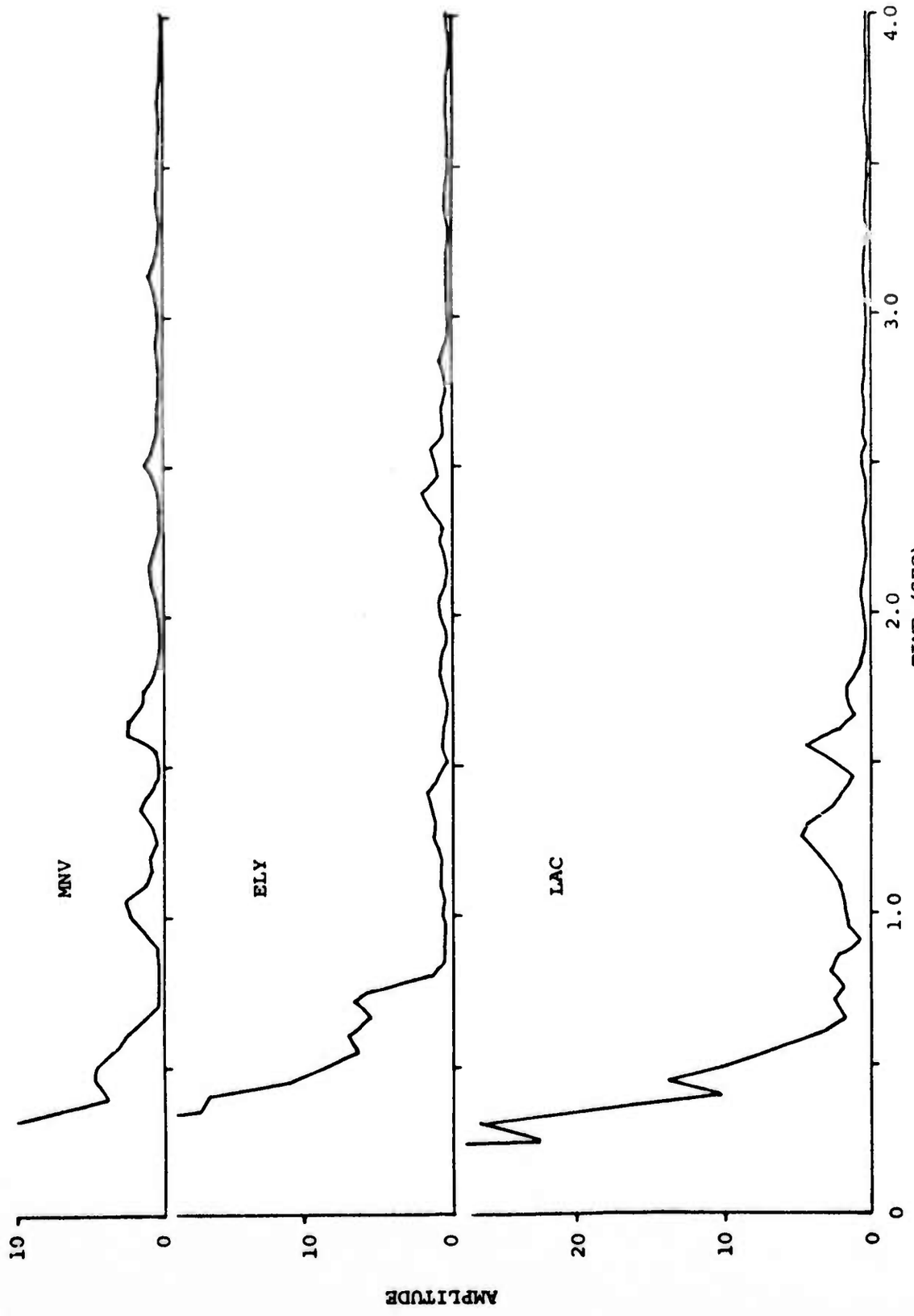

Figure 46. EVENT D cepstra for MNV, ELY, and LAC.

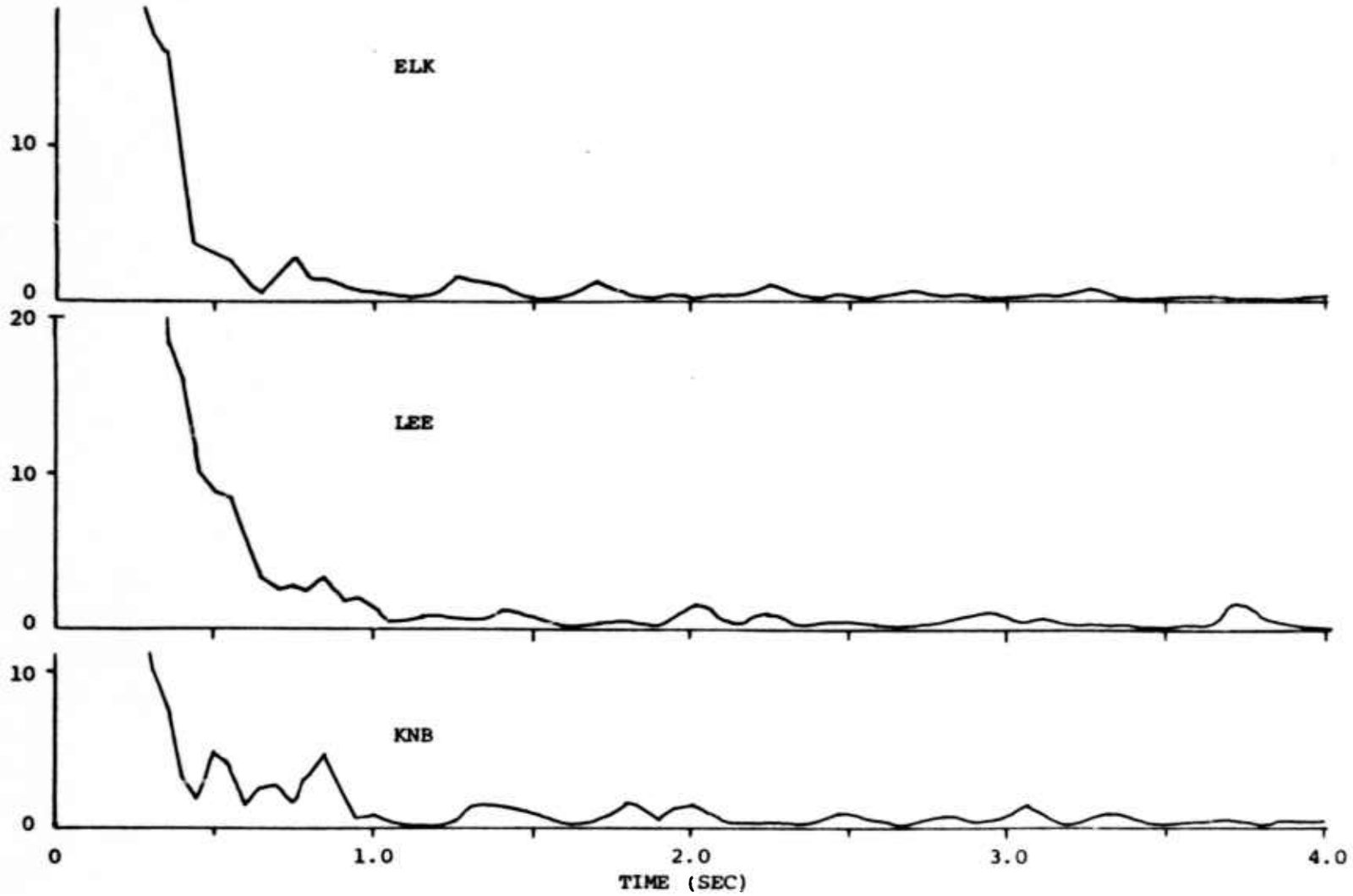

Figure 47. EVENT D cepstra for ELK, LEE, and KNB.

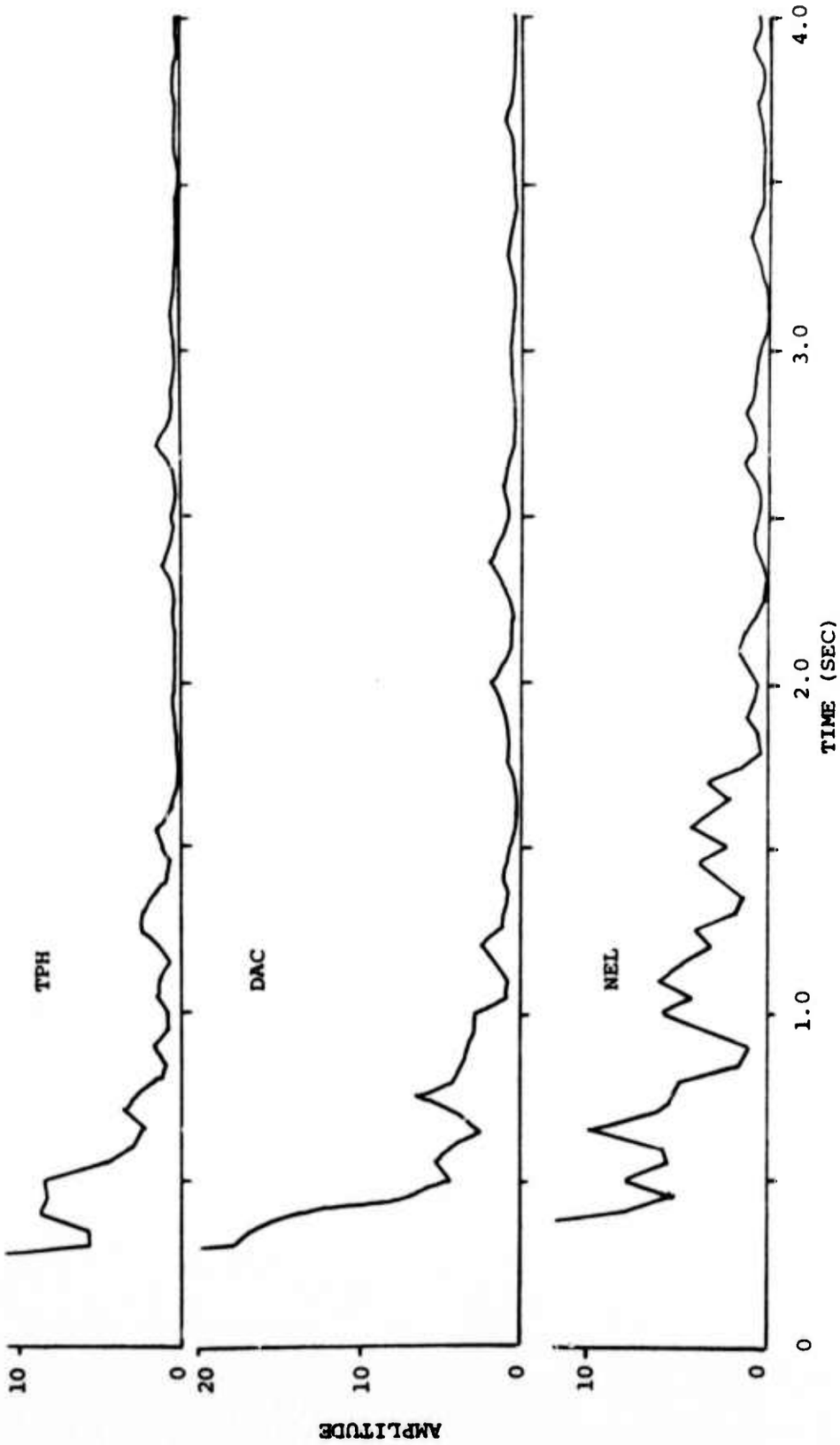

Figure 48. EVENT D cepstra for TPH, DAC, and NEL.

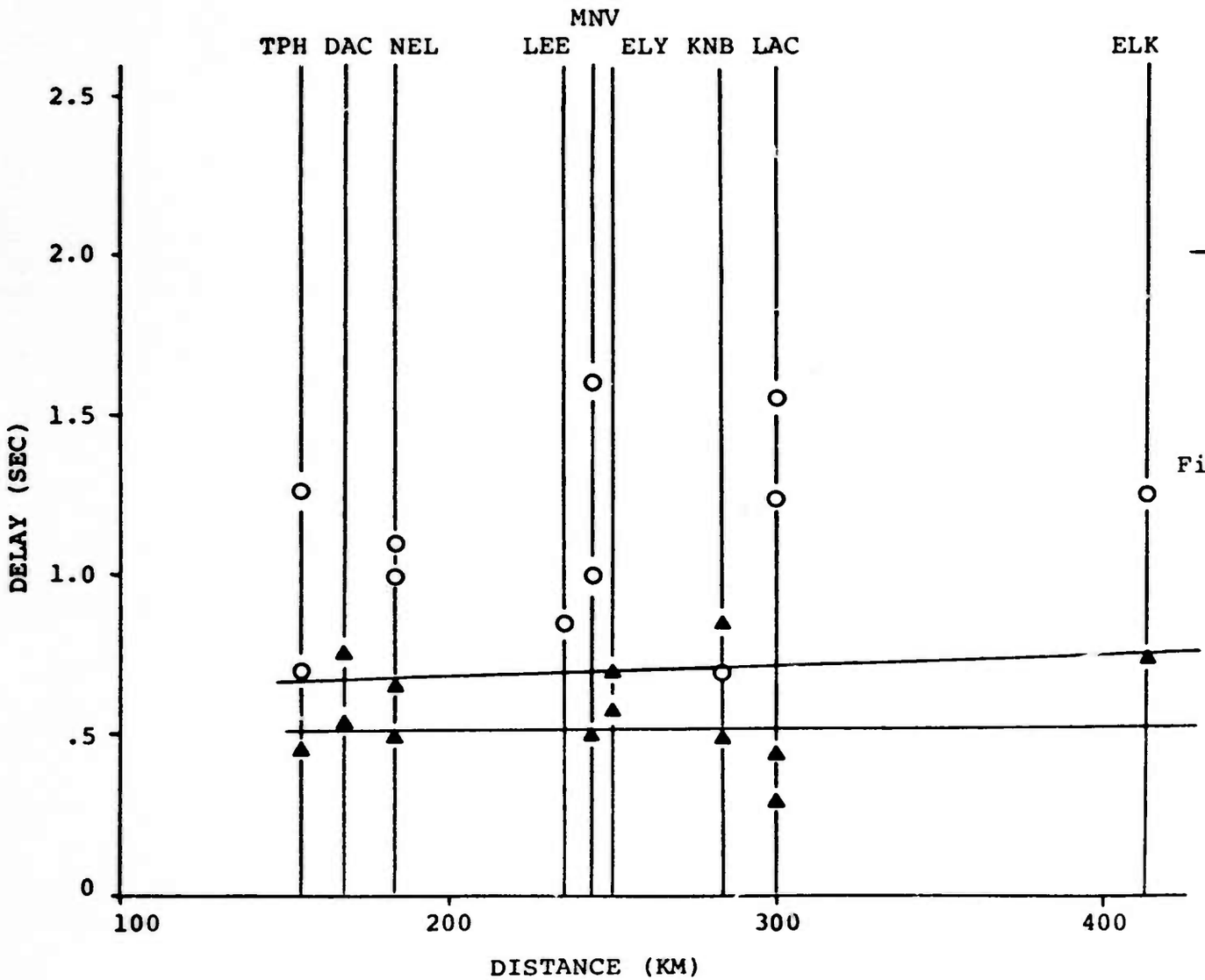

Figure 49. Delay-distance plot for EVENT D.

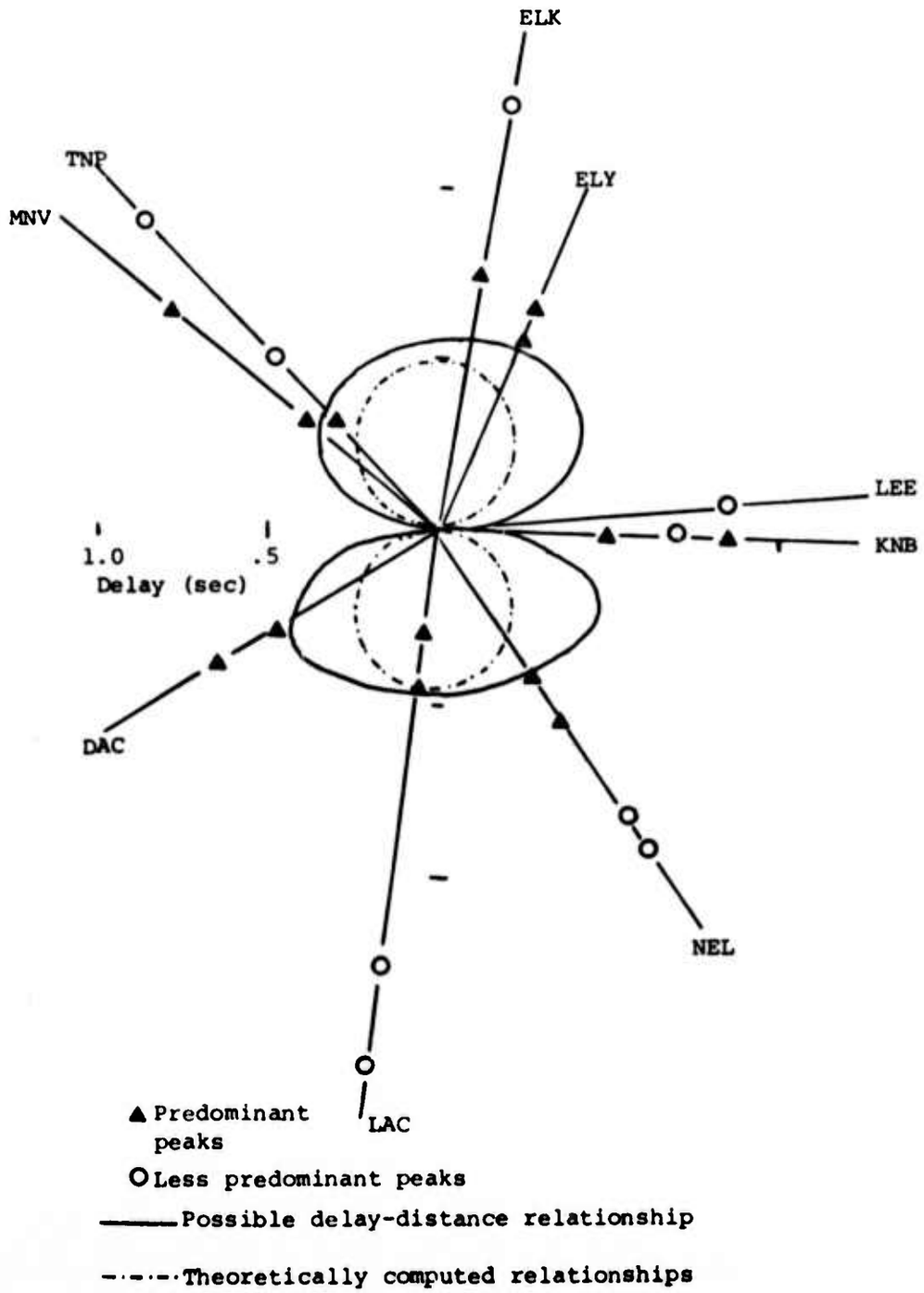

Figure 50. Delay-azimuth plot for EVENT D.

sec is also shown on Figure 50. It is also possible that there is a pP arrival in the .65-.75 sec range with a moveout of .05 sec per 100 km. The corresponding circle with center at the epicenter could be drawn on the delay-azimuth plot. Without data from the 260°-310" azimuth interval the nature of EVENT D cannot be predicted.

Results from EVENT E

Seven EVENT E records were available for analysis. The cepstra are shown in Figures 51 and 52, the delay-distance plot in Figure 53, and the delay-azimuth plot in Figure 54. Four of the cepstra have first peaks occurring in the .45-.55 sec range. This could be an indication of an arrival. There is also an indication of a possible pP arrival in the .80-1.00 sec range with moveout of .09 sec per 100 km. Lines of delay-distance dependence have been placed on Figure 53, but are dashed because of limited data. The possible delay-azimuth pP relationship has been drawn on Figure 54. The lack of data in the 330°-80° azimuth range makes impossible any prediction of the nature of EVENT E.

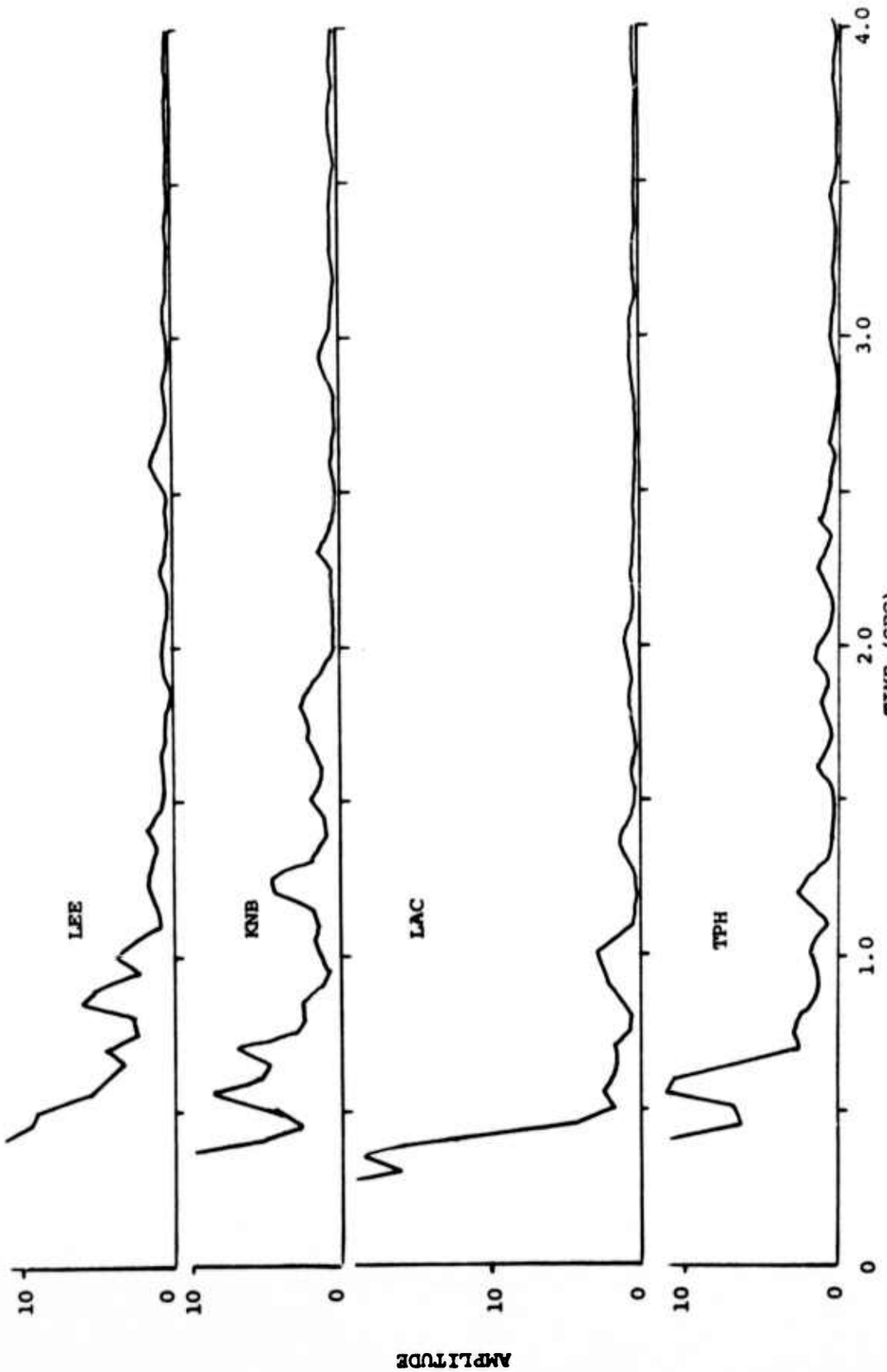

Figure 51. EVENT E cepstra for LEE, KNB, LAC, and TPH.

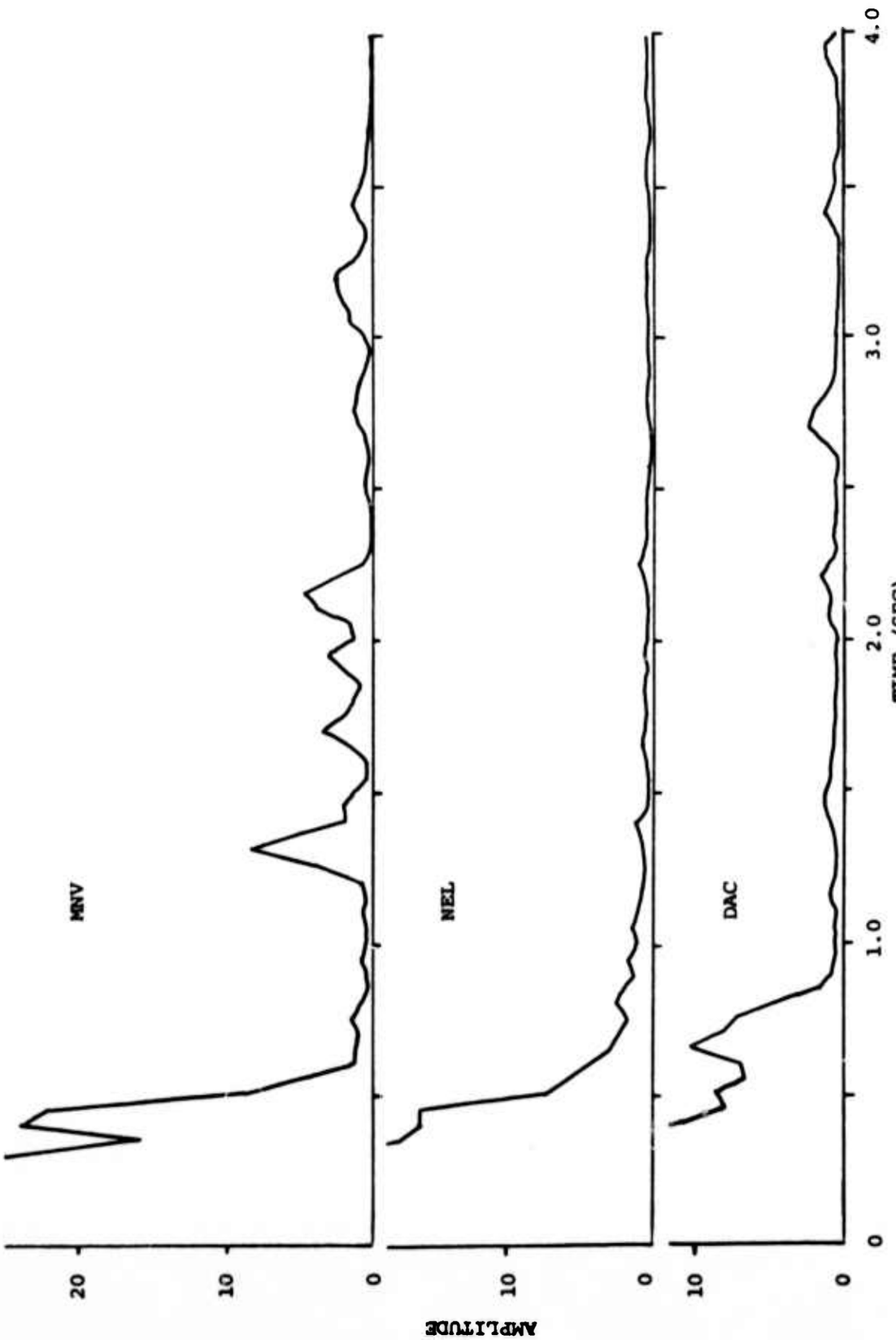

Figure 52. EVENT E cepstra for MNV, NEL, and DAC.

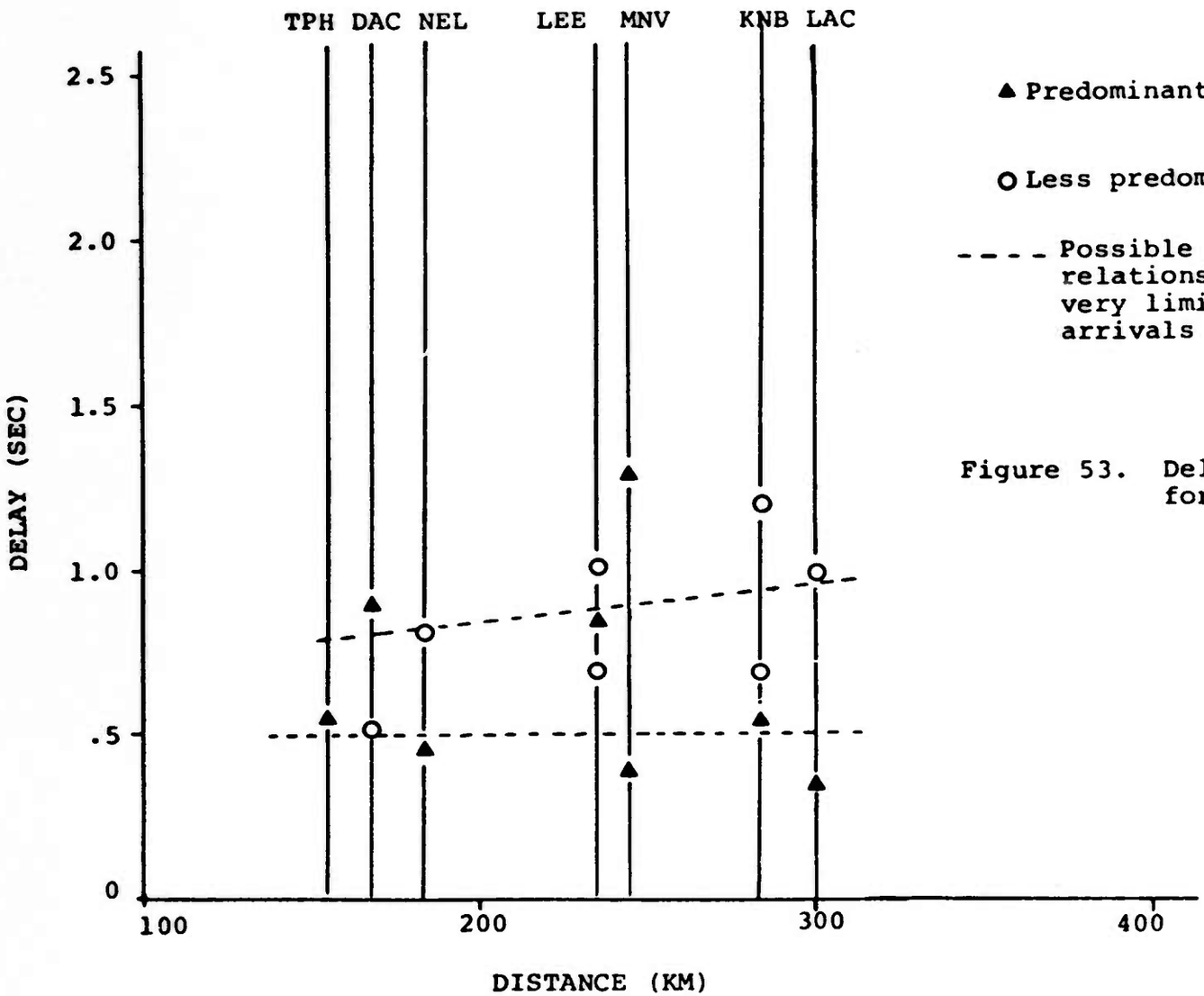

Figure 53. Delay-distance plot for EVENT E.

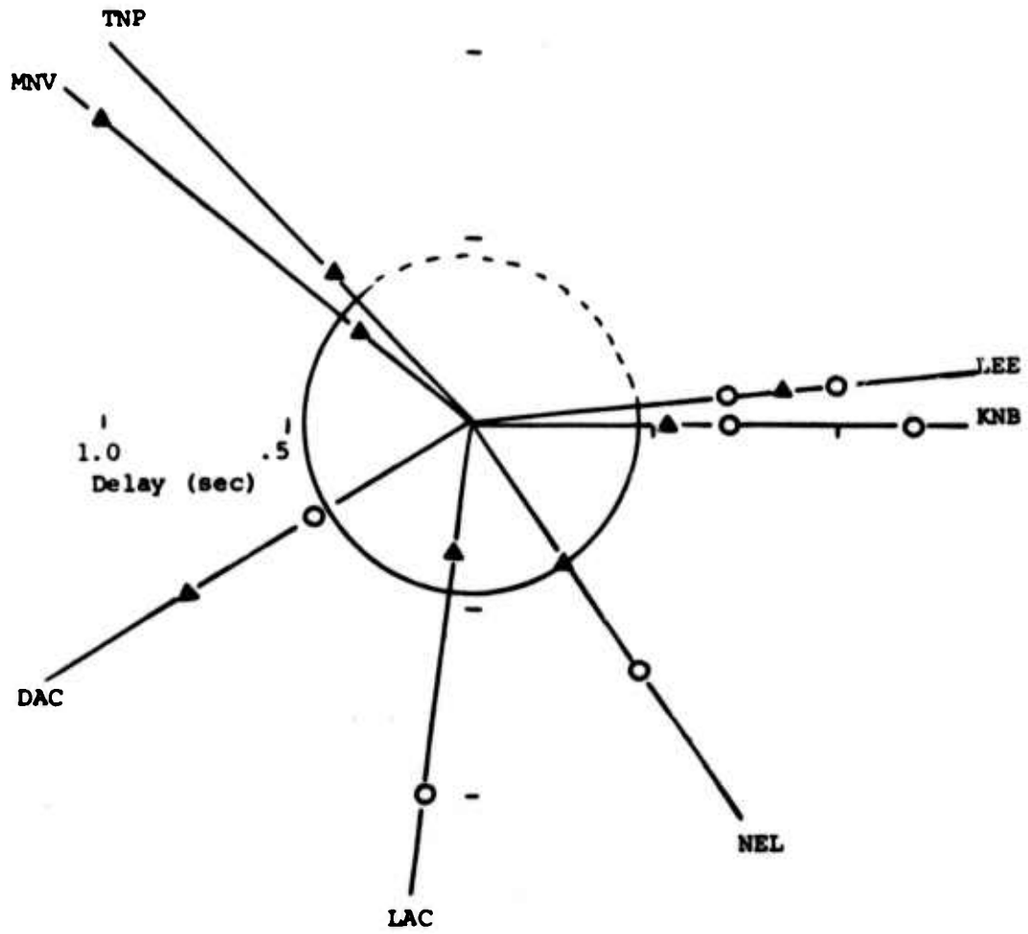

Figure 54. Delay-azimuth plot for EVENT E.

Suggestions for Further Research

The use of cepstrum analysis in connection with the establishment of delay dependence on azimuth and distance, as proposed in this study, should be extended to include additional natural earthquakes. This would provide a more valid basis for determining the ability of such procedures to differentiate earthquakes from nuclear events.

Any future application of cepstrum analysis should involve the recovery of the scale factor "a". This would be particularly important in attempts to identify pP at first zone distances. The "a" factor might also prove of some value in eliminating extraneous peaks. The utility of "a" in this connection, however, will be severely limited by its ambiguous nature.

The use of the pseudo-autocorrelation, suggested by Bogert, Healy, and Tukey (1963), should be investigated. The pseudo-autocorrelation would be particularly valuable in the identification of the pP arrival. This method also has the potential of improving the detection of all arrivals as it should reduce the overall noise level.

REFERENCES CITED

Bogert, B. P., Healy, M. J. R., and Tukey, J. W., 1963, The quefrency alanysis of time series for echoes: cepstrum, pseudo-autocovariance, cross-cepstrum and saphe-cracking: in Proceedings of the Symposium on Time Series Analysis, M. Bosenblatt, ed.: John Wiley and Sons, Inc., New York.

Cohen, T. J., 1970, Source-depth determinations using spectral, pseudo-autocorrelation and cepstral analysis: Geophys. Jour. R. Astr. Soc., v. 20, p. 223-231.

Ekren, E. B., 1968, Geologic setting of the Nevada Test Site and Nellis Air Force Range: Geol. Soc. America Memoir 110, p. 11-19.

Eisler, J. D. and Chilton, F., 1964, Spalling of the earth's surface by underground nuclear explosions: Jour. Geophys. Res., v. 69, p. 5285-5293.

Evernden, J. F., 1969, Identification of earthquakes and explosions by use of teleseismic data: Jour. Geophys. Res., v. 74, no. 15, p. 3828-3856.

Fischer, F. G., Papanek, P. J., and Hamilton, 1972, The Massachusetts Mountain earthquake of 5 August 1971 and its aftershock, Nevada Test Site: U.S. Geol. Survey Rept. USGS-474-149, 20 p.

Flinn, E. A., Cohen, T. J., and McCowan, D. W., 1973, Detection and analysis of multiple seismic events: Bull. Seismol. Soc. America, v. 63, no. 6, p. 1921-1936.

Greenfield, R. J., 1969, Short-period P-wave generation by Rayleigh-wave scattering at Novaya Zemlya: Jour. Geophys. Res., v. 76, p. 7988-8002.

Hinrichs, E. N., 1968, Geologic structure of Yucca Flats area: Geol. Soc. America Memoir 110, p. 239-246.

Huang, Y. T., 1966, Spectral analysis of digitized seismic data: Bull. Seismol. Soc. America, v. 56, no. 2, p. 425.

IBM, 1968, IBM application program system 1360 scientific subroutine package: H20-0205-3, White Plains, IBM Technical Publications Department.

King, C. Y., Abo-Zena, A. M., and Murdock, J. N., 1974, Teleseismic source parameters of the LONGSHOT, MILROW, and CANNIKIN nuclear explosions: Jour. Geophys. Res., v. 79, no. 5, p. 712-718.

Lobeck, A. K., 1957, Physiographic diagram of the United States: Maplewood, New Jersey, The Geographical Press, C. S. Hammond and Co.

Rohrer, R. and Springer, D., 1972, The Massachusetts Mountain earthquake at the NTS, August 5, 1971, compared to an underground explosion at NTS: Lawrence Livermore Laboratory Memorandum, 9 p.

Springer, D. L., 1974, Secondary sources of seismic waves from underground nuclear explosions: Bull. Seismol. Soc. America, v. 64, no. 3, p. 581-594.

Springer, D. L. and Kinnaman, R. L., 1971, Seismic source summary for U.S. underground nuclear explosions, 1961-1970: Bull. Seismol. Soc. America, v. 61, p. 1073-1098.

Stockholm International Peace Research Institute, 1969, Seismic methods for monitoring underground explosions: Almquist and Wiksett, Stockholm, Sweden, 99 p.

Thornbury, W. D., 1965, Regional geomorphology of the United States: New York, John Wiley and Sons, Inc., 609 p.

United States Arms Control and Disarmament Agency, 1964, Documents on disarmament 1963: Government Printing Office, Washington, D. C., p. 291-293.

Zindars, Marjorie A., 1974, Cepstrum analysis applied to the problem of multiple event discrimination: unpub. M.S. thesis, Department of Geological Sciences, Univ. Wisconsin-Milwaukee, 124 p.

APPENDIX A

TYPICAL ANALOG RECORDS

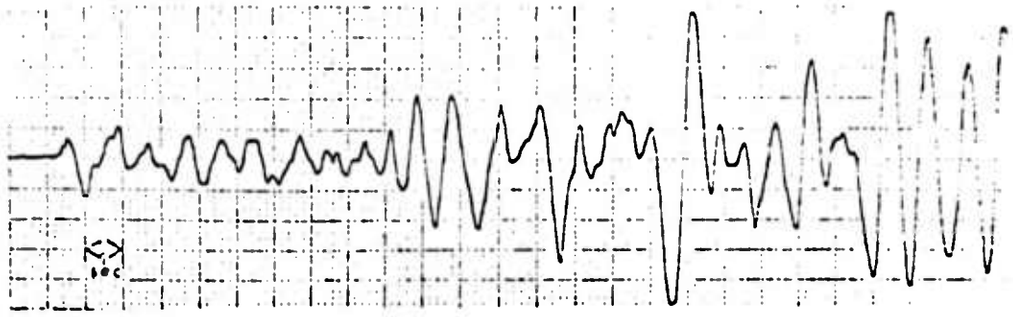

DIDO QUEEN LEE-VWB

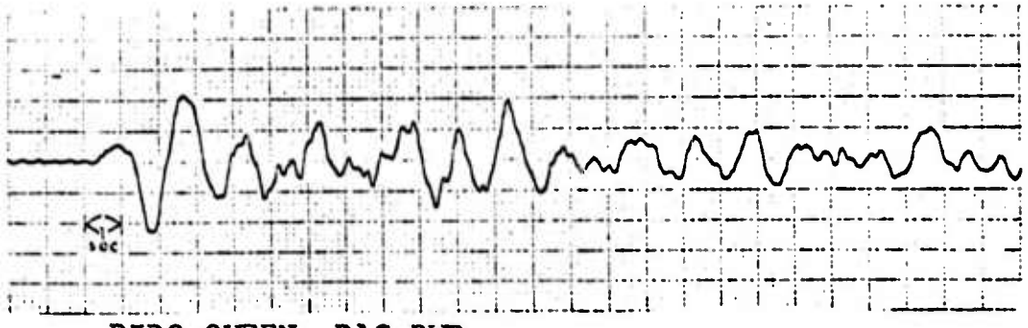

DIDO QUEEN DAC-RWB

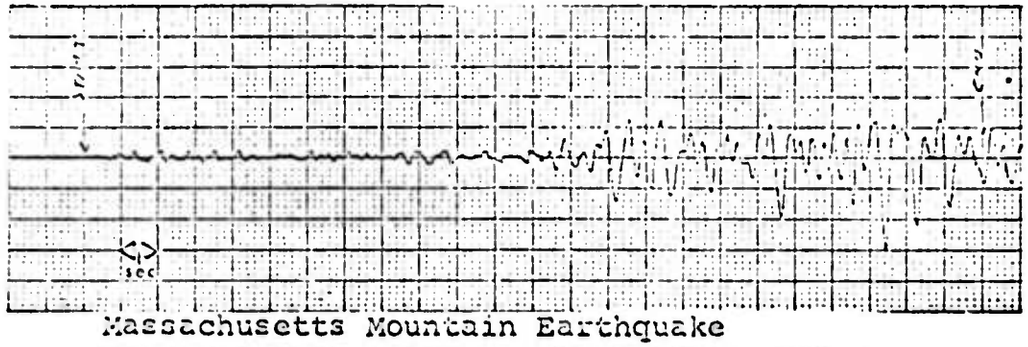

Massachusetts Mountain Earthquake
ELK-Medium Gain through Benioff Simulator

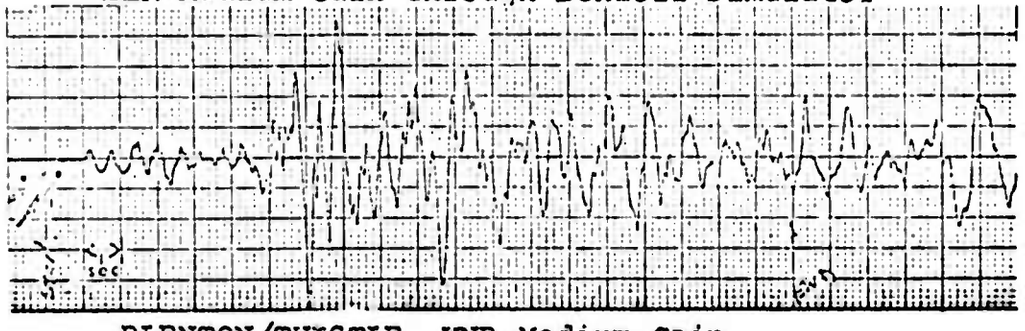

BLENTON/THISTLE KNB-Medium Gain

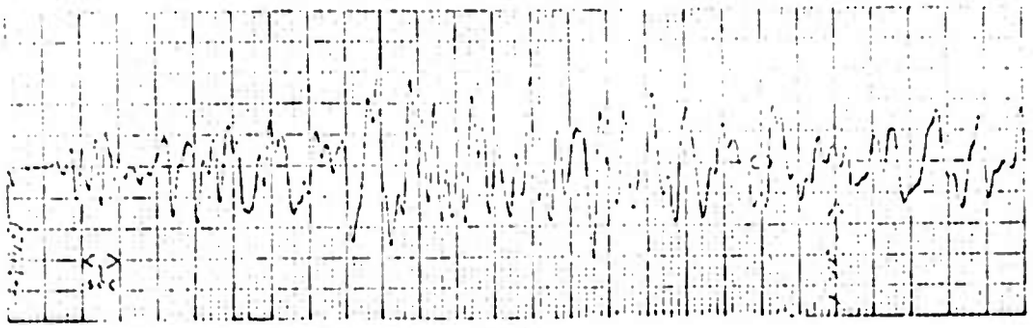

EVENT A MNV-Medium Gain

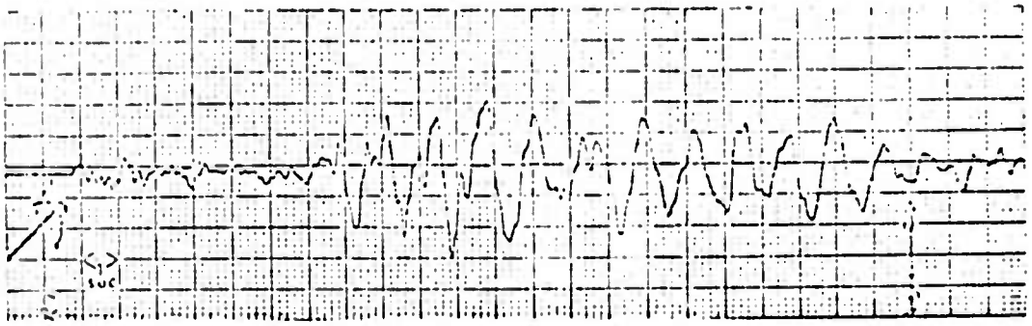

EVENT B LAC-Medium Gain

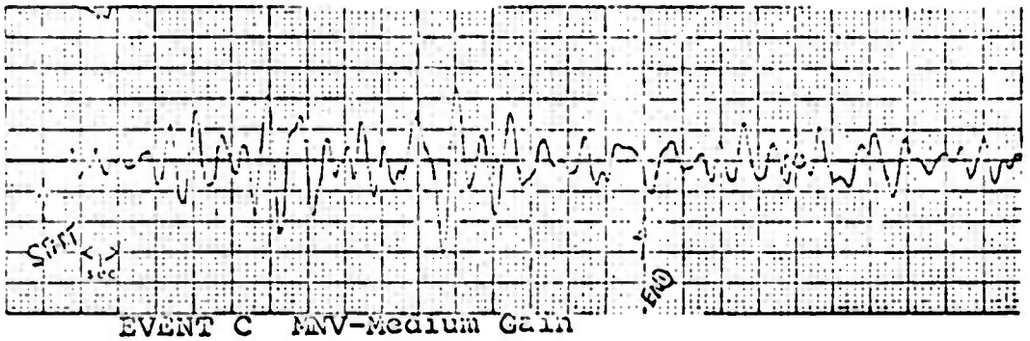

EVENT C MNV-Medium Gain

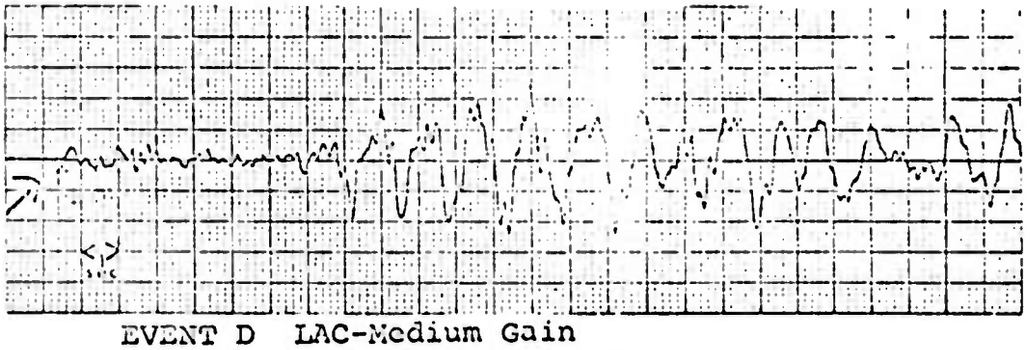

EVENT D LAC-Medium Gain

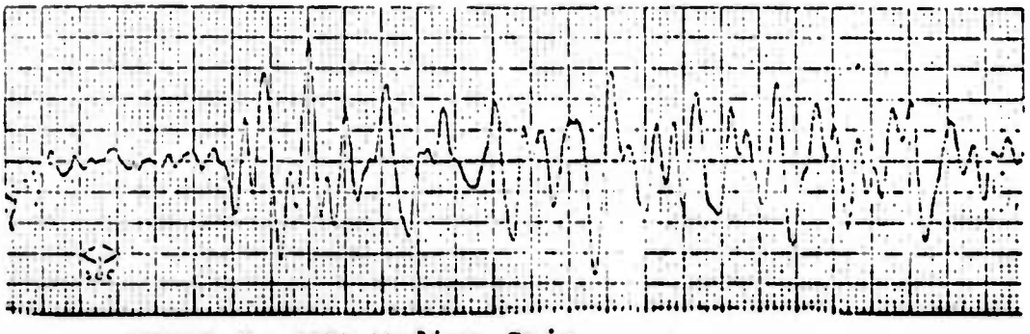

EVENT E KNB-Medium Gain

APPENDIX B

CEPSTRUM PROGRAM LISTING

```
C
C          $$$$$$$$$$          $$$$$$$$$$          $$$$$$$$$$          $$$$$$$$$$
C
C          PROGRAM FOR CEPSTRUM ANALYSIS OF DATA SET X WINDOWED AT TIMES
C          T1 AND T2
C
C          PROGRAM WILL DETERMINE THE POWER SPECTRAL DENSITY OF THE
C          POWER SPECTRAL DENSITY OF THE INPUT SET IF THIS FINAL OUTPUT
C          HAS A STRONG PEAK IT SUGGEST A SECOND ARRIVAL DELAYED BY
C          THE DELAY OF THE PEAK
C
C          $$$$$$$$$$          $$$$$$$$$$          $$$$$$$$$$          $$$$$$$$$$
C
C
C
C          DIMENSION STATEMENTS
      COMPLEX CMP
      DIMENSION L(3),INV(1000),TITLE(28)
      DIMENSION AX(10),AP(10,10)
      DIMENSION AN(10),COEF(30)
      COMMON X(2050),S(2050),CMP(2050)
      DATA L/11,0,0/
C
C
      READ(5,1006) (TITLE(J),J=1,28)
      WRITE(6,1009) (TITLE(J),J=1,28)
C
C
      READ(5,1007) NQA,AINC,SF,ACC,T1,T2,SCALF,DISTM
      READ(5,1017) NPP1,NPP2,HR
C
C          NQA IS THE DEGREE OPERATOR TO USE IN INTERPRETING THE DATA
C          AINC IS THE INCREMENT TO INTERPRET DATA AT
C          SF IS THE SCALE FACTOR
C          ACC IS THE ACCURACY REQUIRED OF THE INTERPRETATION ROUTINE
C          ACCURACY IS NOT REALLY CORRECT BUT NEVER MIND
```

```
C          T1 IS THE START OF DATA WINDOW MEASURED FROM START OF DATA
C          T2 IS THE END OF DATA WINDOW
C     SCALF IS THE NUMBER OF DATA INCREMENTS, PER MILLIMETER
C     DISTM IS THE NUMBER OF MILLIMETERS PER SECOND IN THE DATA
C     NPP1 IS THE NUMBER OF DATA POINTS TO BE PLOTTED FOR THE AMPLITUDE SPECTRA
C     NPP2 IS THE NUMBER OF DATA POINTS TO BE PLOTTED FOR CEPSTRUM
C     HR IS THE HEIGHT OF THE PLOTS TO BE PRINTED
C
C
C
C
C
C          READ IN THE DATA SET
C
C          ALSO DETERMINE NP, ASSUMING TEN DATA POINTS PER CARD
C
      DO707 J=1,2051,10
      JN=J+9
      READ(5,1776,END=708) (S(J1),X(J1),J1=J,JN)
  707 CONTINUE
      JN=JN+10
  708 NP=JN-10
  712 IF(S(NP).LT.0.1) GO TO 713
      GO TO 711
  713 NP=NP-1
      GO TO 712
  711 CONTINUE
C
      WRITE(6,1010) NP,AINC,NQA,ACC
C
      CALL CONVRT(NP,SCALF,DISTM)
C
C     WRITE(6,2) (X(J),J=1,NP)
C     WRITE(6,03)
C     WRITE(6,2) (S(J),J=1,NP)
C     WRITE(6,03)
```

```
C
C            SCALE THE GIVEN DATA SET
      DO 14 J=1,NP
   14 X(J)=X(J)/SF
C
C
C            SELECT THE DESIRED SIGNAL FROM THE DATA SET RETURN IN ARRAY X
      CALL WINDOW(NP,T1,T2)
      IF(NP.EQ.0) GO TO 10000
C
C
C            WRITE OUT THE TIME SERIES
C
      WRITE(6,1001)
      WRITE(6,2) (X(J),J=1,NP)
      WRITE(6,63)
      WRITE(6,1008)
      WRITE(6,2) (S(J),J=1,NP)
      WRITE(6,63)
C
C            SET NECESSARY CONSTANTS
C
      NA=1
      NON=0
      XX=0.0
      N=NOA
      ISET=2
C
C            INTERPRET DATA AT EQUAL INCREMENTS AINC
C
 3020 DO3011 I=ISET,NP
      IOUT=I
      IF(S(I-1).LE.XX.AND.S(I).GE.XX) GO TO 3010
 3011 CONTINUE
      GO TO 94
 3030 ISTRT=1
```

```
      IEND=NQA
      GO TO 3033
 3031 ISTRT=NP-NQA+1
      IEND=NP
      GO TO 3033
 3010 ISET=IOUT
      ISTRT=ISET-NQA/2
      IEND=ISET+NQA/2-1
      IF(ISTRT.LT.1) GO TO 3030
      IF(IEND.GT.NP) GO TO 3031
 3033 J=1
      DO3040 I=ISTRT,IEND
      AX(J)=S(I)
      AP(J,1)=X(I)
      J=J+1
 3040 CONTINUE
      NN=J-1
C     WRITE(6,2) (AP(J,1),J=1,NN)
   82 DO247 I=1,NQA
      AN(I)=AP(I,1)
  247 CONTINUE
      CALL AISPIN(AX,AN,NQA,2,0.0,0.0,COEF,TITLE)
      CALL AISPEV(AX,AN,NQA,COEF,XX,VALUE,FRSTD,SCNDD)
      CMP(NA)=CMPLX(VALUE,0.0)
      NA=NA+1
      XX=XX+AINC
      IF(NON.LT.0) GO TO 94
      IF(S(IOUT).LT.XX) GO TO 91
      GO TO 82
   91 N=N+1
      IF(N.GT.NP) GO TO 93
      GO TO 3020
   93 N=N-1
      NON=-1
      GO TO 82
   94 AB=S(NP)-XX
      IF(AB.GT.0.0) GO TO 82
      NP=NA-1
C
```

```
C           DATA IS NOW INTERPRETED AT EQUAL INTERVALS AINC
C
C           ESTABLISH IN ARRAY X
C
      DO 95 J=1,NP
   95 X(J)=REAL(CMP(J))
C
C
C           WRITE OUT INTERPRETED DATA
C
      WRITE(6,83)
      WRITE(6,1001)
      WRITE(6,2) (X(J),J=1,NP)
C     WRITE(7,1776) (X(J),J=1,NP)
      WRITE(6,63)
C
C           FIND THE AUTOCORRELATION
C
      CALL COREL(NP,N)
      CALL TAPER(NP,N)
      WRITE(6,63)
      K=NP+1
C
C           ADD APPROPRIATE ZEROS TO GIVE TOTAL DATA SERIES OF 2048 POINTS
      DO 15 J=K,2048
   15 X(J)=0.0
C
C           WRITE OUT TOTAL SERIES TO BE TRANSFORMED
      WRITE(6,1002)
      WRITE(6,2) (X(J),J=1,NP)
C
C           FIND THE FOURIER TRANSFORM
C
      NP=2048
      DO 20 J=1,NP
   20 CMP(J)=CMPLX(X(J),0.0)
      CALL HARM(CMP,L,INV,S,1,IFERR)
```

```
C
C          FIND AMPLITUDE SPECTRA OF COMPLEX FOURIER TRANSFORM CMP
C
      DO 50 J=1,1025
   50 X(J)=CABS(CMP(J))
C
C          WRITE OUT AMPLITUDE SPECTRA
      WRITE(6,1003)
      WRITE(6,2) (X(J),J=1,1025)
      WRITE(6,63)
      CALL PLOTF(X,NPP1,HR,AINC)
      X(1)=X(1025)
C
C          FIND LOG SPECTRA
      DO 52 J=1,1025
   52 X(J)=ALOG10(X(J))
C
C          SET BASELINE NEAR ZERO
      DO 53 J=1,1025
   53 X(J)=X(J)-X(1025)
C
      NN=1025
C
C          FIND THE AUTOCORRELATION OF THE LOG SPECTRUM
      CALL COREL(NN,N)
      K=N
      CALL TAPER(NN,N)
      WRITE(6,63)
C
C
C          FIND FOURIER TRANSFORM OF AUTOCORRELATION OF LOG SPECTRA
C
```

```
      DO 55 J=1,2048
   55 CMP(J)=CMPLX(X(J),0.0)
      CALL HARM(CMP,L,INV,S,1,IFERR)
C
C          FIND AMPLITUDE SPECTRA OF COMPLEX FOURIER TRANSFORM CMP
C          THIS IS CEPSTRUM OF DATA SET X
C
      DO 60 J=1,1100
   60 X(J)=CABS(CMP(J))
C
C          WRITE OUT THE CEPSTRUM
C
      WRITE(6,1005)
      WRITE(6,2) (X(J),J=1,1100)
C
      DO 62 J=1,N
   62 S(J)=FLOAT(J-1)*AINC
      WRITE(6,63)
      WRITE(6,1011)
      WRITE(6,2) (S(J),J=1,N)
      CALL PLOTF(X,NPP2,HR,AINC)
C
C          FORMATS FOLLOW
C
    2 FORMAT(' ',10F12.3)
   63 FORMAT(' ','  ',////)
 1001 FORMAT('1','INPUT TIME SERIES',//)
 1002 FORMAT(' ','AUTOCORRELATION FUNCTION ',//)
 1003 FORMAT(' ','AMPLITUDE SPECTRA',//)
 1005 FORMAT(' ','FINAL OUTPUT',//)
 1006 FORMAT(13A6,A2)
 1007 FORMAT(I10,7F10.3)
 1017 FORMAT(2I5,F10.3,I5)
 1008 FORMAT(' ','TIME INCREMENTS'//)
 1009 FORMAT('1',20X,'++++++++++           ++++++++++           ++++++++++
     1          ++++++++++',2X/' ',30X,13A6,A2,3X/' ',30X,13A6,A2,2X/' ',2
     220X,'++++++++++           ++++++++++           ++++++++++
     3++++++++++',//)
```

```
 1010 FORMAT(' ','NUMBER OF POINTS = ',I5/' ','INTERPOLATED EVERY ',F5.3
     1,2X,'SECONDS',5X,'USING DEGREE ',I5,2X,'WITH REQUIRED ACCURACY OF
     2 ',F7.5,//)
 1011 FORMAT(' ','CEPSTRUM TIMES',//)
 1776 FORMAT(20F4.0)
10000 STOP
      END
@FOR,AIX  TAPER
      SUBROUTINE TAPER(NP,N)
      COMMON X(2050),S(2050)
      A=0.8*FLOAT(N)
      ALFA=ALOG(0.3)/(A**2)
      DO 1 J=1,NP
      A=(FLOAT(N-J))**2
    1 X(J)=X(J)*EXP(ALFA*A)
      RETURN
      END
@FOR,AIX  COREL
      SUBROUTINE COREL(NP,N)
      COMMON X(2050),S(2050)
      DO 11 J=1,NP
      SUM=0.0
      DO 12 I=1,J
   12 SUM=X(I)*X(NP+I-J)+SUM
      S(J)=SUM
   11 CONTINUE
      N=NP-1
      DO 13 J=1,N
   13 S(NP+J)=S(NP-J)
      NP=2*NP-1
      N=N+1
      DO 14 J=1,NP
   14 X(J)=S(J)/S(N)
C     WRITE(6,1)
C     WRITE(6,2) (X(J),J=1,N)
```

```
    1 FORMAT(' ',' NORMALIZED AUTOCORRELATION FUNCTION',///)
    2 FORMAT(' ',10F12.3)
      RETURN
      END
@FOR,AIX  WINDOW
      SUBROUTINE WINDOW(NP,T1,T2)
      COMMON X(2050),S(2050),CMP(4100)
C
C
      NTF=4
      NTB=6
C          NTF AND ETB SHOULD BE PASSED FROM THE MAIN PROGRAM AS VARIABLES
C          SINCE THIS IS TEST PROGRAM THIS WAS NOT DONE
C
C
      DO 10 J=1,NP
      K=J
      IF(S(J).GT.T1) GO TO 11
   10 CONTINUE
      WRITE(6,1)
      NP=0
      RETURN
   11 A=T1-S(K-1)
      B=S(K)-T1
      IF(A.LE.B) K=K-1
      I=K-NTF
      DO 15 J=I,NP
      K=J
      IF(S(J).GE.T2) GO TO 16
   15 CONTINUE
      WRITE(6,2)
      NP=0
      RETURN
   16 A=T2-S(K-1)
      B=S(K)-T2
```

```
      IF(A.LE.B) K=K-1
      K=K+NTB
      IF(I.LT.1) GO TO 30
      IF(K.GT.NP) GO TO 31
      WRITE(6,3) S(I),S(K)
      NA=1
      BASE=X(I)
      T=S(I)
      DO 20 J=I,K
      S(NA)=S(J)-T
      X(NA)=X(J)-BASE
      NA=NA+1
   20 CONTINUE
      NP=NA-1
      CALL ENDS(NTF,NTB,1,NP)
C
C          FORMATS FOLLOW
C
    1 FORMAT(' ',' START OF WINDOW GREATER THAN DATA SERIES LENGTH PROGRA
     1M ABORTED'//)
    2 FORMAT(' ',' END OF WINDOW GREATER THEN END OF DATA SERIES PROGRAM
     1ABORTED'//)
    3 FORMAT(' ',' DATA WINDOW FROM TIME ',F7.3,2X,'TO TIME ',F7.3//)
      RETURN
   30 WRITE(6,4)
      NP=0
    4 FORMAT(' ',' START OF WINDOW IS TOO CLOSE TO START OF DATA SERIES
     1PROGRAM ABORTED'//)
      RETURN
   31 WRITE(6,5)
      NP=0
    5 FORMAT(' ',' END OF WINDOW IS TOO CLOSE TO END OF DATA SERIES  PROG
     1RAM ABORTED'//)
      RETURN
      END
```

```
@FOR.AIX  ENDS
      SUBROUTINE ENDS(NF,NB,NS,NE)
      COMMON X(2050),S(2050),CMP(4100)
      A=3.0*3.14159/2.0
      PI=3.14159
      B=PI/2.0
      PHEF=A-(PI*S(NS))/(S(NS+NF)-S(NS))
      PHEB=B-(PI*S(NE-NB))/(S(NE)-S(NE-NB))
      TF=2.0*(S(NS+NF)-S(NS))
      TB=2.0*(S(NE)-S(NE-NB))
      N=NS+NF
      DO 10 J=NS,N
   10 X(J)=((1.0+SIN(2.0*PI*S(J)/TF+PHEF))/2.0)*X(J)
      N=NE-NB
      DO 11 J=N,NE
   11 X(J)=((1.0+SIN(2.0*PI*S(J)/TB+PHEB))/2.0)*X(J)
      RETURN
      END
@FOR.AIX  CONVRT
      SUBROUTINE CONVRT(NP,SCALF,DISTM)
      COMMON X(2050),S(2050)
C
      NPT=NP-1
      DO40 I=1,NPT
      II=I+1
      IF((X(II)-X(I)).GT.5000.0) X(II)=X(II)-10000.0
   40 CONTINUE
C
      SFIRST=S(1)
      DO10 I=1,NP
      S(I)=(S(I)-SFIRST)/(SCALF*DISTM)
   10 CONTINUE
```

```
C
      XTOT=0.0
      DO20 I=1,NP
      XTOT=XTOT+X(I)
   20 CONTINUE
      XMED=XTOT/NP
C
      DO30 I=1,NP
      X(I)=(X(I)-XMED)/(SCALF*DISTM)
   30 CONTINUE
      RETURN
      END
```